SELECTIVE DISPROPORTIONATION OF TOLUENE TO PRODUCE BENZENE AND p-XYLENE

A DISSERTATION

Submitted in partial fulfilment of the
requirements for the award of the degree

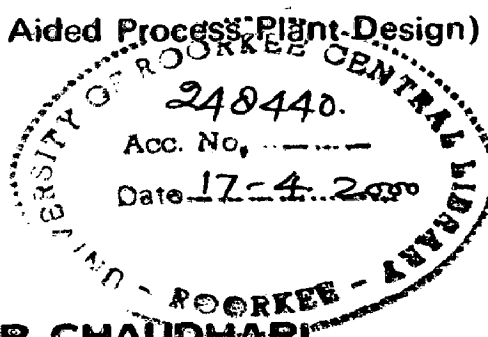*of*

MASTER OF ENGINEERING

in

CHEMICAL ENGINEERING

(With Specialization in Computer Aided Process Plant Design)

By

PARMESH KUMAR CHAUDHARI

DEPARTMENT OF CHEMICAL ENGINEERING
UNIVERSITY OF ROORKEE
ROORKEE-247 667 (INDIA)
FEBRUARY, 2000

CANDIDATE'S DECLARATION

I hereby certify that the work presented in this dissertation entitled "SELECTIVE DISPROPORTIONATION OF TOLUENE TO PRODUCE BENGENE AND P-XYLENE", in partial fulfilment of the requirements for the reward of the degree of MASTER OF ENGINEERING IN CHEMICAL ENGINEERING with specialisation in COMPUTER AIDED PROCESS PLANT DESIGN, at University of Roorkee, Roorkee, is an authentic record of my own work carried out between July 1999 and February 2000 under the guidance of Dr. Sri Chand, Assistant Professor, Department of Chemical Engineering, University of Roorkee, Roorkee.
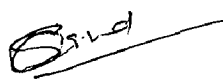
The matter presented in this dissertation has not been submitted by me for the award of any other degree of this or any other University.

Dated 21st February , 2000

(Parmesh Kumar Chandhari)

This is certify that the above statement made by the candidate is correct to the best of my knowledge.

Date: 21. 2. 2000

(Dr. Shri Chand)
Assistant Professor
Deptt. of Chemical Engg.
Roorkee - 247 667 (India)

ABSTRACT

Due to the increasing demand of benzene and xylenes in global market as intermediate raw material for the manufacture of polyester fibers and synthetic resins in recent years, newer techniques in converting toluene to benzene and xylenes is being explored. Among the xylenes, p-xylene is of considerable importance as raw material for terephthalic acid and dimethyl terephthalate manufacture required for polyester fibers, vitamin synthesis and other pharmaceuticals.

Toluene disproportionation has the advantages for producing both xylenes as well as benzene. This reaction to produce equimolar amounts of benzene and xylenes is well known. Earlier studies on disproportionation has been done using Friedel Craft catalysts of metal halides; solid acid catalysts, such as silica-alumina and synthetic zeolites. Apparently none of these satisfied the need of industry. Zeolites are shown to be superior compared to amorphous solid acid catalysts for disproportionation reaction. Several studies have been performed using H-mordenite, X- and Y-zeolites and ZSM-5 zeolites in ion-exchanged forms. The ion-exchange was done using base metals/transition metals/rare earth cations.

Among all the catalysts HZSM-5 zeolites were found to be superior catalysts in giving better activity and selectivity towards the desired products.

The present work is aimed at using modified and unmodified zeolites as prospective catalysts for the reactions. Modification has been done by cation exchange of rare earth/transition metal. The compound which has been used by previous workers for chemical deposition on HZSM-5 and other zeolites having much cost compare to the compound which has been used at present work for cation exchange. Previous workers have performed the disproportionation reaction at high pressure, whereas, in the present work, the reactions were performed at atmospheric pressure. By choosing the conditions as mentioned above operating cost as well as the material cost may be minimized. The parameters such as, effect of preparation method of catalysts, surface acidity,

shape selectivity, crystal size and operating condition on the activity and selectivity for p-xylene have been studied.

In suceeding part of the work, the best catalyst from the above study was used to explore some of the kinetic aspects and the various reaction constants were evaluated. The thesis has been presented in five chapers, the summary of each is given below:

Chapter I has been divided into two parts.

(a)   Part (a) deals with the introduction to the disproportionation process and the statistics consisting of present and future demands and supply of benzene, toluene and xylenes.

(b)   Review of the existing literature on toluene disproportionation catalyst as well as kinetics of the reaction.

Chaper II describes the different methods employed for the preparation of catalysts. A discussion regarding zeolites structure and nature of acid sites has also been included in this chapter alongwith the methods of analysis of the catalyst samples.

Chapter III gives the details of the experimental set-up and operational technique employed for taking runs. The studies conducted in different ranges of operating parameters for all the catalysts is given below.

Chaper IV comprises of the calculation procedures and kinetic derivation. Homogeneous and heterogeneous model have been derived. The calculation procedure for ΔH, K_e etc. are also encorporated in this Chapter.

Chapter V deals with the calculation procedures of conversion and selectivity of the disproportionation reaction In this chapter results of disproportionation reaction is tabulated as well as some graphs have been presented.

Chapter VI deals with the result of the present investigation and interpretation with pertinent discussion.

The possible explanation to the variations in the activities of the catalysts related to their acidity, crystallinity, nature of cations and the extent of exchange

have been given in detail which are in accordance with the findings of the previous workers. Kinetic study was carried out using over 1.756%Cr1.923%Th HZSM-5 SAR(32), HZSM-5 SAR(19) and PbHY SAR(3) catalysts.

III

ACKNOWLEDGEMENT

CONTENTS

LIST OF FIGURES

LIST OF TABLES

NOMENCLATURE

A_T, A_B, A_{P-X}, A_{M-X}, A_{O-X}	Area of toluene, Benzene, Para xylene, Metaxylene, ortho xylene obtained in gas chromotograph analysis.
B	Benzene
$B(v)$	Spectral power density
C_t	Total concentration of active sites of catalyst
C_v	Total concentration of vacant active sites of ctalyst
d	Distance between the surface of X-rays, falling on the crystal surface.
F	Mole of toluene leaving per unit time from differential amount of catalysts.
F_{T0}	Mole of toluene fed in reactor
ΔF_T^0	Standard free energy change at temperature $T(^\circ K)$
ΔH_T^0	Standard heat of reaction at temperature $T(^\circ K)$
ΔH_R^0	Change in enthalpy of reactant
ΔH_p^0	Change in enthalpy of product
ΔH^0_{R298}	Standard heat of reaction of reactant at $298^\circ K$
ΔH^0_{P298}	Standard heat of reaction of product at $298^\circ K$.
k_1, k_2, k_3	Rate constant of hetogeneous toluene dipropornations model for adsorption of toluene, surface reaction , desorption of xylenes respectively.
$k_e = K_x\ K_T\ K_s$	Thermodynamic equilibrium constant of toluene disproportionation reaction of hetrogeneous model.
$K_T = K_A$	Equlibrium rate constant of adsorption of toluene on catalyste surface.
K_X	Equilibrium rate constant of desorption of xylene from catalyst surface.

K_S	Equilibrium rate constant of surface reaction on catalyst surface.
k_P	Reaction rate constatn of toluene disproportionation reversible second order reaction = k_e at atmospheric pressure.
K_P	Thermodynamic equlibrium constant = K_e at 1 atmosphere.
n_{T0}	Number of mole of toluene initially fed on reactor
M_1, M_2	Molecular weight of material formign the bond.
n_T	Number of mole of tolouene at any time.
$\bar{P}_B$, $\bar{P}_N$, $\bar{P}_T$, $\bar{P}_x$	Partial pressure of benzene, nitrogen, toluene, xylenes respectively
P_{T0}	Partial pressure of toluene in feed
P_{m-x}	Partial pressure of meta xylene
P_{p-X}	Partial pressure of Para xylene
R	Gas constant
r_T	Rate of dispropornation of toluene for homogeneous reaction model
S-A_T, S-A_B, S-A_{m-x}, S-A_{P-X}, S-A_{O-X}	Standard area of toluene, Benzene, Meta xylene, Para xylene, Ortho xylene at oven temperature of gas chromotograph.
T	Temperature K
V_F	Volume of reaction product fed in gas chromotograph for analysis.
W	Weight of catalyst
x	Mole fraction conversion of toluene
X	Xylene
M_T, M_B, M_{P-X}, M_{M-X}, M_{O-X}	Molecular weight of toluene, Benzene, Para xylene, Meta xylene, Ortho xylene

M_{XS}	.	Total mole of xylens
S_{P-X}		Selectivity of p-xylene

Greek Symbol

ϕ_B, ϕ_X	Mole fraction of Benzene and xylenes in feed
ν	Wave number, cm^{-1}
2θ	Angle of diffraciton of X-ray falling on crystal surface
λ	Wave length of X-ray
α, β, γ	Constant of heat capacity

INTRODUCTION AND LITERATURE REVIEW

1.1 INTRODUCTION

Toluene disproportionation is one of the modern techniques to convert less valuable toluene to more valuable benzene and xylenes. The relevance of disproportionation process especially with reference to our country is enormous when we look into the available toluene as well as the short supply of benzene and xylenes for the petrochemical industry. From last two decades, there has been a phenomenal growth in the use of benzene and xylenes in organic synthesis. The large amount of toluene produced in the world do not find much use as a raw material for petrochemical industry except for production of TNT (trinitrotoluene) and benzoic acid, which require relatively smaller amounts. Bulk of toluene produced is used as reagent and as a solvent for paint industry. Benzene is the largest volume aromatic hydrocarbon having uses for the production of plastics, synthetic fibres, elastomers, phenolic resins, synthetic detergents, lube oil additives and insecticides like benzene hexachloride, DDT, etc. Among the three xylenes para and ortho are more important as feed stock for petrochemical industry. Para xylene finds its use in the production of dimethyl terephthalate and terephthalic acid which are intermediates in production of polyester fibers, synthesis of vitamins and other pharmaceuticals production, which is expected to be in still high demand in coming years. it is estimated that para-xylene production will increase by 60% or more by the year 2000. Orthoxylene is used for the manufacture of phthalic anhydride, which is an intermediate for the plastic industry. Meta xylene does not find much use and it has to be isomerized to p-xylene or o-xylene for better utility.

Table 1.1 shows benzene, toluene and xylenes yields from the two major types of crudes of our country after reforming.

Table 1.1 [1]

	Bombay High	Assam
Benzene	3.27 wt.%	1.89 wt%
Toluene	5.30 wt.%	3.67 wt.%
Xylenes	4.59 wt.%	3.77 wt%

Table 1.2 Projected demand and short fall of petrochemicals [1]

	Demand 1000 MTA		Short fall 1000 MTA	
	1983-84	1987-88	1983-84	1987-88
Benzene	301	441	176	316
o-xylene	58.	91	34	67
p-xylene	94	162	59	124

Table 1.3 The cost of benzene, toluene and xylenes in Indian market [2]

	Rs./ liter
Benzene	22.00 + ST
Toluene	24.00 + ST
p-xylene	43.00 + ST
0-xylene	30.00 + ST
Mixed xylene	22.0 + ST

ST → Sales Tax

The projected demand and short fall of benzene and xylenes in India during previous years are given in Table 1.2. Presently, the gap between demand and production has been filled. As per the significant demand of p-xylene, the

2

Reliance industry is going to start the world's third largest p-xylene production plant. It is estimated that 12 percent of total demand of benzene will be fulfilled by disproportionation reaction by year 2003 (Oil & Gas J., Nov. 23, 1998).

In order to bridge the present and the future import gaps relying on the procrastinated demands, a lucrative process for the conversion of surplus toluene to more valuable benzene and xylenes has, therefore become indispensible and disproportionation of toluene is one such process.

1.2 Disproportionation of toluene [3]

This reaction to product equimolar amounts of benzene, xylenes is a well known reaction and is represented as

$$2 \; \text{Toluene} \; \rightleftharpoons \; \text{Benzene} \; + \; \text{Xylenes} \qquad (1.1)$$
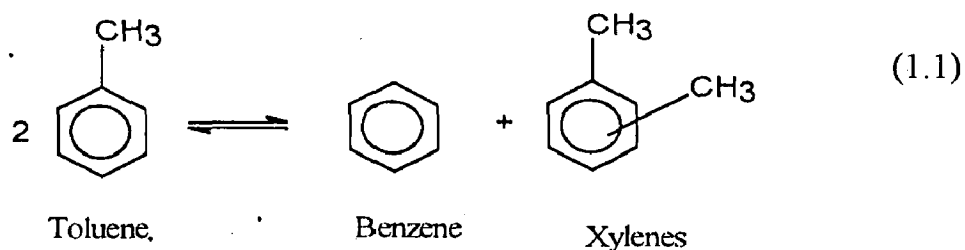
Here, the two mole of toluene molecules are converted to one mole benzene and one mole xylene molecule by an interchange of a CH_3 group and a H-atom between two toluene molecules.

The reaction may be carried out in the presence of nitrogen oxygen or hydrogen as a carrier gas. In the present experiment nitrogen has been used. Toluene and nitrogen are mixed together and are passed over the catalyst. The subsequent use of nitrogen resulted in conversion rates and product distributions. Which were similar to those obtained on fresh catalyst. However, no effect of

acceleration of the toluene conversion was found by the use of oxygen as a carrier gas, if a fresh catalyst was applied.

Hydrogen is employed to suppress cracking and to presserve the activity of catalyst. Since hydrogen is also a component in the feed strem, toluene will also have a tendency to combine with hydrogen in the presence of a catalyst to give benzene and methane i.e. **dealkylation** of toluene and is represented by following reaction.

$$\text{Toluene} \qquad\qquad\qquad \text{Benzene} \quad \text{Methane} \qquad (1.2)$$
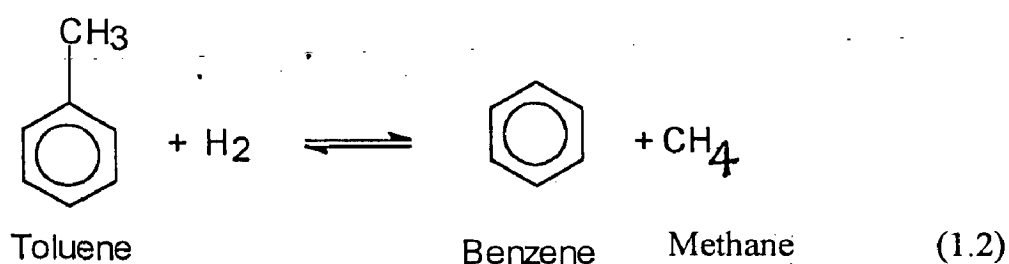
Initially at equlibrium 24% p-xylene 52% m-xylene and 24% o-xylene is formed. The xylenes may isomerise, depending upon the nature and pore size of the catalyst. The **isomeridation** reaction is given below.

$$\text{o-Xylene} \qquad\qquad \text{m-Xylene} \qquad\qquad \text{p-Xylene} \qquad (1.3)$$
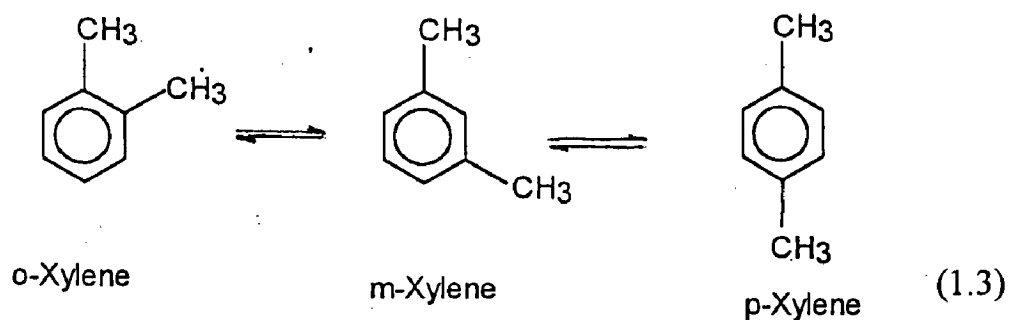
Toluene may also be produced back by subsequent reaction between primary products. This is generally defined as **transalkylation** reaction which is given by the backward reaction of equation (1.1).

The product also contains trimethyl benzene. The formation of trimethyl benzene takes place as high temp (>450°C) by xylenes alkylation (1.4) and xylenesdisproportionation reactions (1.5).

Toluene   Xylenes   Tri methyl benzene   Benzene   (1.4)

Xylenes   Toluene   Tri methyl benzen

(1.5)
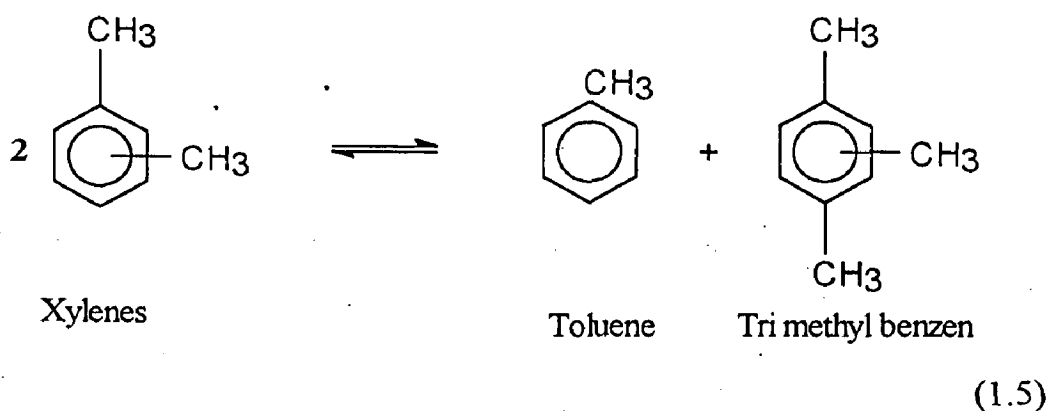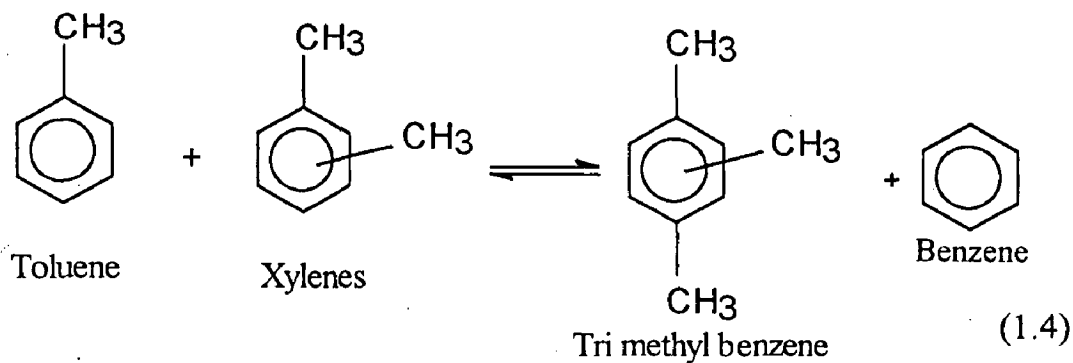
Apart from these side reactions, some amount of xylenes also also converted to ethyl benzene as per the reaction given below.

Xylenes   Ethylbenzene   (1.6)
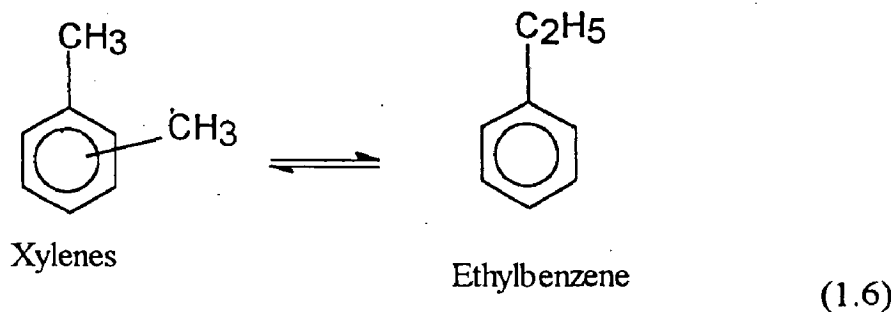
1.3 ADVANTAGE OF DISPROPORTIONATION REACTION

Converting toluene to more useful products such as benzene and xylenes (particularly p-xylene) is accomplished by mainly two methods : alkylation of toluene and disproportionation of toluene.

The advantages of the later method over the former are

i) alkylation does not produce benzene which is a very important chemical intermediate.

ii) an additional reagent, methanol, is required in alkylation.

iii) alkylation produces methane gas which is not of immediate use in a petrochemical process. This leads to loss of hydrocarbons.

iv) the proportion of liquid products in disproportionation is much higher in comparison to alkylation.

1.4 LITERATURE REVIEW

The disproportionation of toluene was first reported in 1884 by Anschutz, who refluxed toluene at atmospheric pressure with aluminum chloride as catalyst. Since that time many studies were carried out over different catalysts. The literature that are available, since 1979, are presented below in chronological order.

Aneke et al (1979)[3] have reported toluene disproportionation over HY/β-AlF₃/Cu catalyst. The catalyst performance measurements were carried out in a standard continuous flow apparatus at atmospheric pressure. They found that more and more active sites are eliminated as the reaction proceeds (progressively lower conversion) and that the remaining sites are the ones that are active for toluene disproportionation. They found that selectivity of p-xylene increases appreciably with stream time.

The best activation temp for catalyst appears to be 500°C. Above this temperature the performance of the catalyst clearly deteriorates. As the

temperature of activation increases above 500°C, it results in dehydration of the catalyst and the formation of inactive and possibly Lewis acid sites. Catalyst used was 72 wt% HY, 18 wt% β AlF$_3$, and 10 wt% copper. The performance (selectivity) of the above catalysts was better than HY zeolite, but conversion was low.

Bhavikatti et al (1981) [4] used 0.2-wt% nickle-loaded aluminum-deficient mordenite (SAR 23). They found that as temperature increases from 350-450°C selectivity of p-xylene was very high (>90%). Toluene conversion was found to increase with time factor, W/F (g-cat.hr/gmol toluene). The activity of catalyst does not decrease till one hr. of operation but after one hr the activity decreases exponentially ($\theta = \theta_o e^{-mt}$) from 40 to 20% in seven hrs.

Here, θ_o is initial activity at time t = 0,

t is time-on-stream expressed in minutes and

$m \approx 3 \times 10^{-3}$

To maintain the activity, the system was flushed with nitrogen and the catalyst was regenerated in oxygen between 400 and 500°C. In all the test runs the hydrogen/toluene molar ratio was kept constant at 5.

Kaeading et al. (1981) [5] reported 70-90% para isomer selectivity over ZSM-5 zeolites modified with phosphorus and boron compounds. The compounds used for modification were trimethylphosphite and boric acid respectively. For 3.5 wt% phosphorous, para selectivity was 64% and conversion was 4.4% at 700° compared to 67% para selectivity and 3% conversion at 550°C. The weight hourly space velocity was maintained at 2.1.

With boron modified ZSM-5 the toluene conversion increased with temperature (to 24.5% at 650°C) and declined after 650°C. The concentration of para isomer in xylene product increased gradually until the highest temperature was reached (700°C), where a substantial increase of 73% para xylene was

7

observed. After the calcination at 700°C the para selectivity increased to 87.2% from 73% at this temperature and conversion decreased to 8.4% from 12.7%.

For magnesium oxide modified ZSM-5 containing (Mg = 11 wt%) p-xylene in xylene product was found to be 90% at 5% conversion level and 80% at 10% conversion. Conversion at 550°C was noticed to be maximum for magnesium oxide modified ZSM-5. The decrease in conversion and increase in p-xylene selectivity was said to be due to some coking.

Disproportionation reaction was also performed without modification of HZSM-5. In this case para xylene selectivity was found 24.7% and 24.1%. Corresponding to toluene conversion varying conversions of 8.2 and 5.16% at temperature 450°C and 600°C respectively. At the lowest temperature the mole ratio of benzene/xylenes was 1. The B/X ratio was observed to increase with temperature to a value of 1.77 at 600°C. This was due primarily to a demethylation reaction of dimethyl benzene, indicated by corresponding increase in the yield of methane. Only a small amount of transalkylation occurred to give C_9 aromatic hydrocarbons. A near equilibrium mixture of xylene isomers was obtained.

The HZSM-5 modified with Mg, B and P gives high selectivity of p-xylene because the zeolite pores were reduced in size so that the para isomer, with the smallest minimum dimension, was able to diffuse out of the pores in comparison to ortho and meta isomers which could not.

Beltrame et al. (1985) [6] studied toluene disproportionation catalysed by various zeolites. Activity, selectivity and stability of the catalysts were tested at temperatures upto 500°C, but mostly in the range 350°-400°C. The activity was obtained in the following order.

HZSM-11<HZSM-5 (LA)<HY<HZSM-5(HA).

Variation in selectivity of p-xylene was found in the following order.

HZSM-5 (LA)>HZSM-5 (HA)>HZSM-11 > HY.

Selectivity of p-xylene in xylene product was highest for HZSM-5 (LA) up to 60% while on other catalysts the selectivity was approximately in the range 24-28%.

The stability of zeolites was found in the following order.

HY<HZSM-11<HZSM-5 (HA)<HZSM-5 (LA).

8

It was found that the stability of HZSM-5 (LA) does not change appreciably with temperature and time of operation.

Beltrame et al (1987) [7] performed toluene disproportionation over HZSM-5 crystals of different size by poisoning the external surface by 4-methyl-quinoline. The results indicate that toluene disproportionation reaction occurs mainly in the zeolite pores, with marked para shape selectivity. It is usually followed (in the absence of surface poison) by fast isomerization of the preferred primary product at the pore mouth. There is evidence that 4-methyl-quinoline, as a poison is not specific to the external surface, slightly affecting the zeolite pores. The rate of toluene disproportionation over HZSM-5 at 300°C was compared with a recent experimental evaluation of the rate of sorption, diffusion for benzene, toluene and p-xylene within the zeolite channels in the same temperature range. It reveals that the chemical reaction is approx. 104 times slower than sorption diffusion. They concluded that

- at 300°C, there is no diffusive hindrance to toluene disproportionation in the channels of HZSM-5 with p-xylene as the main product.

- since the products, obtained over different samples of HZSM-5, in any case contained xylene isomers in the equilibrium ratio, there is evidence of a fast isomerization after the disproportionation.

- since catalytic activity depends strongly on their surface acidity, but does not seem correlated with their external surface area, the rate controlling step is in any case is toluene disproportionation. While the external surface is always sufficient to catalyse the fast isomerization.

Uguina et al (1993) [8] studied toluene disproportionation over modified and unmodified ZSM-5 zeolites. It has been found that xylene dealkylation is the major secondary reaction, where as toluene dealkylation can be considered negligible. The catalyst used in this section was a ZSM-5 zeolite modified by impregnation with silica and magnesium compound (Si and Mg/ZSM-5). The silicon modification was carried out using a dimethyl silicon polymer as precursor. Due to its large molecular size the silicon polymer did not penetrate into the zeolite channel systems and got deposited on the external surface of the crystals thereby deactivating the non-selective sites. On the other hand, the size and nature of the precursor used in the magnesium

modification allow this agent to be located inside the zeolite pore, leading to an enhancement of diffusional limitations. They reported 90% para xylene selectivity and 20% conversion at $510^{\circ}C$. The benzene/xylene molar ratio was 1.5 at 400 g.h/mole-space time. The p-xylene selectivity decreased with space-time. The conversion increased from zero to 20% as space-time increased from zero to 400 (gm.h/mole).

Das et al (1994) [9] studied toluene disproportionation over ZSM-5 modified by deposition of SiO_2 using 6.5% Si $(OC_2H_5)_4$ solution in 50:50 toluene and methanol. The effect of reaction parameters such as temperature and weight hourly space velocity (WHSV) on para selectivity was considered. They found that the silica deposited catalyst (16 wt%) exhibit appreciable toluene conversion of 23% with 89% of p-xylene selectivity. With increase in reaction temperature from 723 to 803 K the toluene conversion and benzene formation increases, while xylene formation is decreased. p-Xylene selectivity was affected little up to 773 K. Above this temperature, it was lowered due to the dealkylation reaction. At higher WHSV of 4.35 h^{-1}, toluene conversion decreased to 9%.

CATALYST SELECTION, PREPARATION AND CHARACTERISATION

2.1 SELECTION OF CATALYST

The types of catalysts employed for the disproportionation of toluene can be grouped into four categories.

(a)   Friedel-Crafts Catalysts

(b)   Silica-alumina Catalysts

(c)   Zeolite type Catalysts

(d)   Composite Catalysts

In general zeolites have been found to be superior catalysts as compared to amorphous solid acids. Apart from being less active amorphous solid acid catalysts show a low selectivity for disproportionation as a result of side reaction such as hydrodealkylation. Benesi et al [10] used toluene disproportionation reaction as one of the model reactions for the comparison of catalytic activities of mordenite and faujasite zeolites and concluded that H-mordenite showed higher activity compared to H-Y zeolite.

Bhavikatti et al [4] observed that toluene can be converted on H-mordenite with high yield of benzene and xylenes, however, the activity of catalyst fall after one hour of operation exponentially. Many of the researchers have worked on HZSM-5 zeolite catalyst. They found better results than H-mordenite zeolite catalyst. The performance of disproportionation reaction towards p-xylene production on HZSM-5 zeolite was better because its pore size is slightly greater than p-xylene causing p-xylene to diffuse rapidly while m-xylene and o-xylene are restricted due to their larger size and subsequently get isomerised to p-xylene. It was also noticed that the activity of HZSM-5 zeolites is maintained for longer time of operation.
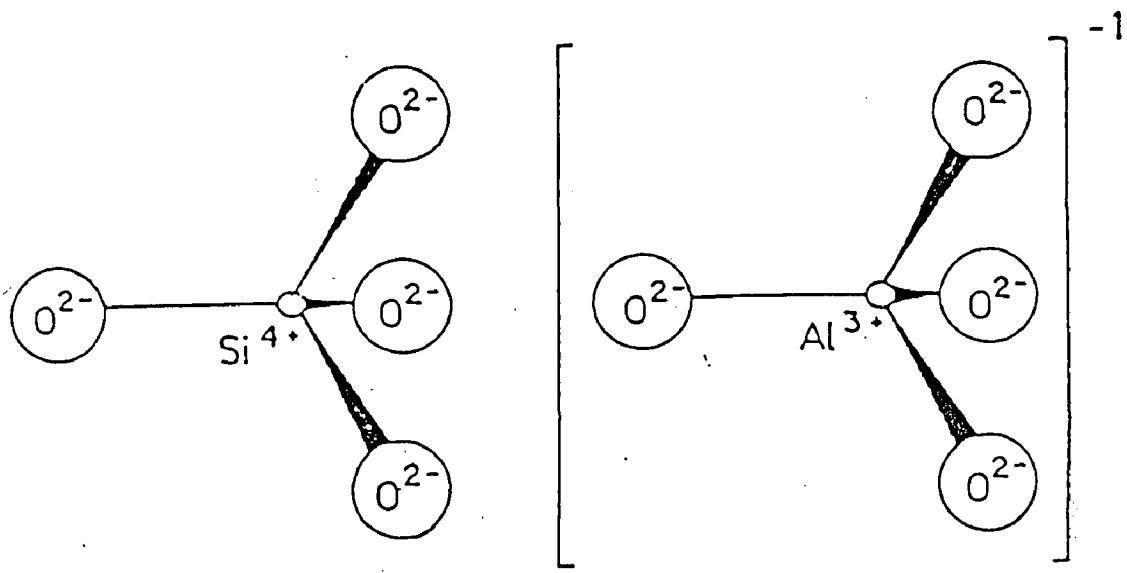
Silica Tetrahedron   Alumina Tetrahedron

Fig. 2.1   PRIMARY BUILDING BLOCKS OF ZEOLITE

It was reported that the activity and selectivity of HZSM-5 catalysts further improved. HZSM-5 when it was modified by deposition of various metals, such as, Si, B, Mg and P.

In the present work, therefore, the activities of HZSM-5 in particular alongwith some other zeolite types were tested under variety of operating conditions.

2.2 ZEOLITES AS CATALYSTS

2.2.1 X and Y zeolite [11]

Structurally, X zeolite, Y zeolite and natural faujasite are similar. However, they differ in their characteristic silica-alumina ratios and consequently differ in their crystallattic parameter. They also differ somewhat in such properties as cation composition, cation location, cation exchangeability, thermal stability and adsorptive and catalytic character. The typial unit-cell formula is Na_j $[(AlO_2)_j(SiO_2)_{192-j}]$. $z.H_2O$ where z is about 260. The value of j is between 48 and 76 (typically 57) for the Y zeolite and between 77 and 96 (typically 86) for the X zeolite.

In the X and Y zeolites and faujasite, the silica and alumina tetrahedra are joined together to form a cuboctahedron as shown in Fig. 2.2. This unit containing 24 silica and alumina tetrahedra is called a sodalite unit or a truncated octahedron, which is the secondary building block of a number of zeolites like X zeolite, Y zeolite and faujasite etc.

The unit cell of X zeolite, Y zeolite and faujasite is cubic with a unit-cell dimension of 25Å, and it contains 192 silica and alumina tetrahedra. The unit cell dimension varies with the Si/Al ratio. Each sodalite unit in the structure is connected to four other sodalite units by six bridge oxygen ions connecting the hexagonal faces of two units (Fig. 2.3). The oxygen-bridging unit is referred to as a hexagonal prism, and it may be considered another secondary unit. This structure results in a supercage (sorption cavity) surrounded by 10 sodalite units, which is sufficiently large with a diameter or 12 Å. The opening into this large
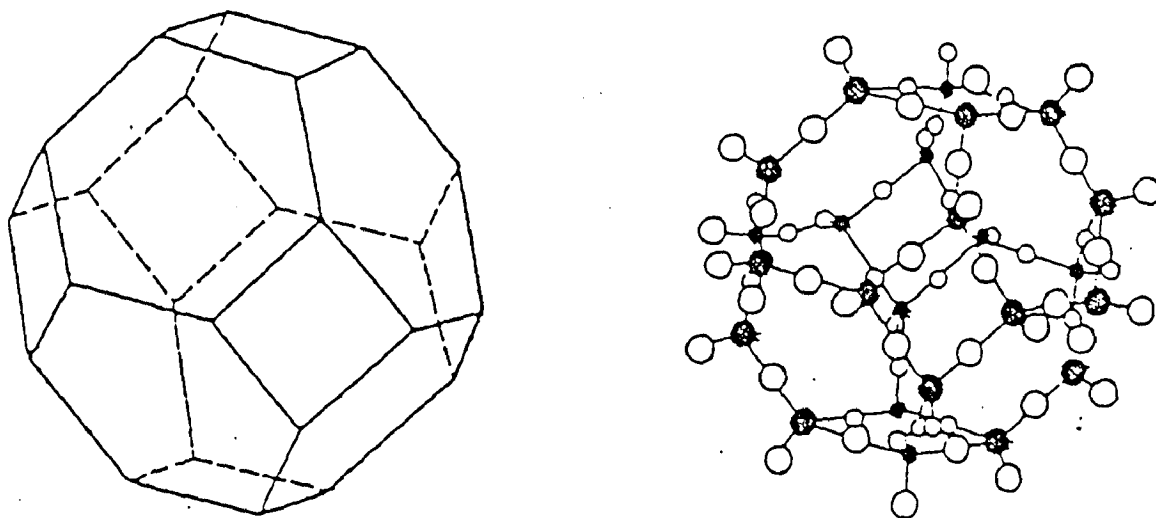
O Oxygen

● Aluminum or silicon

Fig. 2.2   SODALITE CAGE STRUCTURE. A FORMAL REPRESENTATION OF A TRUNCATED
OCTAHEDRON IS ON THE LEFT, AND INDIVIDUAL ATOMS ARE INDICATED ON THE
RIGHT.
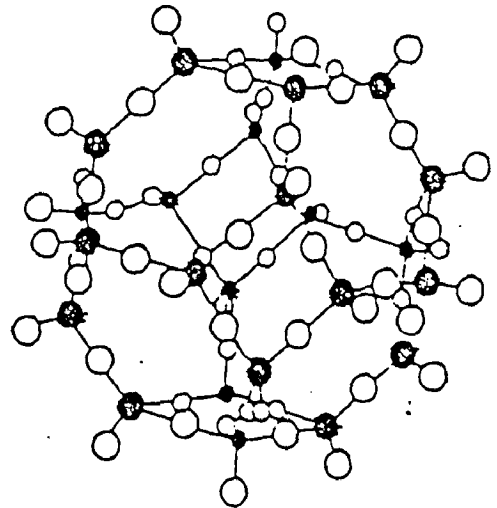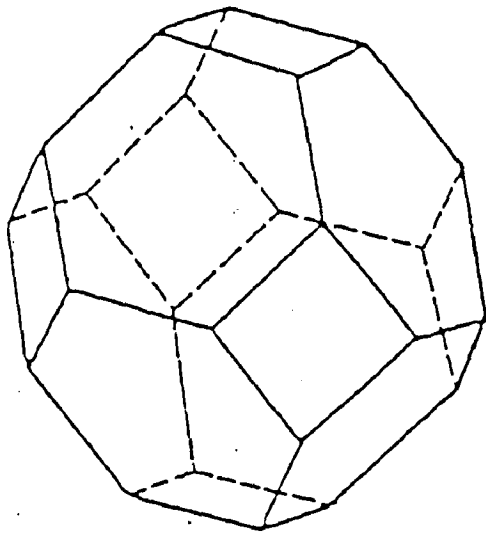
O Oxygen

● Aluminum or silicon

Fig. 2.2   SODALITE CAGE STRUCTURE. A FORMAL REPRESENTATION OF A TRUNCATED
OCTAHEDRON IS ON THE LEFT, AND INDIVIDUAL ATOMS ARE INDICATED ON THE
RIGHT.

cavity is bound by 6 sodalite units, resulting in a 12-membered oxygen ring with a 7.4 Å free diameter. Each cavity is connected to four other cavities, which in turn are themselves connected to three additional cavities to form a highly porous framework structure. The supercage volume represents 45 percent of the unit cell volume. The main pore structure is three dimensional and large enough to admit large molecules, such as, naphthalene and fluorinated hydrocarbons. It is within this pore structure that the locus of catalytic activitiy resides for many reactions. A secondary pore structure involving the sodalite units exists, but its apertures are too small to admit most molecules of interest in catalysis.

The zeolite structure carries an effective charge per unit cell equivalent to the number of alumina tetrahedra per unit cell. The charges are neutralized by the sodium cations originally present in the structure. In the X zeolite containing sodium ions (referred as Na-X or 13X molecular sieve) there are, depending on Si/Al ratio, about 85 sodium cations per unit cell. These cations are readily exchangeable with other ions having charges of +1, +2 or +3. Just as the framework structure is precisely defined, the positions of the cations within this structure are also precisely defined. The several cation sites, which exist, are filled to different degrees by the cations present. These cations, even in the dehydrated form of the zeolite, are frequently exposed, essentially unshielded, on the surface and produce their own microchemistry within the zeolite pore, depending upon their charge, electronic structure and surroundings.

Essentially complete removal of Na^+ is best obtained by exchanging the zeolite several times with multivalent ions then calcining at 350°C and exchanging again. A hydrogen form of the zeolites can be prepared by exchange with weak acid or by exchanging with NH_4^+ and decomposing the ammonium ions into NH_3 (g) and H^+, which maintain the charge balance in the structure. NH_4^+ exchange technique is considered to be better than that of the acid exchange as high degree exchange with acid typically results in structural collapse of the zeolite.
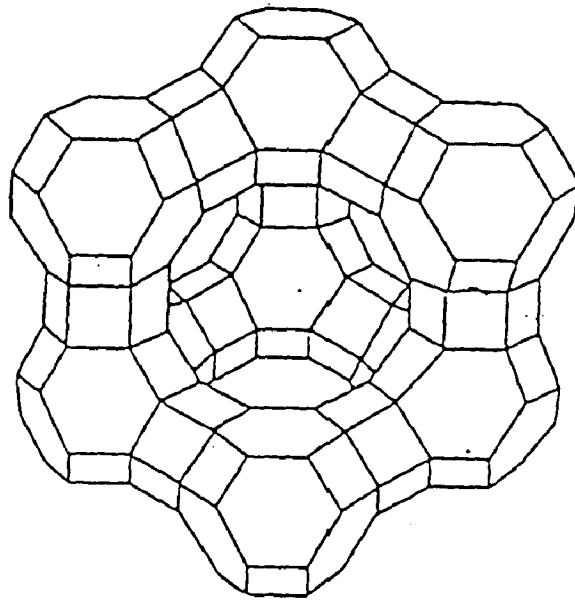
Fig. 2.3   PERSECTIVE VIEW OF THE FAUJASITE STRUCTURE. THE Si OR Al IONS ARE AT THE CORNERS AND OXYGEN NEAR THE EDGE. THE SUPER CAGE IS AT THE CENTER.

2.2.2 Morderite [11]

The fundamental building of block of all zeolites is a tetrahedron of four oxygen anions surrounding by smaller silicon or aluminum ions (see Fig. 2.1). These tetrahedron are arranged in such a way that each of the four oxygen anions is shared in turn with another silica or alumina tetrahedron.

The mordenite crystal structure consists of five-membered rings with each Si or Al tetrahedron associated with at least one such ring. The rings are interconnected to form chains and the chains are cross-linked to identical chains to form the crystal structure. The structure of mordenite is having relatively high thermal and acid stability. It has an unit-cell represented by the formula Na_8 $(AlO_2)_8$ $(SiO_2)_{40}$, $24H_2O$ which show the silica-alumina ratio of 10.

The mordenite pore structure consists of elliptical, non-interconnected channels as shown in Figs. 2.4 and 2.5. These channels or tubes have approximately elliptical openings with Major and minor diameters of 7.0 and 6.7 Å respectively [12]. This structure is unique amongst the zeolites, since the adsorption tubes do not intersect one another. For this reason the pore structure is frequently referred to as two-dimensional. The major channels are circumscribed by 12-membered oxygen rings. There are side pockets opening from the main channel along with b-direction which have a free diameter of 3.9 Å. These side pockets however, do not interconnect the main channels, because half way between the two main channels, the pore is constricted by the distorted eight-membered ring of 2.8 Å free diameter. In the sodium form of the zeolite, this pore is further blocked by a sodium cation located in the centre of each distorted ring fig. (2.4). Consequently, each main channel is isolated from all other main channels for transport of even the smallest molecules. Even in the hydrogen form, the main channels of mordenite are essentially isolated forms each other for transport of all molecules except possibly He and H_2 because of the small free diameter of the distorted eight-membered oxygen rings of the side pocket.
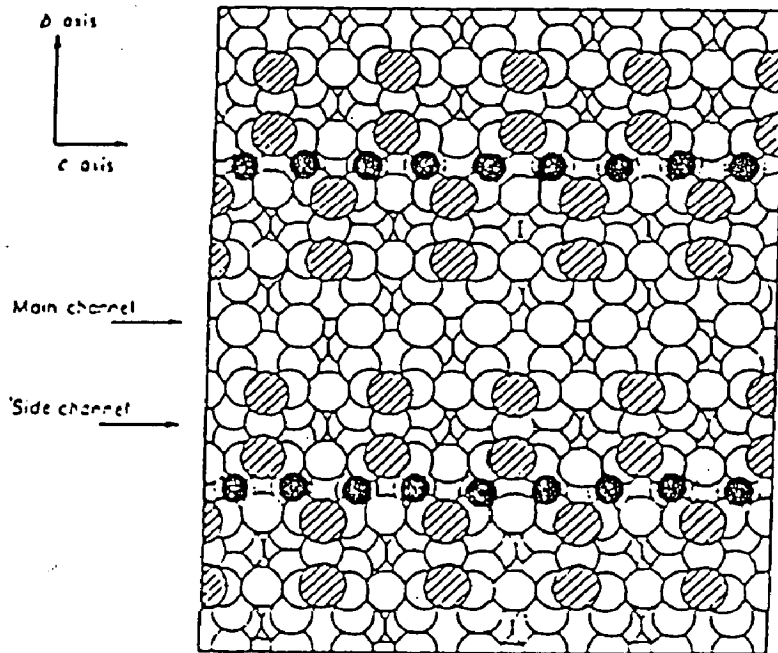
Fig. 2.4   CROSS SECTION OF A WIDE CHANNEL IN MODENITE :
○ O-atoms ◎ O-atoms IN PLANE OF PAPER.
Na ions ● .   Al AND Si ARE NOT SHOWN

Main sorption channel

Side cavity

a axis

b axis

18.13 Å

c

7.52 Å

c axis

b

20.49 Å
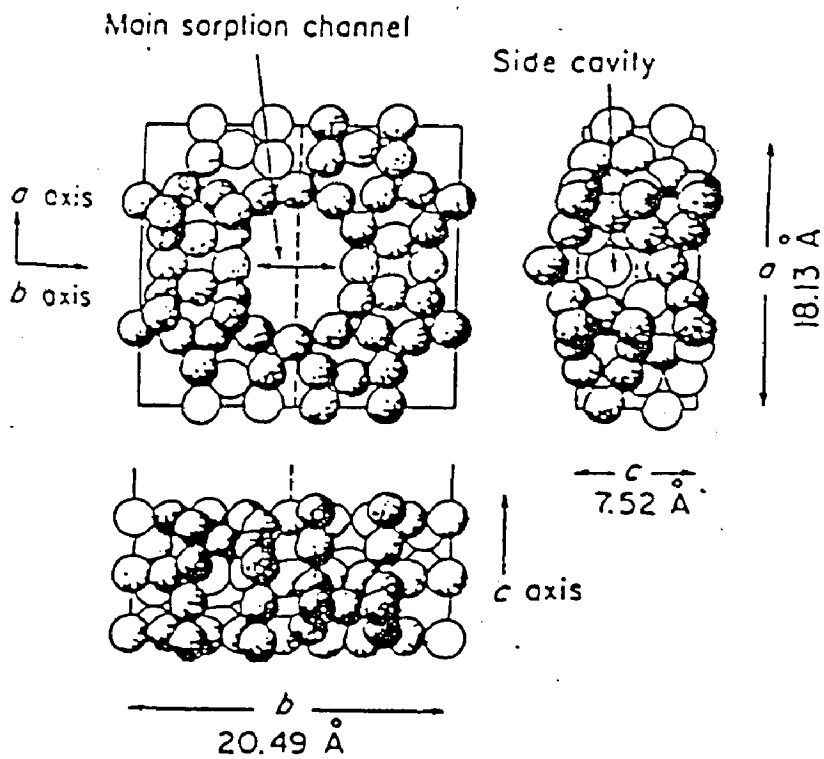
Fig. 2.5   CRYSTAL STRUCTURE OF MORDENITE. ONLY O-ATOMS ARE SHOWN, SHADING
INDICATES THE VERTICAL POSITION OF O-atoms.

In sodium mordenite, diffusion is hindered by sodium cations in the main channels, but in hydrogen mordenite this cation hindrance i.e is significantly reduced. The locus of catalytic activity is within this pore structure.

Because of the narrowness of the pores, the mordenite surface can exert stronger forces on the sorbed reactants than are expected with other catalysts. This characteristic appears to be important in determining some of the unique catalytic properties of hydrogen mordenite.

2.2.3 ZSM-5 [13]

HZSM-5 is a representative member of a new class of high silica zeolites having considerable significance as catalyst materials (Olson et al, 1981) . Examples of their use include conversion of methanol to gasoline, dewaxing of distillates, interconversion of aromatic compounds, p-xylene shape selective toluene disproportionation reaction etc.

ZSM-5 has an effective three-dimensional channel defined by 10 membered ring (See Fig. 2.6). Straight channel parallel to [010] have openings defined by 10 rings of size 5.4 x5.6 Å based on oxygen ratio of 1.35 Å. Intersecting this channel at right angles is a channel along [100] with opening 5.1x5.5 Å. Diffusion in the [001] direction can readily take place between the overlapping channels parallel to [100] and [010].

ZSM-5 zeolite contains 10 membered rings of tetrahedra. Among many other trial structures, five models were developed from heulandite units joined together through an edge. Atom co-ordinates obtained from these models were refined with the distance least square model [DLS] , which adjust the co-ordinates to fit prescribed T-O bond distances and angles within the constraints imposed by the space groups and the cell dimensions. The numbering of the framework atoms in the symmetric unit is shown in fig. 2.7. The resultant T-O distances are presented in Table 2.1.

Y Zeolite 12 Ring

ZSM-5 10 Ring
(Straight Channel)

Sinusoidal Channel
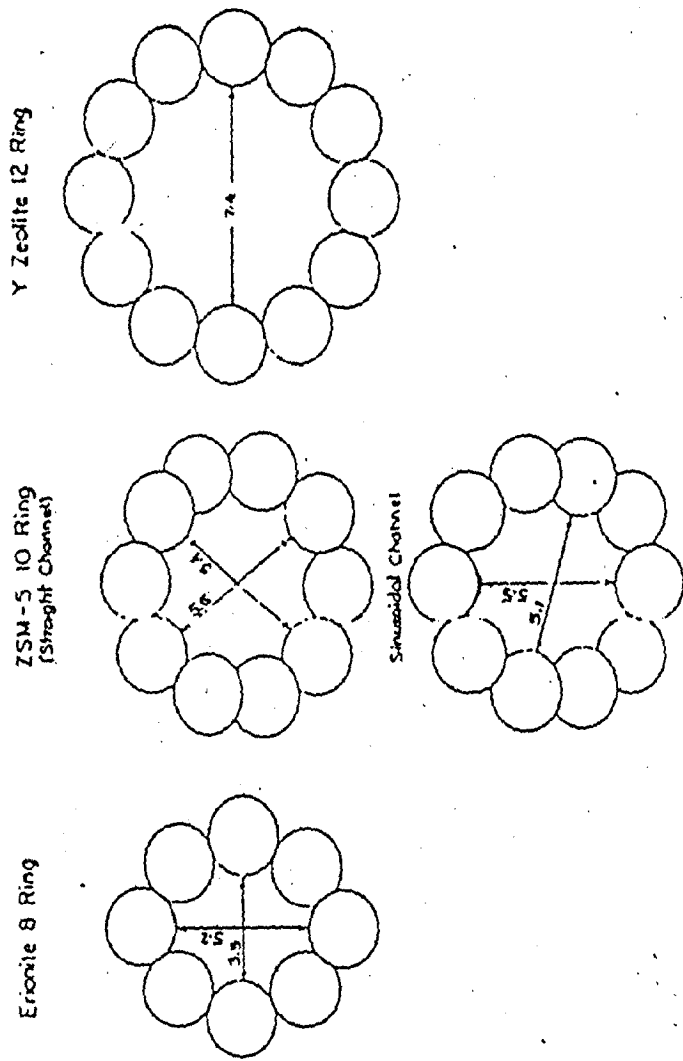
Erionite 8 Ring

Fig. 2.6   COMPARISON OF THE LIMITING PORTS OF ERIONITE, ZSM-5, AND FAUJACITE.

2.1.3 Structure related Properties of ZSM-5

(a) **Sorption Properties** : With a channel size intermediate between small pore (8-ring) and large pore 12 ring (Fig. 2.6), ZSM-5 possesses distinct sorption and diffusion properties. ZSM-5 sorbs molecules between the former and latter zeolites. The sorption isotherm of ZSM-5 for various hydrocarbons is shown in (Fig. 2.8).

(b) **Influence of channel dimension on diffusion**

The channel dimension of ZSM-5 (5.4 x 5.6Å for straight channel) is similar to the diameter of benzene kinetic benzene 5.8 Å and p-xylene 6.3 Å. Thus while benzene and p-xylene has high mobility in ZSM-5, diffusion of meta and ortho di-substituted distributed and poly-substituted aromatics is substantially slower (Table 2.2). For example, the diffusion coefficient for p-xylene is ~ 3 orders or magnitude greater than diffusion coefficient of o-xylene.

(c) **Influence of Structure on Catalytic Properties**

Numerous reactions catalysed by ZSM-5 reflect the influence of its structure, e.g. having product selectivities and/or aging rates distinctly different from those of large-pore zeolites such as mordenite and faujasite type zeolites. In some of these reactions, steric factors are primarily involved, whereas, in others diffusion effect play a significant role.

The steric effects of the ZSM-5 structure are well illustrated by the product distribution in the methanol to gasoline process. In this process the reaction proceeds from methanol to olefins to aromatics. When catalysed by ZSM-5, less than 1% of the product is heavier than C_{10} (tetramethylbenzne) whereas more than 70% of the product is heavier than C_{10} with a large-pore, mordenite catalyst. The C_{10} cut of ZSM-5 results from steric restrictions which limit formation of heaviour (larger) products. Lower diffusivity of the heavier products may also be a factor.

It has been found that the higher para selectivity in toluene disproportionation is directly related to low diffusivity of ortho and meta

TABLE 2.1 T-O DISTANCES (A) FOR ZSM-5

T1-O1	1.59 (3)	T5-O4	1.57 (4)	T9-O8	1.61 (3)
T1-O15	1.53 (3)	T5-O5	1.61 (3)	T9-O9	1.58 (4)
T1-O16	1.67 (3)	T5-O14	1.61 (5)	T9-O18	1.60 (2)
T1-O21	1.62 (3)	T5-O21	1.55 (3)	T9-O25	1.59 (2)
	av 1.60 (2)		av 1.58 (2)		av 1.60 (1)
T2-O1	1.66 (3)	T6-O5	1.59 (2)	T10-O9	1.62 (4)
T2-O2	1.61 (2)	T6-O6	1.56 (3)	T10-O10	1.50 (4)
T2-O6	1.60 (3)	T6-O18	1.63 (3)	T10-O15	1.60 (3)
T2-O13	1.60 (4)	T6-O19	1.53 (3)	T10-O26	1.61 (2)
	av 1.62 (2)		av 1.58 (1)		av 1.58 (2)
T3-O2	1.57 (2)	T7-O7	1.59 (3)	T11-O10	1.65 (4)
T3-O3	1.60 (4)	T7-O17	1.57 (4)	T11-O11	1.53 (4)
T3-O19	1.58 (3)	T7-O22	1.60 (3)	T11-O14	1.56 (5)
T3-O20	1.61 (4)	T7-O23	1.64 (2)	T11-O22	1.57 (3)
	av 1.59 (2)		av 1.60 (2)		av 1.58 (2)
T4-O3	1.56 (4)	T8-C7	1.58 (4)	T12-O11	1.64 (4)
T4-O4	1.60 (3)	T8-O8	1.63 (3)	T12-O12	1.66 (3)
T4-O16	1.65 (4)	T8-O12	1.52 (3)	T12-O20	1.62 (3)
T4-O17	1.52 (3)	T8-O13	1.53 (4)	T12-O24	1.59 (1)
	av 1.58 (2)		av 1.56 (2)		av 1.63 (2)

Average T-O = 1.59 (1)

TABLE 2.2 DIFFUSIVITY OF AROMATICS IN ZSM-5 (315 °C)

	size, Å	diff, cm²/s
benzene	6.3	$\sim 10^{-7}$ (est)
p-xylene	6.3	$\sim 10^{-7}$
o-xylene	6.9	$\sim 10^{-10}$
1,3,5-trimethylbenzene	7.8	$\sim 10^{-12}$
pentamethylbenzene	~ 7.8	$\sim 10^{-12}$ (est)
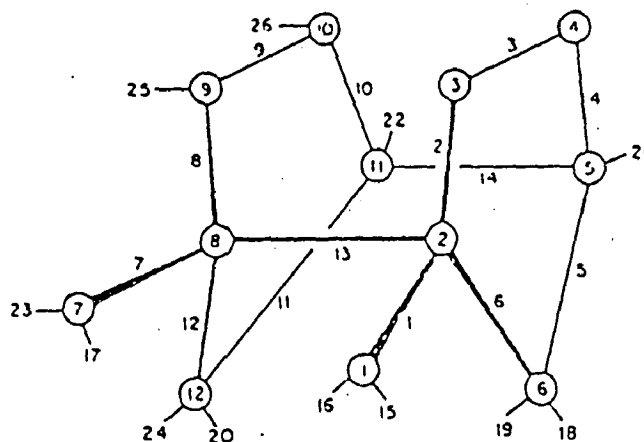
Fig 2.7   NUMBERING SCHEME OF THE FRAMEWORK ATOMS

xylene relative to p-xylene and para selectivity may be increased by increasing crystal size or by chemical modification which results in reduced diffusivity. Steric factors affecting the primary intra crystalline isomer distribution may also be important.

(d)   Catalyst Aging Properties

ZSM-5 based catalysts have low coke formation and aging rates relative to large-pore zeolite catalysts. If a zeolite contains cavities or cage with dimensions larger than the ports leading to the crystal exterior, large intracrystalline products, "coke", may form which can not escape through the ports. Reverse molecular size selectivity results in aging via pore filling and site blockage. Thus, a zeolite's intrinsic aging rate would be related to how closely its cavity size approaches its port dimensions.

2.2.4   Zeolite Surface Chemistry

The surface of the zeolite structure can be represented in a simplified way, which for the sodium form is
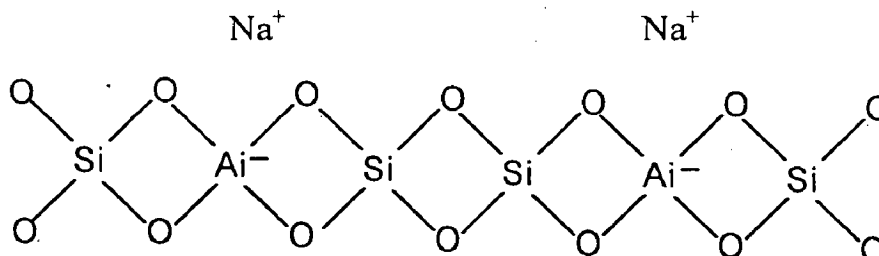
The formation of the hydrozen zeolite by ion exchange with an ammonium salt to replace the Na^+ followed by heating to decompose the NH_4^+ into NH_3 and H^+ is shown schematically below.

23
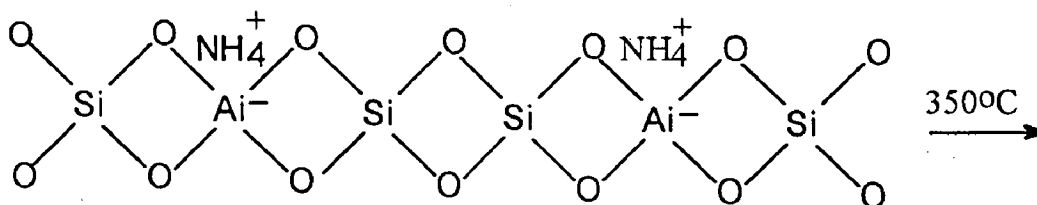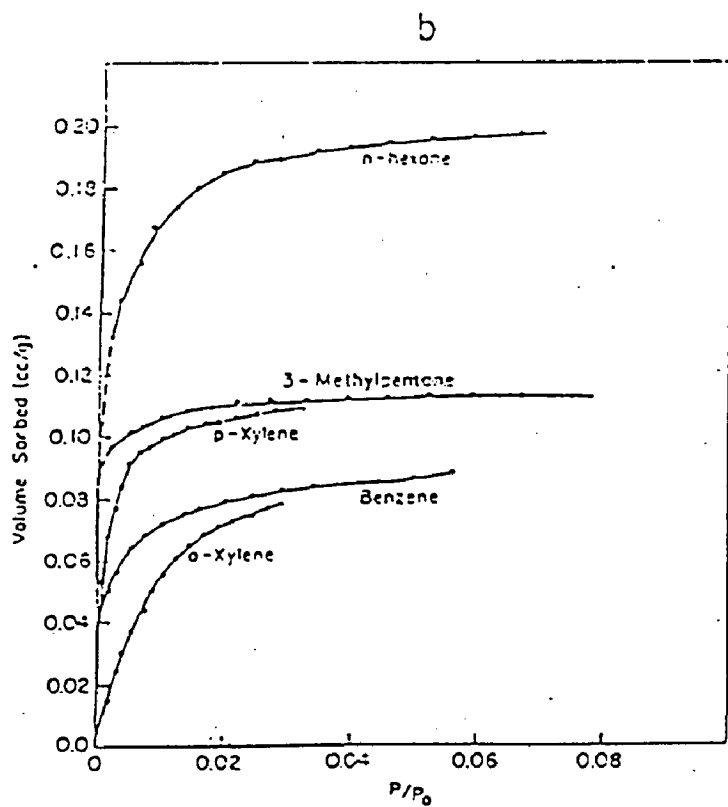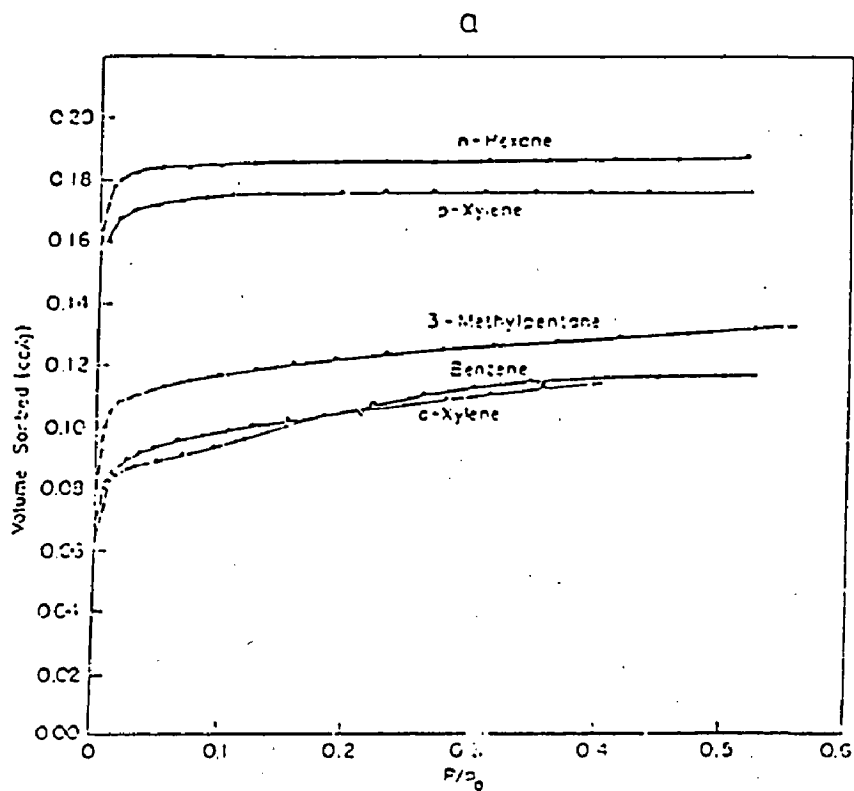
Fig. 2.8   SORPTION ISOTHERMS FOR VARIOUS HYDROCARBONS ON HZSM-5 (SiO_2/Al_2O_3 = 290): (a) at 30 °C; (b) at 90 °C

$$H^+ \quad\quad H^+$$

O—Si—O—Ai⁻—O—Si—Ai⁻—Si—O   + 2NH₃
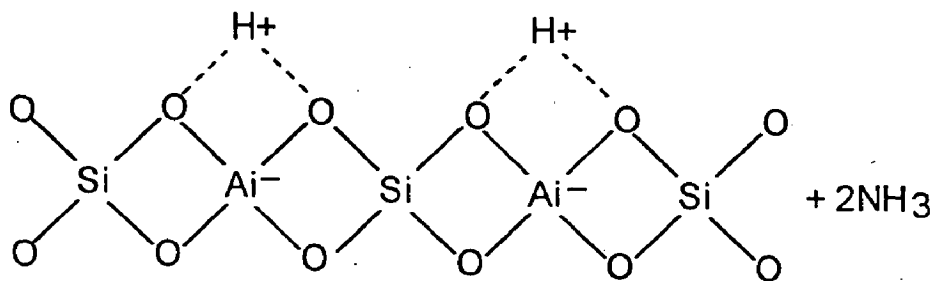
The protons probably bond immediately with one of the lattice oxygens to give OH groups as shown below. These sites represent potential Bronsted acid sites.

$$H^+ \quad\quad H^+$$

O—Si—Ai⁻—O—Si—Ai⁻—Si—O
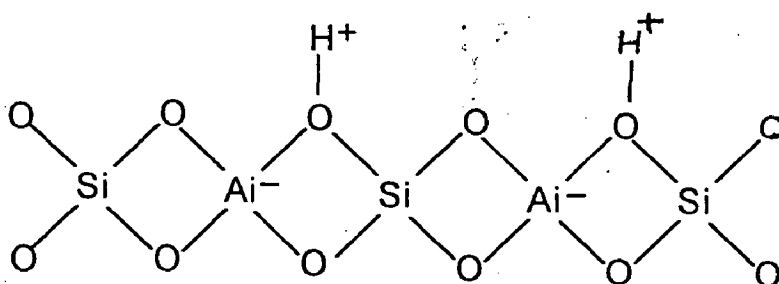
Upon further heating to temperature above 450⁰C, dehydroxylation of the above structure occurs to give the following.

O—Si—Ai⁻—O—Si—Si—Ai—O   +   Si⁺—O
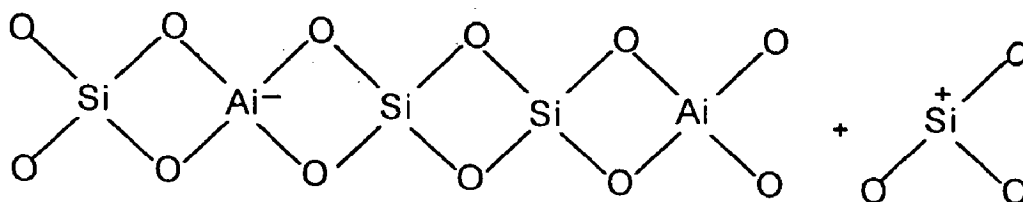
These structural considerations suggest that two Bonsted acid sites are lost for every Lewis acid site generated. The dehydroxylation can be reversed if water is added back. Starting as the highest temperature of dehydroxylation and coolign is done in presence of water vapor [14].

These Broncted acid sites are found to be main active catalytic sites of a zealites. cation exchanged zeolites have broader distributions of acid strengths than H-zealites, the more strongly acidic sites appearing at higher degree if exchange. The braod distribution of acid srengths may be indicative of cations in different sites interact intracting with OH-group involving different oxygens. The

exchanged action could increase the aciditonof the OH-groups by withdrawing electrons from the OH bonds [15].

2.3 PREPARATION OF CATALYSTS

In the present work mordenite, ZSM-5 and Y-zeolites having different silica alumina ratio were used to test the disproportionation reaction. The mordenite, ZSM-5 and Y zeolites in form of Na mordenite, NaZSM-5 and NaY which were less active, were first converted to H-mordenite, HZSM-5 and HY, which were further subjected to ion exchange with active rare earth or transition metal cations.

For converting Na-zeolites into H-zeolited, $0.5M-NH_4NO_3$ was taken in a beaker and mixed with zeolites under constant stirring. 500 ml of 0.5 M NH_4NO_3 and added to 10 gm of zeolite powder. The mixture was subjected to ion-exchange for 16-18 hrs at temperature around 90°C under total reflux conditions. After ion exchange, the solution was filtered and the NH_4^+ exchanged zeolites was dried at 110°C for 12 hrs. The dried NH_4 zeolite was calcined at 570°C for 5 hrs where the NH4-zeolites got transformed to H-zeolite. The above step was repeated three times for greater exchange to H-zeolite.

The H-zeolites were subsequently modified by rare earth, transition metal cations. the overall procedure for preparation of catalyst is given below :

(a)   Ion Exchange

Calculated amount of ion exchangeable metal salt was dissolved in distilled water. The solution was taken for ion exchange in a round bottomed flask and heated alongwith the H-form of zeolite under total reflux condition for a period of 16-18 hrs at 90°C.

The ion exchanged zeolite was filtered and the catalyst obtained at the top of the filter paper was dried at 110°C for 12 hrs. The filtrate was used for atomic absorption spectrophotometric analysis by which degree of exchange of cation in zeolite was determined.

The dried catalyst was calcined at temperature of 400-580°C for 5 h. The structure of zeolites may slightly change due to dehydroxylation, which may vary with temperature.

After calcination the catalyst was pelletized at 10-15 tonns pressure in a hydraulic press pelletizing machine. The binders may also be used to facilitate the pelletization.

The peletized catalyst was crushed to desired size range for toluene disproportionation reaction tests. Size of the catalyst particles may also be a parameter for reaction.

Table 2.3 summary of Catalyst Prepared

S. No.	Catalyst	Ion exchange temp. & duration	Calcination time & duration
1.	1.4613 wt%CuHZSM-5(SAR-32)	98°C, 18 h	570°C, 5 h
2.	0.589 wt%NiHZSM-5(SAR-32)	98°C, 18 h	570°C, 5 h
3.	1.248wt%PbHZSM-5(SAR-32)	98°C, 18 h	570°C, 5 h
4.	3.952wt%PbHY (SAR-3)	98°C, 18 h	570°C, 5 h
5.	2.973 wt%LaHZSM-5(SAR-32)	98°C, 18 h	570°C, 5 h
6.	3.80wt%ThHZSM-5(SAR-32)	98°C, 18 h	570°C, 5 h
7.	3.71wt%CeHZSM-5(SAR-32)	98°C, 18 h	570°C, 5 h
8.	1.756wt%Cr1.923wt%ThHZSM-5(SAR-32)	98°C, 18 h	570°C, 5 h
9.	HZSM-5 (SAR-19)	--	400°C, 5 h
10.	3.34wt%CrHZSM-5 (SAR-19)	98°C, 18 h	570°C, 5 h
11.	2.71wt%CrHZSM-5 (SAR-40)	98°C, 18 h	570°C, 5 h
12.	2.33wt%SrHZSM-5 (SAR-32)	98°C, 18 h	570°C, 5 h
13.	Hmordenite (SAR-13)	98°C, 18 h	570°C, 5 h

2.4 CHARACTERISATION OF THE PREPARED CATALYSTS

Catalytic properties of a catalyst are a function of its characteristics. The toluene disproportionation reaction depends on the following characteristics of the catalysts.

1. Acidity and acid sites distribution
2. Structure and crystallinity
3. Composition (SiO_2/Al_2O_3, exchanged/deposited metals)

2.4.1 Acidity and Acid Sites

Acidity and acid sites may be determined by FTIR, Microcalorimetric measurement, TPD (Temperature Programmed Desorption) of NH_3. In the present work FTIR spectrometer was used to study the acid sites and relative acidity.

2.4.1.1 FTIR Spectroscopy [16,17,18]

By FTIR Spectroscopy the various functional groups present in catalyst and their intensity can be determined and by studying the spectra of the samples the relative acidity may be determined.

For analysing the sample (solid) by FTIR the prism material an alkali halide KBr (300 mg) and solid sample (1 mg) were mixed, finely ground and pelletized at a pressure of 15 tonnes. The instrument was operated, first by passing the electromagnetic radiation through the air. Now sample was kept in the chamber and electromagnetic rays (impaired radiation having wavelength between 0.8 and 1000 mm) passed through the sample. The sample contains various bands which absorb the radiation (energy) and remaining radiation is transmitted through the thermocouple detector. The detector is connected to data acquisition system. Using computer software interface, a plot between wave number versus % transmittance of radiation was obtained.

The I.R. spectrometer is suitable for qualitative analysis of the sample by various functional groups present. For comparative measurement of functional

group in different catalysts, same amount of prism material, with identical pressure and thickness for all the samples were taken. In the present work, the objective was to identify different functional groups and their relative quantities. By FTIR results, the acidity of various catalysts were calculated based on the measurements of intensities of various functional groups.

Principles of FTIR

A schematic form of the arrangements of obtaining spectra is shown in Fig. 2.9, which shows the experimental arrangement for obtaining emission and absorption spectra. The upper arrangement of Fig (2.9) shows how an emission spectrum may be obtained. The sample is exited in same way which emits radiation. Some of the radiation is collected by a lens and focussed on the spectrometer. The spectrometer sorts out the electromagnetic radiation allowing an emission (infrared) spectrum to be displayed.

The lower arrangement of Fig. (2.9) show the absorption spectrum in which from a certain source electromagnetic waves are emitted, which pass through samples by using lens. The secondary radiation from sample passes to the spectrometer, which sorts out infrared radiations allowing absorption spectrum to be displayed.

The FTIR works on same principleas IR. A source of continuous radiation over the interest is used and essentially collected two spectra, one spectra which passes through sample and the other passes through the blank are collected. The ratio of the two intensities gave the desired result. One indicates the spectrum of the radiation emitted by the source directly and the other, the radiation of the source after it had passed through the samples. The ratio of two represents the absorption spectrum of sample. The equations relating the intensity falling on the detector (I(s)) to the spectral power density (B(Ū)) at a particular wave number, U, is given by
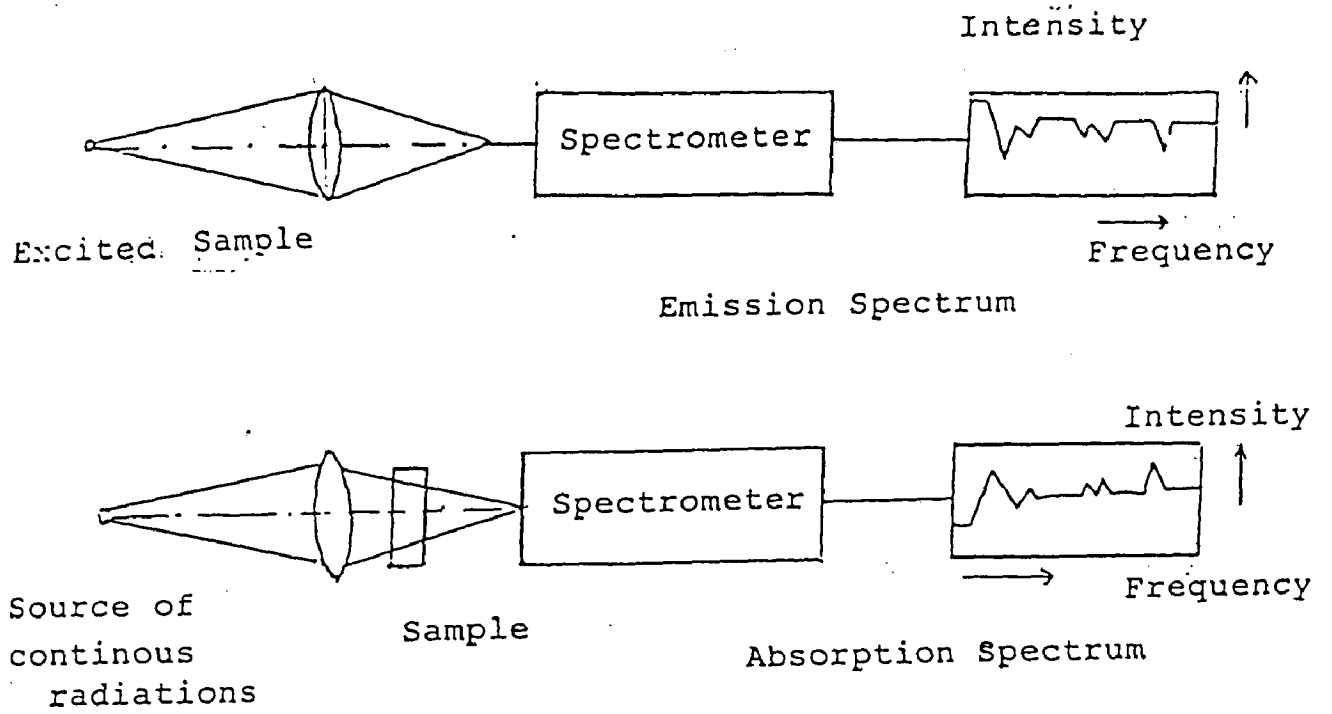
Fig. 2.3 EXPERIMENTAL ARRANGEMENT FOR OBTAINING EMISSION AND ABSORPTION SPECTRA.

$$I(s) = \int_{0}^{\infty} B(\overline{v})\cos 2\pi \overline{v} s\, d\overline{v} \qquad (2.1)$$

$$B(v) = \int_{-\infty}^{\infty} I(s)\cos 2\pi \overline{v} s\, ds \qquad (2.2)$$

These two equations are interconvertible. They are known as Fourier Transform pair. The first shows variation in power density as a function of difference in path length, which is an interference pattern. The second shows variation of intensity as a function of difference in path length, which is a spectrum. The IR operated within frequency range 10^4 cm^{-1} to 100 cm^{-1}.

The various prism material employed in spectrometer are as given below. These are transparent to infrared radiation.

NaCl   650 – 4000 cm^{-1} mid infrared

KBr   400-4000 cm^{-1}

Polyethylene terephthalate   for infrared

By FTIR, the strength of Bronsted and Lewis acid sites can be determined. The approximate wavelength near which particular peak corresponding to a functional group is present in zeolite HZSM-5 are listed below :

Si-OH   3745 cm^{-1}

Si-OH-Al   3610 cm^{-1} (dependent on SAR)

H-OH   3600 cm^{-1} (in structure)

          also

H-OH   1660 cm-1 (Absorbed water)

Si-O-Si   1140 cm^{-1}

Si-O-Al   .   1075 cm^{-1}

Al-O   760 cm^{-1}

The graph for % transmittance versus wave number obtained by FTIR is plotted on graph. The frequency is given by formula material forming the bond.

$$\overline{v} = \frac{1}{2\pi C}\sqrt{\frac{K}{\mu}}$$
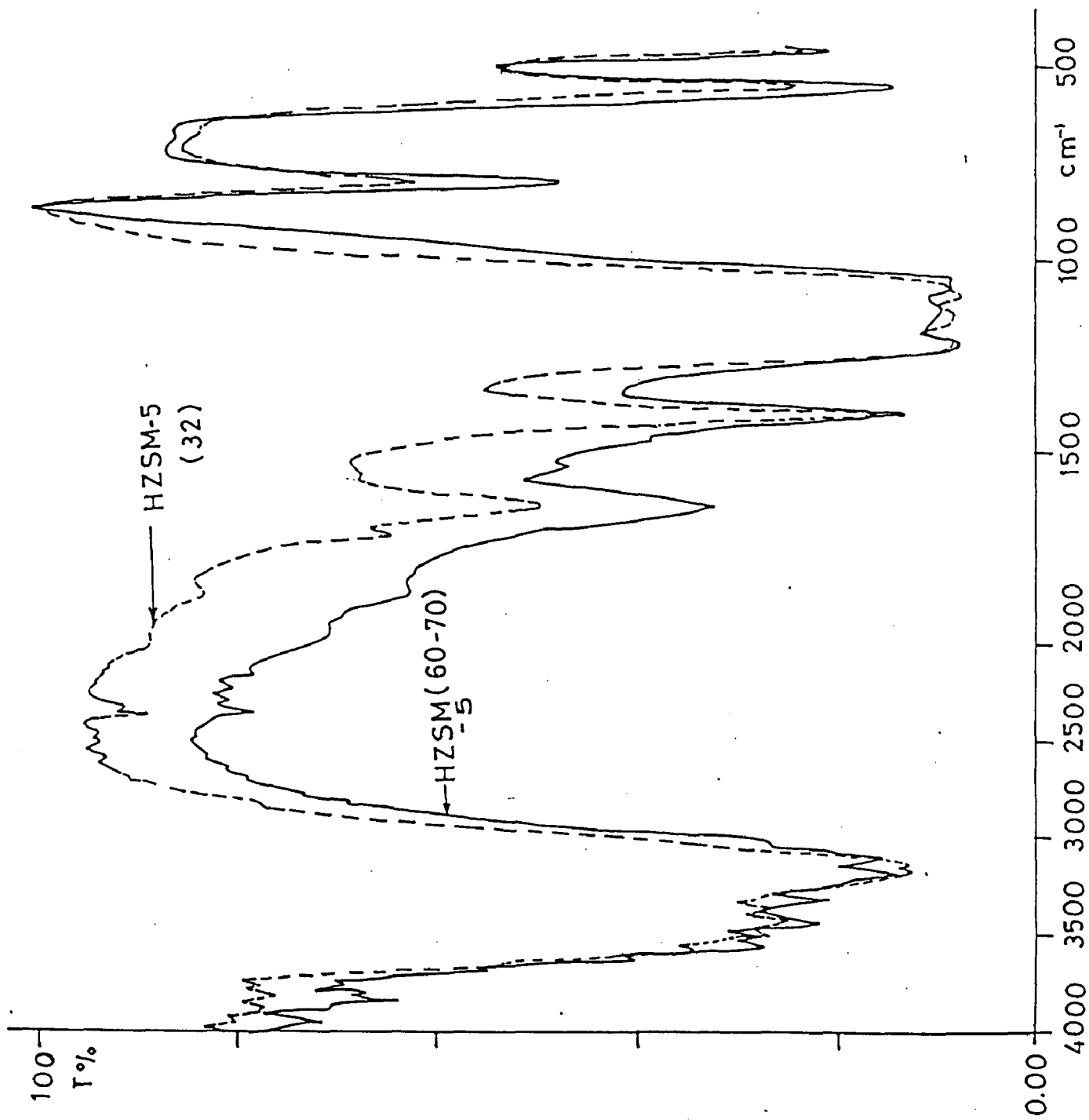
Fig. 2.10. I.R. SPECTRAGRAPH OF ZEOLITE CATALYSTS 32

where $\dfrac{1}{K} = \dfrac{1}{M_1} + \dfrac{1}{M_2}$

$\bar{v}$ is the wave number

C is the speed of light

K is the force constant between two molecules

M_1, M_2 are molecular weight of molecule 1 and 2 forming the bond.

Functional groups (Fig. 2.10, 2.11)

The catalyst samples were analyzed to examine acid strength corresponding to various functional groups by FTIR (Perkin elemer 1600 series) at the Department of Chemistry, University of Roorkee. The prism material used was KBr pellets. The percentage transmittance versus wave number is plotted, which is show in Figs. (2.10 and 2.11). The test sample was prepared by mixing 1mg zeolite with 300 mg of KBr. The pressure applied for pelletization was 15 tonne.

The frequency corresponding to a particular functional group and its transmittance is given in table 2.4.

Table 2.4 Various functional groups with their transmittance

	Functional Group and its Frequency with percentage transmittance (in bracket)						
Catalysts	Si-OH	Al-OH	Si-OH-Al	H-OH	Others		
HZSM-5 SAR (32)	3767 (78)	3660 (53)	3600 (33)	3540 (27)		1977 (87)	2367 (87)
HZSM-5 SAR (60-70)	3767 (74)	3660 (55)	3600 (37.4)	3540 (28)		1977 (71.50)	2337 (78)
NiHZSM-5 SAR (32)	3783 (68)	3660 (45)	3600 (37.4)	3540 (28)	3580 (29.3)	1990 (78.5)	2361 (Nil)

Ce 3.21 wt%
Ni 0.59 wt%
Cu 1.46 wt%

Hzsm-5 (30-40) SAR(32)

Cezsm-5 (30-40) SAR(32)

Nizsm 5(30 40) SAR(32)

Hzsm (60-70)

Cuzsm 5 (30-40) SAR(32)
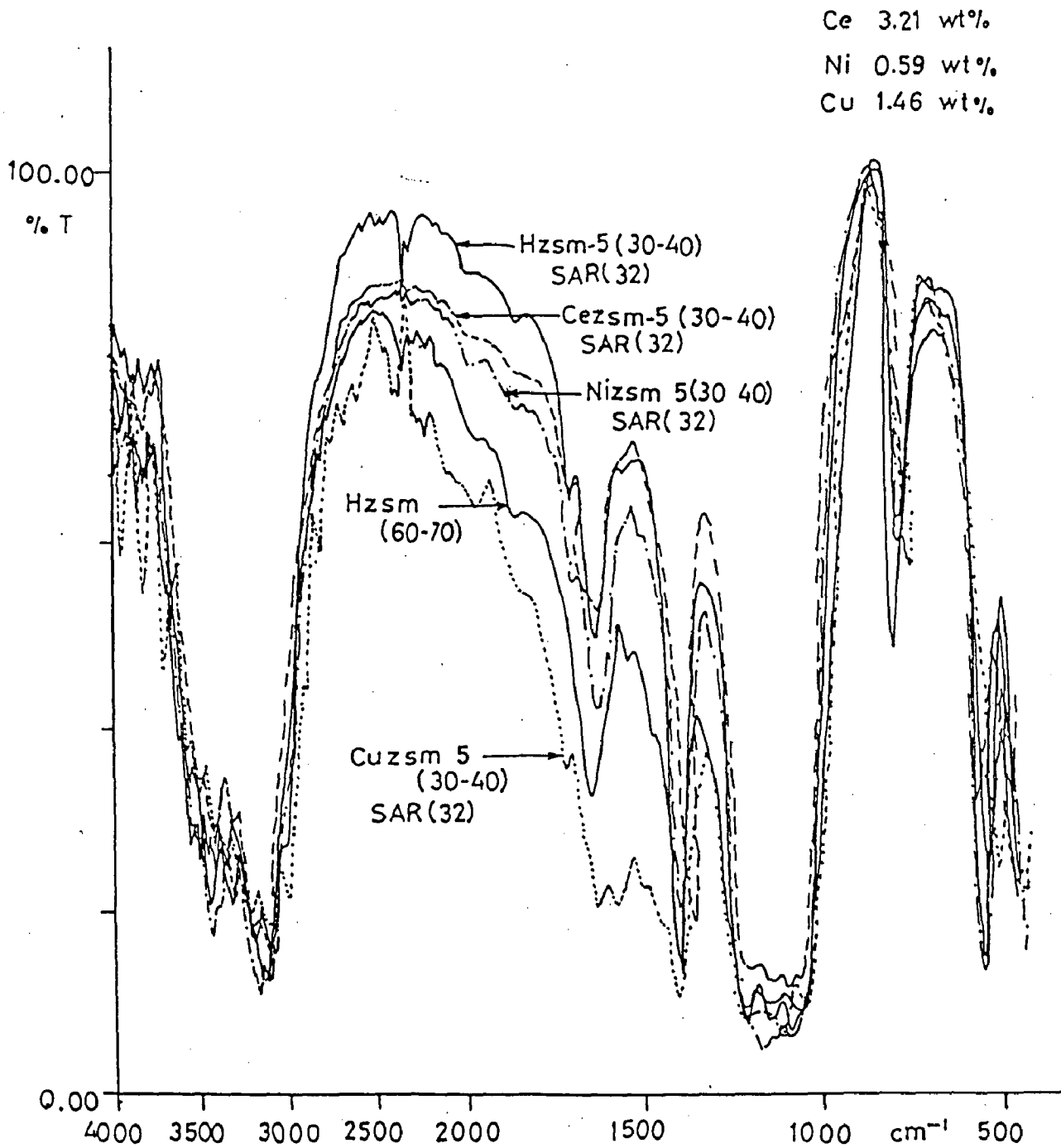
Fig. 2.11 I. R. SPECTRAGRAPH OF ZEOLITES CATALYSIS

CuHZSM-5 SAR (32)	3766 (45)	3660 (45)	3600 (36.6)	3540 (32)	3508 (31.60)	1971 (64)	2361 (Nil)
CeHZSM-5 SAR (32)	3767 (76)	3660 (53)	3600 (34)	3540 (30)	3467 (30)	1977 (82)	2367 (85.61)

Table 2.4 and Fig. 2.10 relate the intensity of functional groups containing two samples of HZSM-5 zeolites having silica alumina ratio 32 and 60-70. From the figure it may be concluded that the Si-OH band intenstiy was greater in SAR 60-70 in comparison to SAR 32 while Al-OH band intensity was larger in 32 in comparison to SAR 60-70. The transmittance of infrared band at 3600 cm^{-1} for SAR (60-70) was 38% compared to 33% for SAR (32). This suggests a higher Si-OH-Al group in SAR (32) compared to SAR (60-70). The intensities of bands at frequencies 1977 cm^{-1} and 2369 cm^{-1} were more in SAR (32) compared to SAR (60-70).

Table 2.2 and Fig. 2.11 relate the intensities of various HZSM-5 (SAR-32) zeolites with Ni, Cu, Ce ion exchange. From Figure it may be concluded that during ion exchange of zeolites the thermal treatment (calcination) leads to dealumination which subsequently breaks Si-OH-Al group into Si-OH-increasing intensity of Si-OH group and decreasing of Si-OH-Al. In cation exchanged zeolites, new hydroxyl group or groups at other places are found as shown in Table 2.4 [3400-3600 cm^{-1}]. The probable origin of these bands is the hydrolytic fission of absorbed water shown by the following reaction

$$\text{Zeolite}^{2-} + M^{2+} + H_2O \rightarrow MOH^- + \text{Zeolite} - OH^-$$
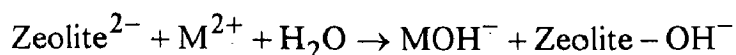
The ability of the zeolite to dissociate absorbed water varies with the cations present. Ni, Cu, Ce exchanged zeolites give peak at different frequencies and having various bands in 1900 to 2400 cm^{-1} frequency range. The transmittance of IR for various bands is presented in Table 2.4. The 2367 cm^{-1} band of HZSM-5 (SAR-32) disappeared in Ni and Cu exchanged zeolites and new
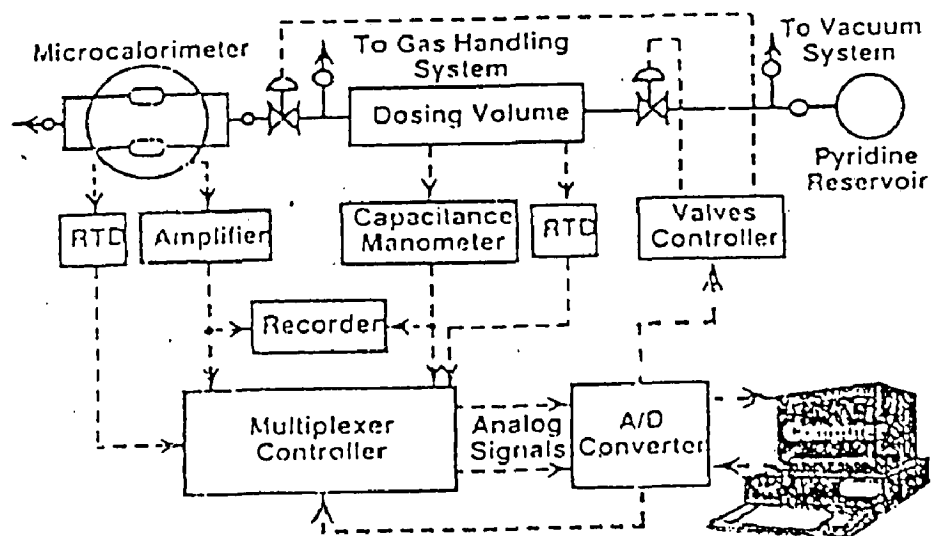
Fig. 2.12   SCHEMATIC OF MICROCALORIMETRIC APPARATUS

bands generated at 1990, 1971 cm^{-1} frequency respectively. For Ce exchanged zeolite intensity at 2367 cm^{-1} decreased and increased at 1977 cm^{-1}.

2.4.1.2 Temperature Programmed Desorption

The acidity of the catalyst samples may also be measured by temperature programmed desorption of NH$_3$ [19] or pyridine. The catalyst (200 mg, 10-20-mesh particle) is loaded in a stainless steel micro reactor connected on line to a gas chromatograph. The catalyst is activated in a flow of dry nitrogen at 323°K for 2 hrs and then cooled to room temperature. NH$_3$ gas is purified by passing through a column of molecular sieve 4 Å. The catalyst is completely saturated with purified NH$_3$ at ambient temperature and the physi-sorbed NH$_3$ is desorbed by flushing with nitrogen (100 ml min^{-1}). The catalyst is thus heated at a linear rate of 10°K min^{-1} in a stream of hydrogen and the amount of NH$_3$ desorbed is continuously monitored by thermal conductivity detector to yield TPD spectrum. Simultaneously, the concentration of NH$_3$ in the exit gas is titrated using standard HCl (0.01 N). The total amount of NH$_3$ desorbed between 283-823 K(25-500°C) may be calculated from the titration data.

2.4.1.3 Microcalorimetric Measurement [20]

Microcalorimetric measurements of the heat of adsorption of puridine is used to determine both numbers and strength of acid sites.

Microcalorimetry Apparatus

A schematic representation of the micro-calorimetry system is shown in fig. 2.12.

The calormeter is placed on a heavy-duty jack that permits the calorimeter to be moved during pretreatment of the sample under study such that the sample is not exposed to air. Gaseous pressures re measured by means of either on MKS Baratron capacitance manometer. The entire calorimetric system is kept constant at 318°K (45°C) using a PID temperature controller. another temperature controller is used to control the temp of the preheated gas entering the cells to the
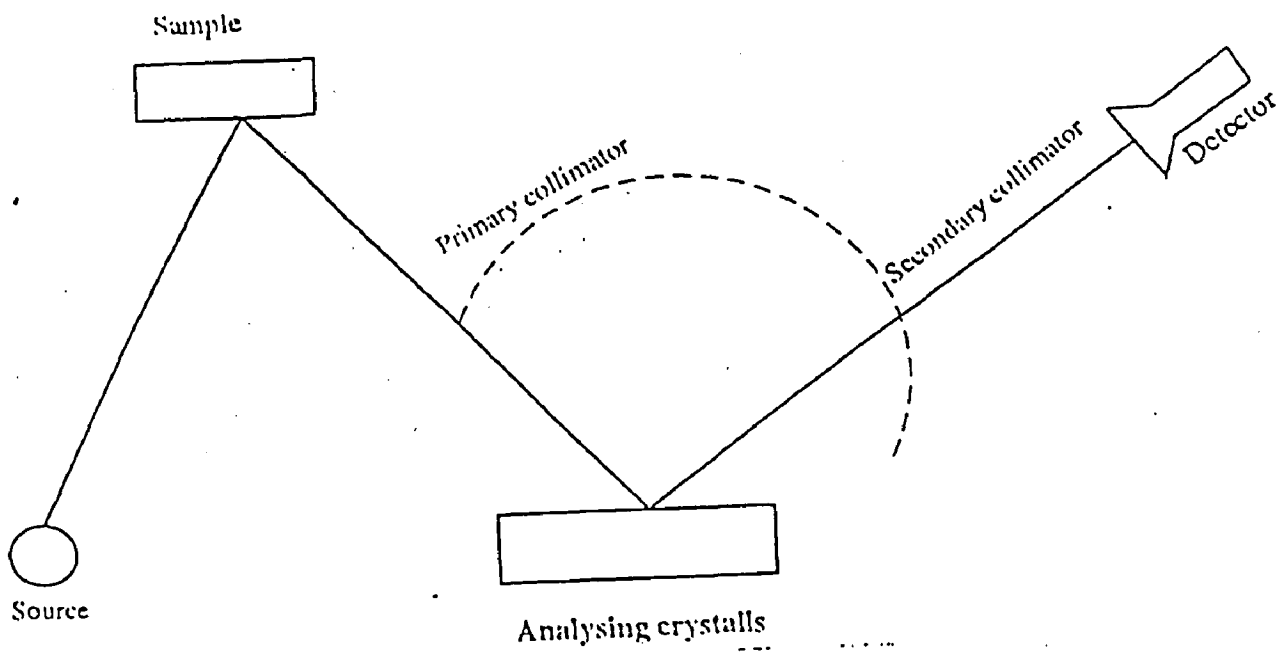
Fig. 2.13   Schematic   diagram   of   X ray   Diffractometer

calorimeter temperature. This is done in minimize heat effects caused by the heating of the gas that can not be completely compensated by the reference cell. in the calorimeter. the temperature of the cells and dosing volume are measured using a pair of precision platinum resistance temperature device (RTD). the dosing volume is attached to a diffusion-pumped glass vacuum system within ultimate dynamic pressure of 4×10^{-7} Torr and to a gas handling and purification system.

The following quantities are monitored continuously by a computer for subsequent data processing. Calorimetric temperature, dosing volume system temperature and pressure, calorimetric signal and time since dosing, calorimetric peak areas and volumetric isotherms give the total heat and total adsorption respectively, as a function of pressure. Integral heats Q, as a function of coverage, provide the total acidity of the system.

$F(g) = -dn/dq$ provide a desorption of the acid strength distribution over the surface of the catalyst

Where,

q	=	differential heat
n	=	amount absorbed
Q	= .	Integral heat

2.4.2 Structure and Crystallinity

Structure and crystallinity of the zeolites may be studied by X-ray diffraction and Scanning Electron microscope (SEM).

2.4.2.1 X-ray Diffraction Spectrometer [21,22]

X-ray spectrometry is a non-destructive technique used to determine by element present in any particular substance. the Schematic operation principle of X-rays spectrometer is shown in Fig. (2.13). A bean of X-rays is diffracted from a source to a sample of the substance causing secondary or florescent X-ray to be emitted. This secondary radiation contains wave length that are characteristics of
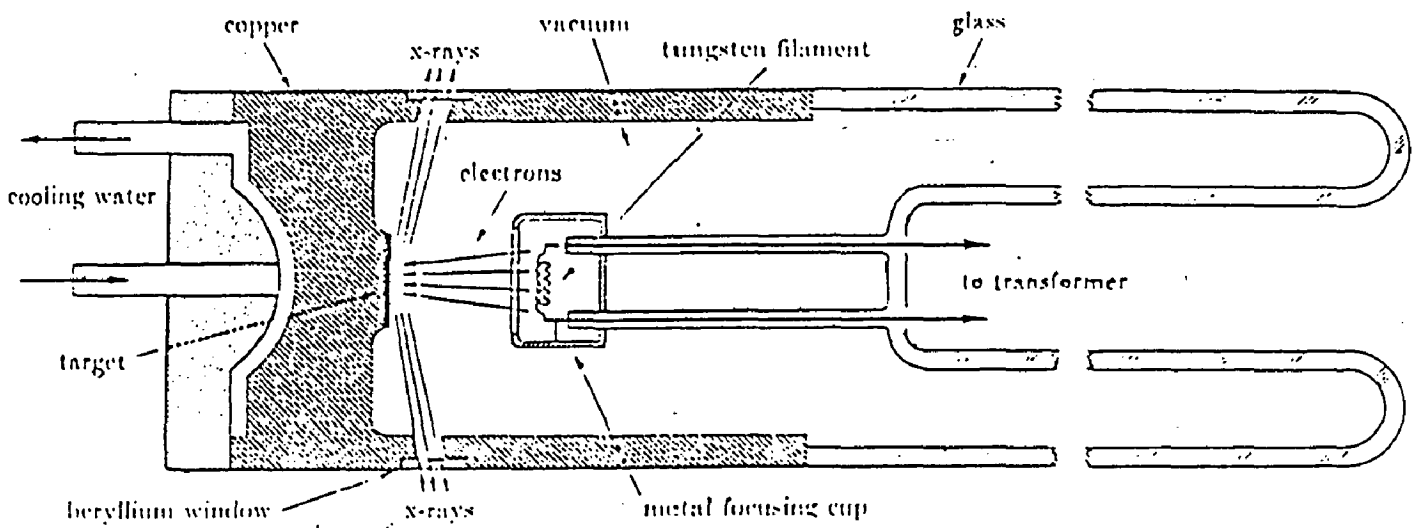
Fig. 2.14   CROSS SECTION OF SEALED-OFF FILAMENT X-RAY TUBE
(SCHEMATIC)

each element present. These runs are directed to analysing crystals by primary collimeter. the analysing crystal moves at angle 2θ with certain speed. The runs are reflected and passes to detector through secondry collimater. The various parts of X-ray spectrometer are presented in detail below.

(a) **X-ray Tube :**

    (i)   A source of electrons

    (ii)   A high accelerating voltage

    (iii)   A metal target.

X-Ray tubes (Fig. 2.14) contain two electrodes, an anode (the metal target) maintained at a high negative potential, normally of the order of 30,000 to 50,000 volts for diffraction work. x-ray tubes may be divided into two basic types' according to the way in which electrons are provided : Filament tubes, in which the source of electrons is a hot filament, and gas tube in which electrons are produced by the ionization of a small quantity of gas in the tube.

Filament tubes consist of an evacuated glass envelope which insulates the anode at one end from the cathode at the other, the cathode being a tungsten filament and the anode a water-cooled block of copper containing the desired target metal as a small inert at one end. One lead of the high-voltage transformer is connected to the filament and the other to ground, the target being grounded by its own cooling-water connection. The filament is heated by a filament current of about 3 amp and emits electrons which are rapidly drawn to the target by the high voltage across the tube. Surrounding the filament is a small metal and maintained at the same high (negative) voltage as the filament; it therefore repels the electrons and tends to focus then into a narrow region of the target, called the total spot. the X-ray are emitted from the focus spot in al directions and escape from the tube through the windows in the tube housing.

    (b)   Collimators: The Collimators consists of circular apparatus of dia d. the collimators directed the rays in desired direction as in Fig. 2.13. the primary collimator directed secondary X-ray into crystal while

the secondary collimator directed the rays into detector. In fig. 2.15 pinhole collimator and sources is presented.

Consider the simplest kind of collimator fig. 2.15 having a point source of radiation at the collimator consisting of circular apegtures of diameter d. If there is a point source of radiation at s, then all the runs in the beam are non parallel. If projected source shape is square fig. 2.19 of collimator having height h and dia d. The beam issuing from the collimator contains not only parallel and divergent rays but also convergent one.

(c)   X-rays Detector System : Two types of detectors are normally employed a gas filled detector for longer (softer) wavelengths, and a scientillation detector for shorter (harder) wavelengths. In the gas filled detector the employing X-ray ionize gas (usually mixture of argon and methane). A short shape voltage pulse is obtained due to the difference in velocity between the electrons moving to the anode and positive ions moving to the earthed casing.

In my samples analysis the Scientillation detector consisting of a phosphor and photomultiplier. The phosphor converts the X-ray photons into (blue) light and photo multiplier converts the eight pulses into voltage pulses.

(d)   Data Output : For qualitative analysis, the goniometer is scanned over the angular range and a record of 20 against intensity is obtained. The intensity peak indicates values of 2θ, where the Brgg's Law $n\lambda = 2$ d sin θ is fulfilled. Since 2 d is known constant. The 2θ setting of each peak corresponds to a certain wavelength. Tables of 2θ versus atomic number and wavelengths can be used to interpart the chart and identify the elements in the analysed sample.

Dispersion used for Elemental analysis :

(a)   Energy dispersion: Elemental analysis of the sample may be done by measuring directly the different photon energies present in the
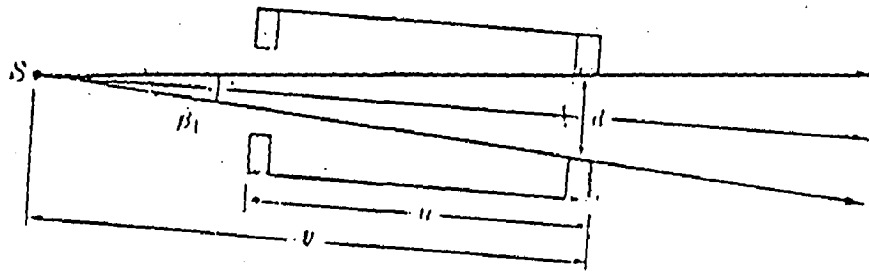
Fig. 2.15   PINHOLE COLLIMATOR AND SMALL SOURCE.
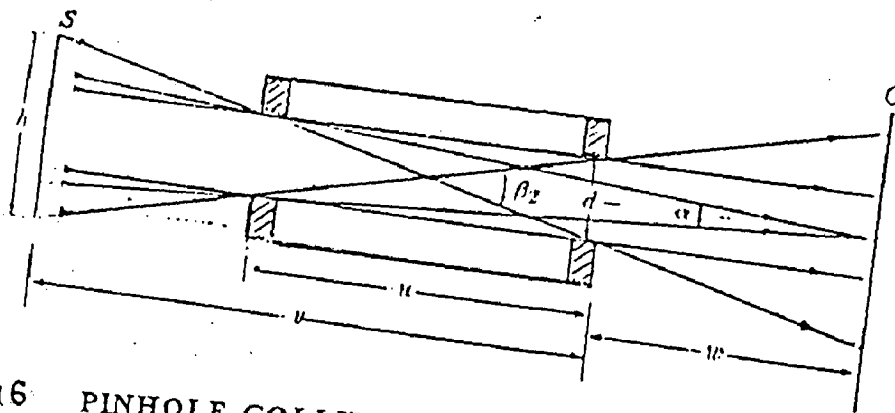
Fig. 2.16   PINHOLE COLLIMATOR AND LARGE SOURCE S= soruce, C= Crystel

secondary radiation energy being inversely propositional to wavelength. The energy is converted into an electrical pulse whose amplitude is proportional to the energy of the detected photon which in turn is related to a specific element. An amplitude selective, multi-channel analyses sorts the difference pulses enabling identification of the different elements present in the sample.

Wavelength Dispersion

Dispersion of the different wavelengths contained in a secondary radiation is achieved by means of a crystal whose lattice planes are parallel to the surface of crystal used and the way in which it has been cut. If secondary radiation is directed on to the crystal at an angle θ, diffraction only occurs when the relationship between θ.d and characteristics wavelength λ fulfill the condition of Braggs law nλ = 2 d sin θ.
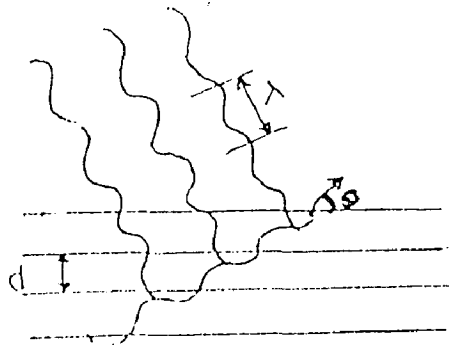
Fig. 2.17 X RAY DIFFRACTOGRAM OF CATALYSTS
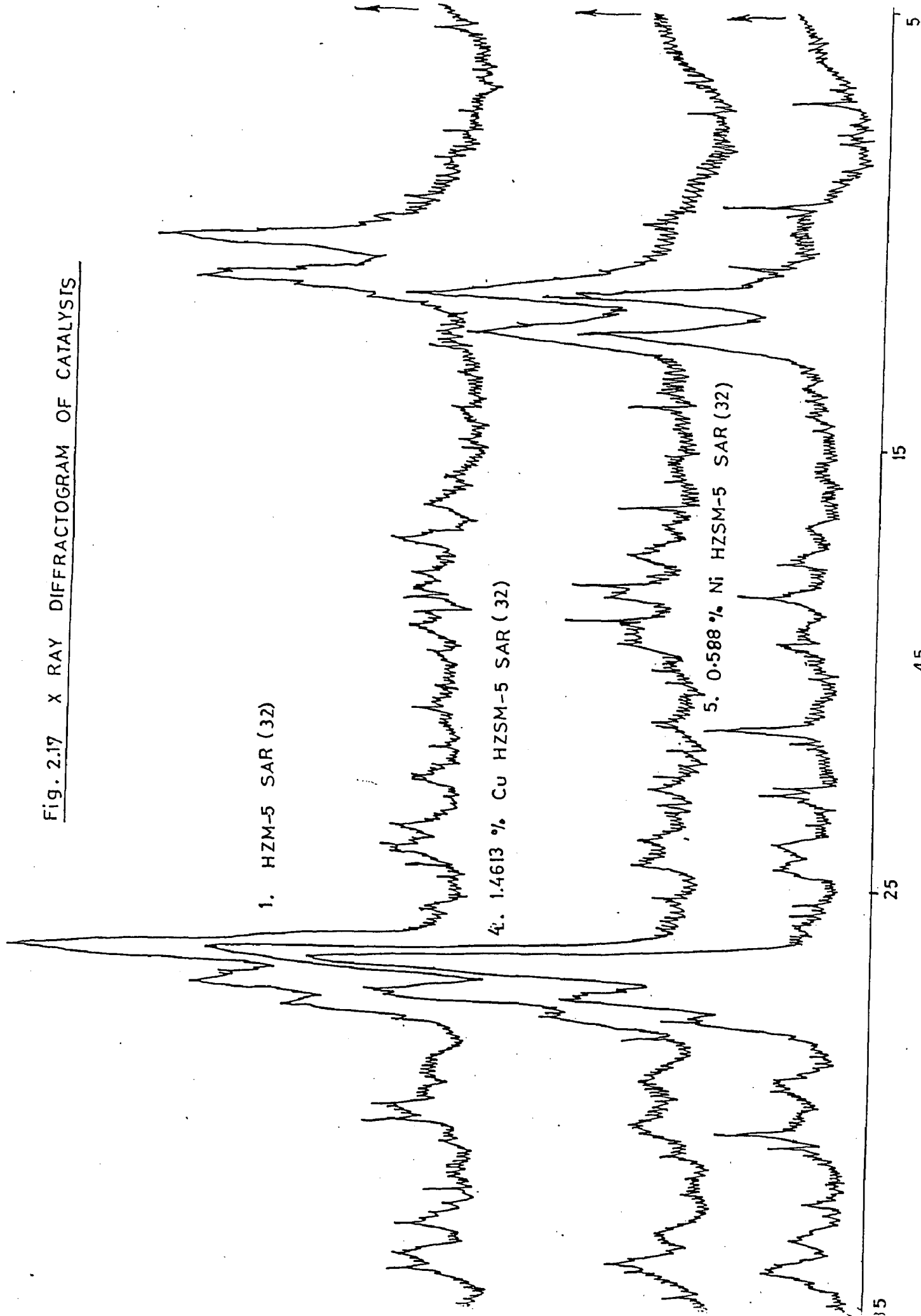
1. HZM-5 SAR (32)

4. 1.4613 % Cu HZSM-5 SAR (32)

5. 0.588 % Ni HZSM-5 SAR (32)

Fig. 2.18 X Ray Diffractogram of Catalysts

1. HZSM-5 SAR (32)

2. 3.6233 % Cr HZSM-5 SAR (32)

3. HZSM-5 SAR (19)

46
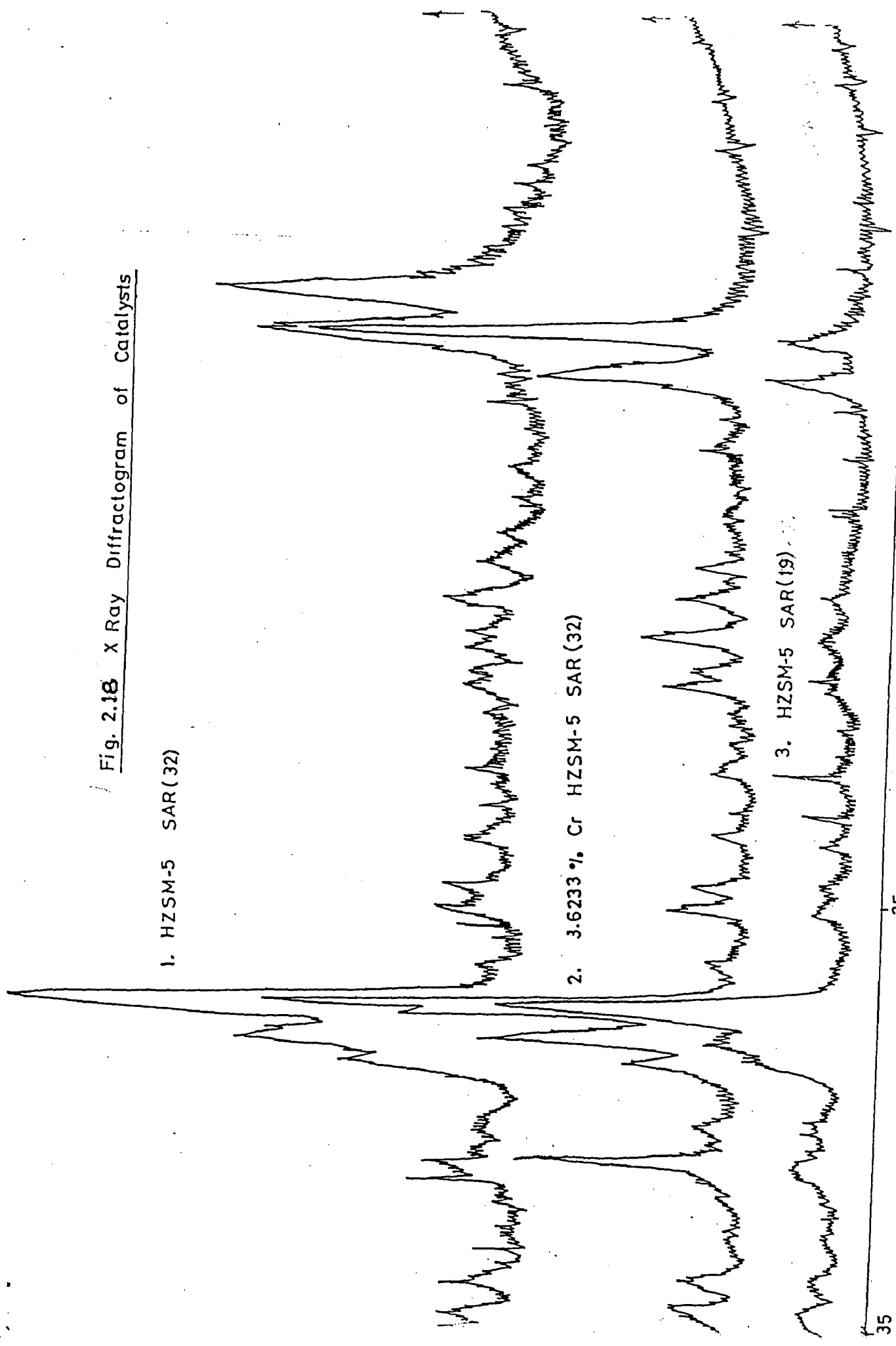
Fig. 2.19   X-RAY   DIFFRACTOGRAM   OF   3.9525%   PbY   CATALYST
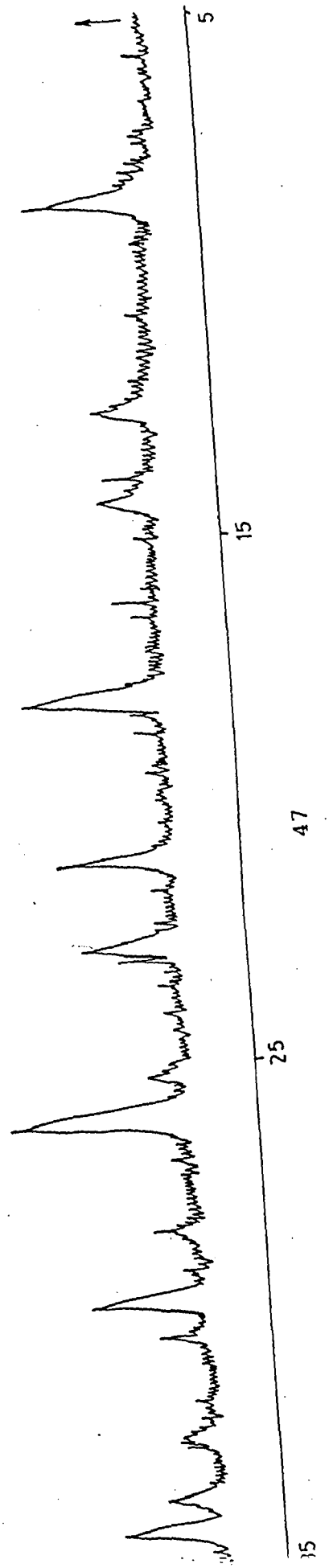
By varying the angle θ, the different wavelengths present and hence different elements in the sample, can be determined (qualitative analysis). Since the intensity of the radiation at each wavelength is proportional to the concentration of the corresponding element, the amount of each element present can be determined quantitative). The peak obtained in X-ray diffraction is shown in fig. 2.17, 2.18 and 2.19.

Study of Crystallinity of Catalyst:

Crystallinity of catalyst was studied by X-ray diffractometer (Philips PW 1140/90) in University Science and Instrumentation Centre (USIC), University of Roorkee, Roorkee. The source used was Cu-Kα and Ni as a filter. Goniometer sepped was kept at 1degree per min and the chart speed was 1 cm/min. The range of diffraction angle (2θ) was kept at 3-50°. A plot of 2θ against intensity was obtained and shown in fig. 2.17-2.19.

By assuming crystacininty of the original HZSM-5 SAR (32) obtained from IOC (R&D), Faridabad as 1, the crystallinity of other samples were determined by a comparison of the peak heights. The heights of the three peaks present in the 28 range of 20-22.5 were measured and an average height was calculated. The percentage crystallinity of any sample can be found as the ratio of the average height for the given catalyst to the average height of the known (original) sample. Table 2.5 presents some of the values.

Table 2.5: Crystallinity of Catalysts

Name of catalyst	(A+B+C)/3	% Crystallinity
H-ZSM-5 SAR(32)	8.167	100
0.5888%Ni-ZSM-5 SAR(32)	7.433	91.0
1.46`3%Cu-ZSM-5 SAR(32)	8.134	99.6
3.6233%Cr-ZSM-5 SAR(32)	7.866	96.3
3.7111%Ce-HZSM-5 SAR(32)	5.133	62.9

Contd...

Th-HZSM-5 SAR(32)	6	73.5
La-HZSM-5 SAR(32)	7.500	91.8
4%CrTh-HZSM-5 SAR(32)	6.93	84.9
1.2486% Pb-HZSM-5 SAR(32)	6.833	83.7
4% Pb 4% Cu HZSM-5 SAR(32)	7.633	93.5
4% Cr 4% Th HZSM-5 SAR(32)	6.6	80.8
2%Cr ThHZSM-5 SAR (32)	6.333	77.5

2.4.2.2 Scanning Electron Microscope (SEM) [23]

Scanning Electron Microscope is normally used to know the shape and size of particles in a given specimen. The specimen may be solid or in powder form. The specimen is fixed in dies by adhesive. The non metallic specimen is activated by silver or gold coating.

For analysis of specimen, a beam of high-energy electrons (Primary electron beam) incident on a surface of sample interacts with it in several ways. The emitted radiation from the surface consists of X-rays, secondary electrons, luminescence and transmitted electrons. The intensity of the various radiations will be characteristics of the chemical composition and the topography of the region of incidence of the beam. These radiations can be detected by suitable and sensitive detectors. Whole signal is then amplified and fed to the cathode ray tube to form an image. The secondary electron gives the most spectacular images. Therefore, it is selected while other is out. By seeding the image the crystal structure of sample is determined. To study surface structure and morphology of the catalysts scanning electron micrograph was obtained using a Philips SEM-501 microscope at the University Scientific Instrumentation Centre (USIC), University of Roorkee.

2.4.3 Composition (SiO_2/Al_2O_3, Percentage Metals Exchanged) Methods

Composition and the percent of exchanged metals in the catalysts were determined by Atomic Absorption Spectrometer (AAS), Inductively Coupled

Plasma Instrument (ICP), Electron Probe Micro Analyser (EPMA) and other analytical methods. Atomic Absorption spectrometer and ICP instruments give component analysis of sample in liquid form, while EPMA analyzes the solid samples directly.

2.4.3.1 Atomic Absorption Spectrometer :

The principles of Atomic Absorption Spectrometer is that when sufficient voltage is applied across electrodes radiation is generated by a hollow cathode lamp containing cathode of element which is to be analyzed and anode of a tungsten metal. An inert gas (Argon or Neon) under low pressure fills the chamber. Approximately 600 V at 1 to 50mA is applied between the anode and cathode. The filler gas is ionized and ions are accelerated towards the cathode. As these ions bombard the cathode they cause the cathode material to "Sputte" and form an atomic vapor in which atom exist in an exited electronic state. In returning to the ground state, the line characteristics of the element are emitted few passed to the monochrometer directly and few to monochromator through the flume were they may be absorbed by vapor of sample. Since generally only the test element can absorb this radiation the method become very specific in addition to being sensitive. The sample, in solution is aspirated as a fine mist into a flame where is converted in the atomic vapor. Most of the atom remaining are capable of absorbing radiation of a suitable wavelength. The descreate radiation is usually supplied by a hollow cathode lamp, which is a sharp line source consisting of a cathode containing the element to be determined alongwith a tungsten anode.

The decrease in energy (absorption) is corresponding to concentration of elements is then measured.

Absorptivity is given by

$$a = A/(b.c)$$

$$\text{where } A = \log_{10}[1/T]$$

$$T = I_t/I_0$$

Where   a   =   absorbtivity

50

A = Absorbence

T = Transmittance of radiation

I_t = Transmittance radiation power

I_0 = Incident radiationpower

b = Path length

Procedure :

Before the analysis of our samples the standard sample is prepared by the method given below:

1000 PPM of given element = [Weight of compound (containing the element) equal to its molicular weight dissolved in 1 litre water]/molicular weight of element.

The 1000 PPM concentration of element was diluted and standard solution of given element having lower concentrations was prepared. The unknown solution is then tested by feeding the sample by peristaltic pump into the flame from the atomic vapor. the line characteristics of cathode lamp passes to the monochromoter directly and few passes through samples. The electrical signal produced in monochromotor is directly related to amount of radiation falling on monochromoter. the electrical signal is then processed by the data acquisition system to present a readout of element concentration.

The data, which generated after atomic absorption spectrometer analysis is given in table 2.6 and 2.7.

Calculation of % elements in zeolites sample

Calculation for $CuNO_3$

	Wt of zeolites taken	=	10 gm
*	Wt of $Cu(NO_3)_3.3H_2O$ ewuivalent to 4% Cu	=	1.5322 gm
	Volume of filtrate	=	300 ml
**	Wt of Cu in filtrate	=	0.2539 gm
++	Wt of Cu in zeolite catalyst	=	1.4613×10^{-2} gm
++	Wt/% Cu in zeolite catalyst	=	1.4613%

+++   % Ion exchanged   =   36.53%

*   Wt. of $Cu(NO_3)_3$. $3H_2O$ equivalent to 4% Cu   =

Molecular of $Cu(NO_3)_2.3H_2O$ x wt. of zeolite x 0.04 / Molecular wt of copper.

$$= \quad \frac{241.60 \times 10 \times 0.04}{63.5} \quad = \quad 1.522 \text{ gm } (CuNo_3)_2. \ 3 \ H_2O$$

$$= \quad 0.4 \text{ gm copper.}$$

**   Wt. of copper in filtrate = (Volume of filtrate x Concentration of Cu given

by   AAS) x Dilution factor

$$= 300.0 \times 1.354 \times 10\text{-}6 \times 625 \text{ gm}$$
$$= 0.253875 \text{ gm . Cu.}$$

+ Wt of copper in zeolotie catalyst = (0.4—0.253875) = 0.146125 gm.

++ Wt of copper in zeolites :

0.4 gm Cu is $\cong$ 4% Cu.

So, 0.146125 gm Cu = 1.46125 %

+++ % Ion exchange of Cu = $\dfrac{0.146125 \times 100}{0.4}$ = 36.53%

Following the above calculation procedure the data obtained is given in Table 2.2 and in Table 2.3. Serial No. (1-6) obtained from AAS. 7 & 8 from ICP, 9 from UV Spectrometer and 10 from EPMA.

Table 2.6: Table of Atomic Adsorption Spectrometers for determintion of weight of elements not ion exchanged

S. No.	Name of zeolites	Volume of filtrate (ml.)	Reading of AAS, ICP (mg/l)	Dilution factor	Wt. of element in filtrate (gm)	Exchanged elements
1.	HZSM-5 (32)	300	1.354	625.00	0.2539	Cu
2.	HZSM-5 (32)	485	1.688	625.00	0.511167	Ni
3.	HZSM-5 (32)	366	8.235	8.333	0.037670	Cr
4.	HZSM-5 (32)	260	12.886	8.333	0.045030	Cr
5.	HZSM-5 (32)	435	1.012	625.00	0.275137	Pb
6.	Y zeolite	450	0.579	8.333	0.002846	Pb
7.	HZSM-5 (32)	410	98.6	10	0.404260	La
8.	HZSM-5 (32)	310	9.32	10	0.028892	Ce

Table 2.7: Table of Wt.% of element in Zeolites

S. No.	Name of zeolites	Wt. of zeolites	Compounds and Wt. taken for elements exchanging	Wt. of exchanged element in zeolites	%age ion exchanged	Name of element with (4% wt.)	Wt.% of elements in zeolites
1.	HZSM-5 (32)	10	Cu(NO$_3$)$_2$.3H$_2$O (1.5322 gm.)	0.14613	36.53	Cu (0.4 gm)	1.4613
2.	HZSM-5 (32)	15	Ni(NO$_3$)$_3$.6H$_2$O (2.973 gm.)	0.08832	14.72	Ni (0.6 gm)	0.5888
3.	HZSM-5 (32)	10	Cr(NO$_3$)$_3$.9H$_2$O (3.078 gm.)	0.36233	90.58	Cr (0.4 gm)	3.6233
4.	HZSM-5 (32)	13	Cr(NO$_3$)$_2$.9H$_2$O (4.0015 gm.)	0.35497	68.26	Cr (0.52 gm)	2.7305
5.	HZSM-5 (32)	10	Pb(NO$_3$)$_2$ (0.639 gm.)	0.124863	31.21	Pb (0.4 gm)	1.2486
6.	Y zeolite	6	Pb(NO$_3$)$_2$ (0.384 gm.)	0.23715	98.81	Pb (0.24 gm)	3.9525
7.	HZSM-5 (32)	10	Ce(NO$_3$)$_2$.6H$_2$O (1.24 gm.)	0.371108	92.78	Ce (0.4 gm)	3.7111
8.	HZSM-5 (32)	10	Th(NO$_3$)$_2$.6H$_2$O (0.6898 gm.)	0.3805	95.125	Th (0.4 gm.)	2.805
9.	HZSM-5 (32)	10	La(NO$_3$)$_2$.6H$_2$O	0.2973	73.32	La (0.4 gm.)	2.973
10.	HZSM-5 (32)	10	Cr(NO$_3$)$_3$.9H$_2$O	0.1756	86.25	Cr (0.2gm)	1.756
			Th(NO$_3$)$_2$.6H$_2$O	0.1923	96.25	Th (0.2 gm)	1.923

2.4.3.2 Inductively Coupled Plasma Spectrometry[24, 25]

Procedure:

The sample, after suitable preparation is introduced into the excitation source. The dispersed light emerging at the respective element wavelength is converted into electrical signal. The magnitude of this signal is proportional to the light emitted and hence the element concentration. The electrical signals are then processed by the data acquisition system to present a radiant of element concentrations in units of operator choice.

The optical component can either be a high speed, high resolution scanning monochromoter which views one wavelength at a time, a polychromator, which can monitor many wavelengths simultaneously, or a combination of both. The data acquisition and instrument control system is a multi-user, multi-processor computing system.

In fig. (2.20) the major constituent parts of an ICP system was identified as [25].

1. The ample Introduction System (nebulizer)
2. The ICP torch
3. The high frequency generator
4. The transfer optics and spectrometer
5. The interface and computers

System in ICP Unit: The system is ICP unit is described below.

The sample introduction (nebulization)

The most commonly used device for the ICP is the pneumatic nebulizer. Efficient aerosol production requires very high gas velocities and consequently the use of fine capillary tubes. With a gas flow of 1 litre per minute a gas capillary of 0.5 mm diameter might well be used. Ideally nebulizer generate droplets of less than 10 µm diameter for efficient transport to the plasma. The larger droplets are simultaneously removed from the aerosol before it enters the ICP torch.
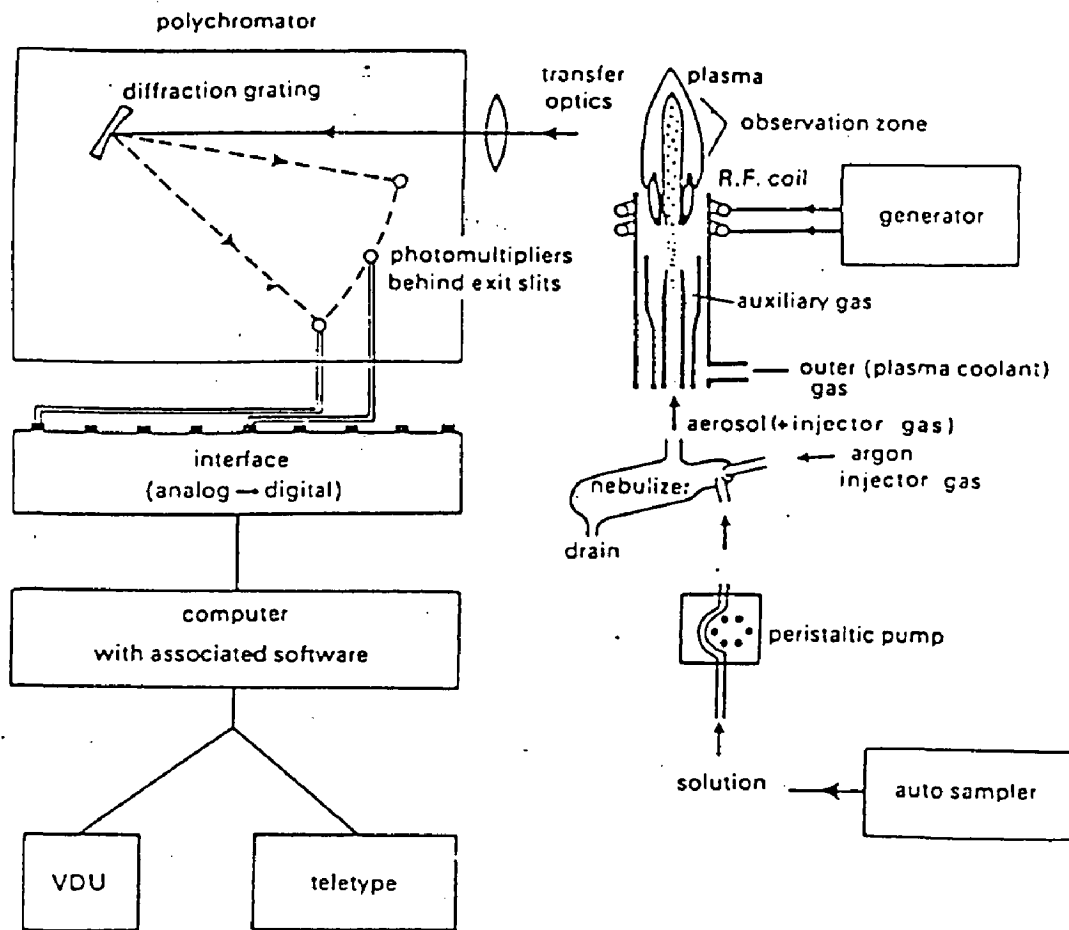
Fig. 2.20 SCHEMATIC DIAGRAM OF A SIMULTANEOUS ICP SYSTEM

Sample Excitation System

A plasma is a gas in which 'atoms are present in an ionized state, and, for the plasma to be sustained by induction, a sufficiently large proportion of those atom must be ionized to make the gas conducting. When a high frequency current flows in an induction coil it generates a rapidly varying magnetic field within the coil. If charged particles (i.e. an ionized gas) flow through a coil in which high frequency current is flowing (cutting the lines of magnetic force) then Joule of ohmic heating follows. This interaction (or inductive coupling) of the oscillating magnetic field with flowing gas generate the ICP flame.

The ICP torch consists of three accurately aligned concentric tubes of silica glass, with the auger most, tallest tube circled by a two-turn, water cooled copper coil (fig. 2.20) and argon gas flows thròugh the silica tubes. The cuter most (coolant) gas flows through the silica tubes. The cuter most (Coolant) gas flow enters the tube tangentially and "Swirls" upwards. The innermost tube contains the aerosol carrier gas which is thereby injected into the flattened base of the plasma, boring a "tunner", through the high temperature "flame". The cooler" tailflame" above the bright plasma is the region used for spectroscopic observation and measurement.

The basis for all emission spectrometry is that atoms or ions in an energized state spontaneously revert to a lower energy state and in so doing emit a photon of energy. For quantitative emission spectrometry it is assumed that the emitted energy is proportional to the concentration of atoms or ions.

Analysis and Quantification of Emission Spectrum.

The light emitted by the atoms of an element in an ICP must be converted to an electrical signal that can be measured quantitatively. This is done by resolving the light into its component radiation by means of a diffraction grating and then measuring the light intensity with a photomultiplier tube at the specific wavelength for each element line.
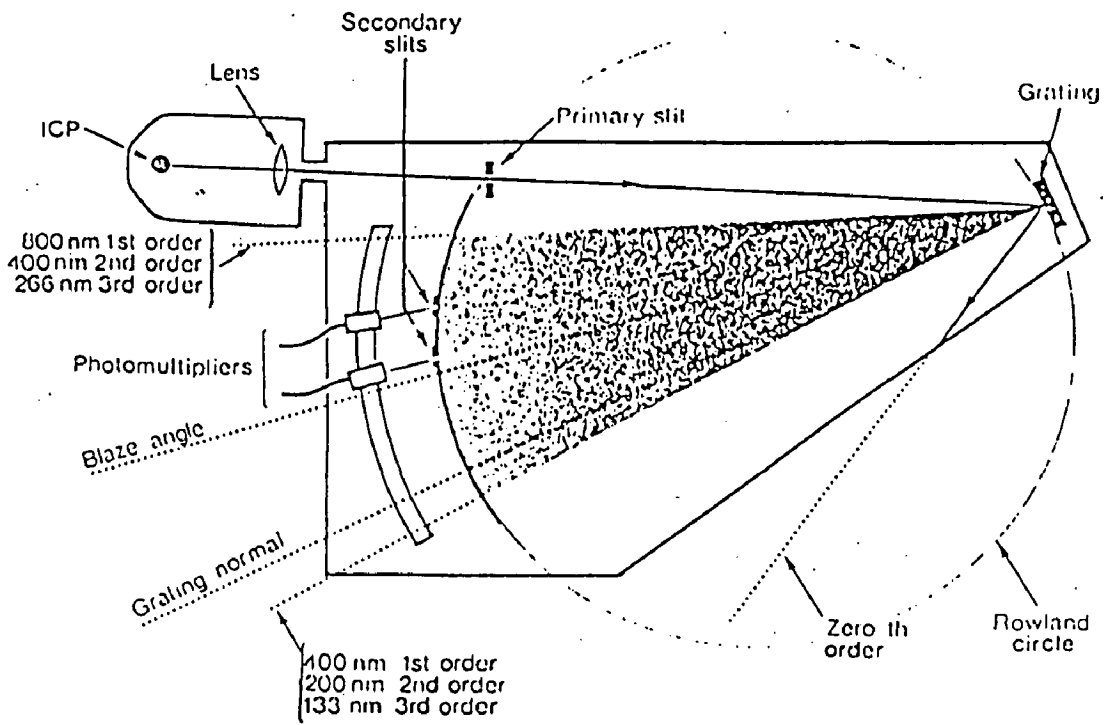
Fig. 2.24 SCALE DIAGRAM FO THE OPTICS OF A POLYCHROMATOR SYSTEM IN THE PASCHEN-RUNGE MOUNTING WITH THE GRATING BLAZED FOR MAXIMUM REFLECTION OF 600 nm IN THE FIRST ORDER.

58

Both monochromater as well as polychromater tube is used for analysis of samples. Polychromators consisting of a lens, a slit, a diffraction grating and secondary slits to isolate the resolved spectral lines. A typical arrangement is shown in fig. (2.21). The components are mounted in a box which is light-tight and, for vacuum spectrometers, air-tight as well.

The lens, the primary optical component, a biconvex lens, is constructed from pure silica and is mounted between the plasma and the primary slit bringing the light. The lens illuminates the primary slit, which is typically 20 mm x 20 mm in size and set parallel with the long axis of the plasma torch. The slit is mounted on the "Rowland circle" of the grating and acts as an optical source for the spectrometer. The movement of slit can be done by means of a stepper motor under computer control. The diffraction grating usually concave grating used are mounted in the Paschen-Runge geometry which is illustrated in fig. (2.21). The secondary slit assembly, an individual channel in a polychromator consist of a secondary slit, a mirror, a photomultiplier, and the electronics required for integrating and amplifying end output of the analytical signal.

Behind the slit frame, an isolated spectral line is brought to a focus on the cathode of a photomultiplier tube by means of a small concave mirror. The number of lines which can be installed is limited by the space available behind the slit frame for the mirrors and photomultipliers. The photomultiplier can be mounted above and below the slit frame. With this arrangement upto hundred channels have been installed in a 1-m spectrometer.

Procedure

The schematic diagram of a ICP system is shown in fig. (2.20). The sample is introduced to the nebulizer by a peristaltic pump, where it is mixed with argon gas. The fine drops of sample (aerosol) and Argon gas (injector gas) is passed through the ICP source in which high current flows in induction coil, it generates a rapidly raying magnetic field within the coil. The magnetic field is responsible for friction, which gas increase the temperature of the sample gas to such an extent that atoms are

present in ionized state called plasma. The light emits from plasma is dispersed passed through polychromotor or monochromoter where the disperse light emerging at the respective element wavelengths is converted into an electrical signal. To magnitude of this signal is proportional to the light emitted hence the element concentration. By using computer with associated software the element concentration is determined.

The liquid sample has been analysed by inductively coupled plasma spectrometer (8440-Plasmalab) in University Science Instrumentation Centre (USIC), University of Roorkee, Roorkee. The results are tabulated in table (2.6).

2.5 CALIBRATIONSAMPLE PREPARATION AND TESTING BY A.A. & ICP

Since A.A and ICP require samples in liquid form only, the analysis was done after preparing the solution of the (solid) zeolite to be analysed and the standard solution in different compositions covering the expected range for the calibration.

Standard solutions for calibration were prepared by dissolving respective nitrates in distilled water (for Ni, Cu, Cr, Pb, Ce, La and Al) in the range of 1 to 10 ppm. The standard solution of Si was obtained from Earth Science dependent.

The liquid form of the zeolite sample (containing the exchanged metal) was obtained as filtrate during the ion exchange process. In each case, a 4% solution of respective nitrate solution was used for ionexchange . After the ionexchange process was completed , the zeolite sample was washed with distilled water and the filtrate was collected for the analysis. Thus, the amount of ion exchange is calculated by the difference of 4% metal initially taken and the percent metal obtained in the filtrate. For analysis by atomic absorption or ICP about 20 ml of the liquid sample is required in each case. Samples are analysed at USIC.

Sample preparation for EPMA.

The zeolite sample is pellitized at 10 tonne pressure in the pelletizing machine and broken into the size range of approximately 1 mm. The particles are then fixed on

a glass plate (size 25 mm x 60 mm x 2 mm) with the help of araldite (done in Earth Science department). The sample was dried over hot plate (at 80°C approx. for 6 h, and polished over a moving wheel having polishing cloth. The sample was then analysed at USIC.

EXPERIMENTAL SET-UP AND PROCEDURES

3.1   EXPERIMENTAL SET-UP

The disproportionation of toluene to benzene and xylenes was carried out in a continuous downflow reactor as shown in Fig. (3.1). Toluene was fed to the reactor at top by a peristaltic pump into the pre-heating zone, where it comes in contact with carrier (nitrogen) gas. After the preheating zone, the toluene vapours and nitrogen gas passed through catalyst bed, which was maintained at the desired reaction temperature. The reaction products from the reactor came out, through a post-heating zone of the reactor. The products were cooled and condensed in an inclined tubular glass condenser and collected. The nitrogen alongwith other gaseous products were passed through a gas flow meter and the sample collected for further analysis. The collected products were analysed by gas-liquid chromotograph to determine the composition. On the whole the reaction system had the following main parts.

1.   Feeding system

2.   Preheater-cum-mixing zone

3.   Reaction zone

4.   Condensor and cooling system

5.   Gas flow measurement.

Figure 3.1 PHOTOGRAPH OF EXPERIMENTAL SETUP

3.1.1 Feeding System

This part comprised of a toluene feeding bottle of ½ litre capacity, a peristaltic pump having maximum capacity 10 ml/min, nitrogen gas cylinder and a rotamter to measure the flow rate of nitrogen. The feeding bottle acted as a storage for the toluene feed, which was connected to the peristaltic pump by a polythene tubing. A glass tube was dipped in reservoir through the cork fitted at the top of the bottle, which was further, connected to polythene tube. The outlet of feeding pump was connected to the reactor through another polythene tube through a T-joint connection, which allowed the simultaneous entry of the carrier gas, nitrogen. The flow rate of nitrogen was controlled by a precision needle valve and measured by a rotameter.

3.1.2 Preheater –cum-mixing zone

The preheater-cum-mixer was the upper part of reactor tube (about 15 cm in length) which was packed with quartz particles. The reactor tube used was made of silica glass, which can be used safely upto 1200°C. The diameter of tube was 12 mm (ID) and length 36 cm. The inlet end was fitted with a glass T joint, where nitrogen and toluene entered. The thermocouple used to measure the temperature of the catalyst bed was placed axially from the top. The temperature in preheating zone was almost the same as of reactor. The preheater cum mixture was heated (simultaneously to the reactor) electrically by means of a kanthal wire coil wound around it. The rate of heating was adjusted by controlling the flow of

Nitrogen   Toluene

Preheating section

Reactor

Post heating section

S.S. Sieve

230 mm

130 mm

Quartz bed

Insulation

Heating coil

REACTOR   TUBE

Material of construction = silica glass
I.D.   = 12mm
O.D.   = 16mm
Wall thickness   = 2mm
Length   = 360mm

To condenser
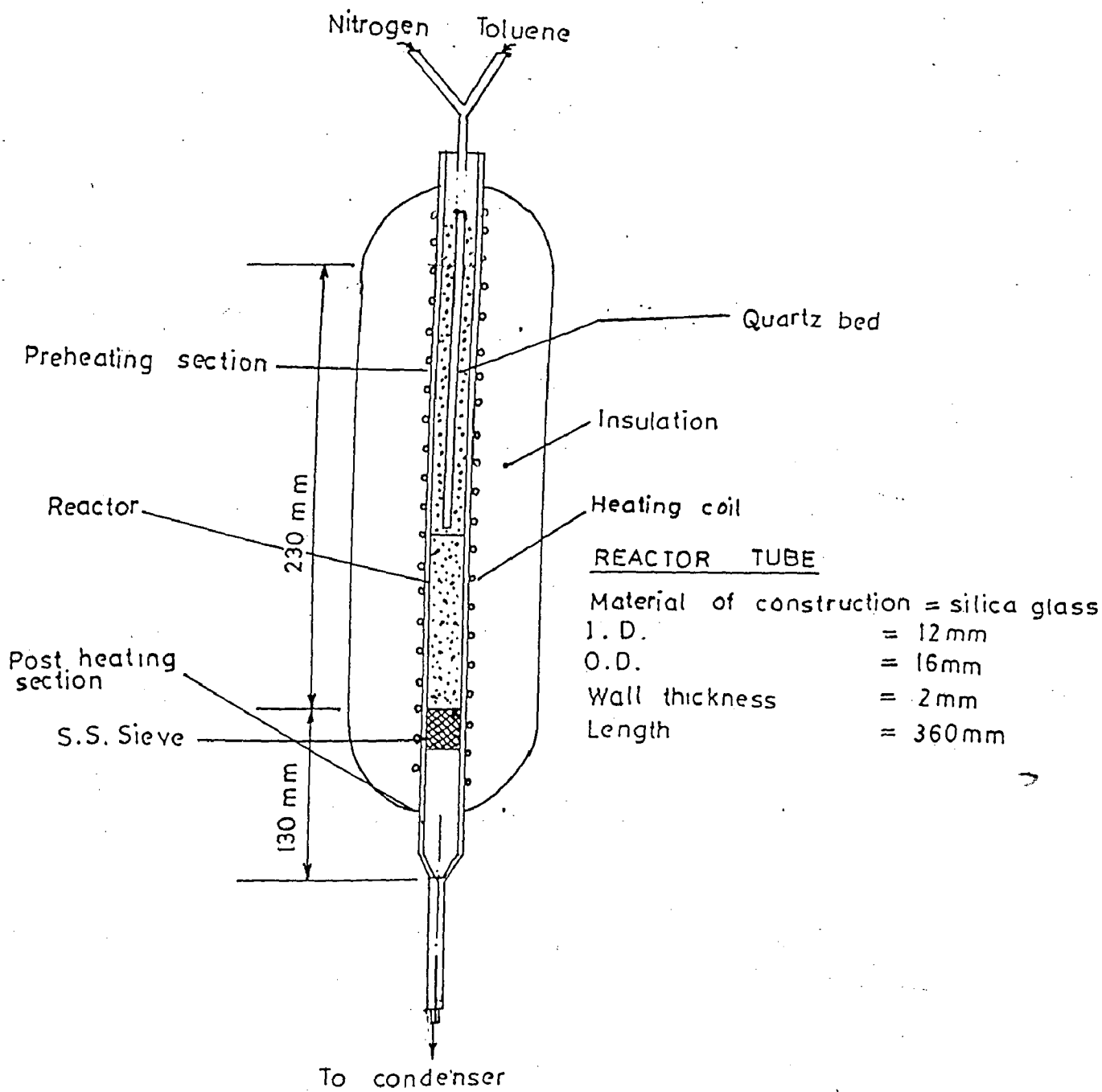
FIG. 3.3   REACTOR   DETAILS

electric current through this wire with the help of the variable autotransformer, which was in turn connected to a temperature controller-cum-indicator to which also the iron-constantan thermocouple was connected.

3.1.3 Reaction Zone

After preheating zone, the reactor zone starts in same tube, which contains 2 gm of catalyst mixed with an equal volume of quartz particles of the same size. The total length of reaction zone in reactor tube was about 9 cm. The catalyst particles were supported on a stainless steel mesh (about 1 cm length). The electrical heating was provided throughout the length of the reactor to keep a uniform temperature. The bottom end of reactor was connected to $120°$ glass bend through which the condensers were joined. The entire reactor system with its heating element was insulated by means of glass wool lagging to avoid the loss of heat.

3.1.4 Condenser and Cooling system

The condensers for condensing the product vapour from the reactor were about 1.0 m long . The chilled water at $4°C$ was passed through inner coil of glass while the product vapour passed through the annular space. The inner dia of condenser was 24 mm. The cooling water was circulated through the condenser by a centrifugal pump. The condensers were kept at an angle of $30°$ with the horizontal.
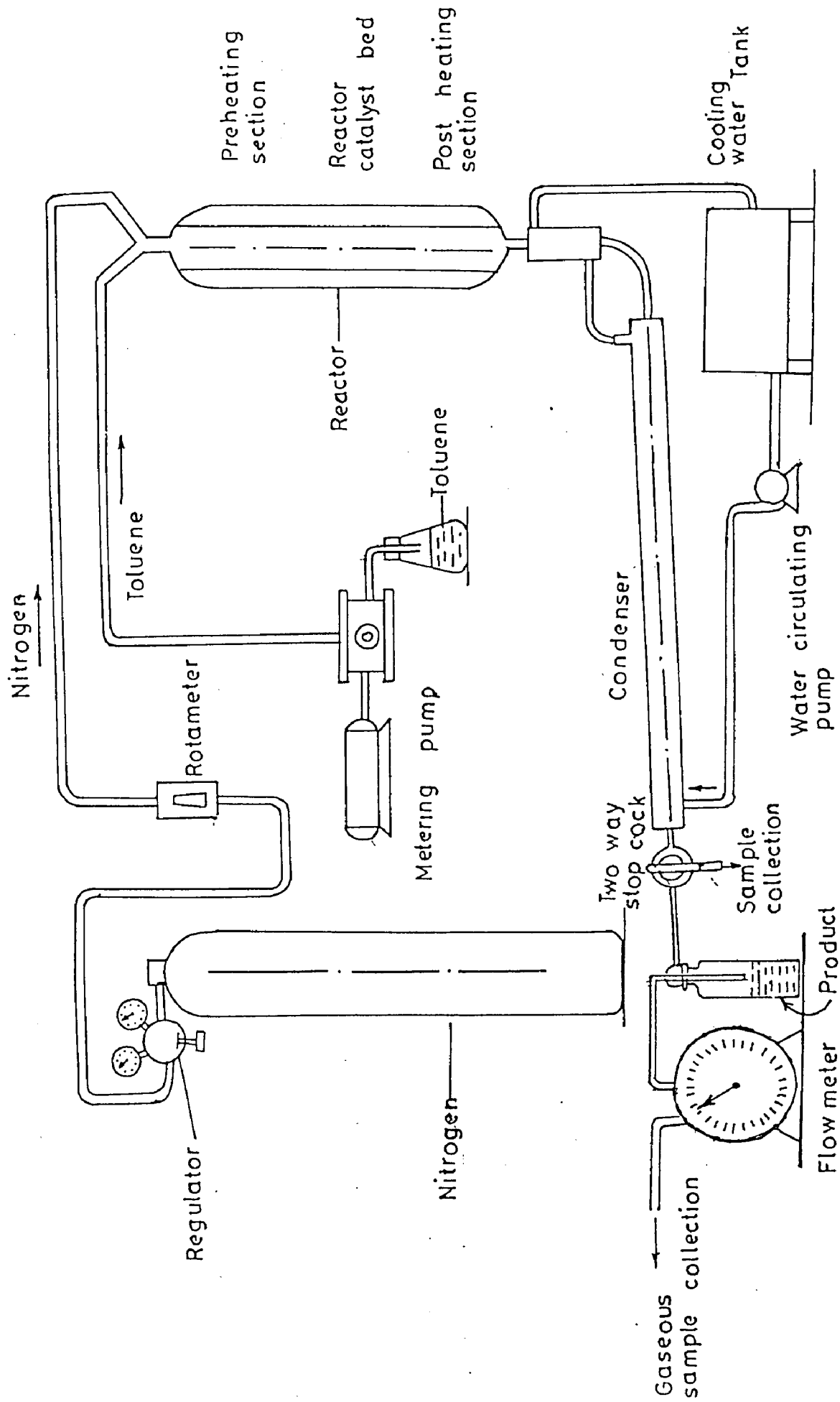
FIG. 3.2 SCHEMATIC DIAGRAME OF EXPERIMENTAL SET-UP

67

3.1.5 Experimental Procedure for activity test

For taking an experimental run the weight reactor was filled with 2 g of catalyst. To do this, the reactor was first removed from the condenser. The mixture of catalysts and quartz particles (both in the size range $-14 + 22$ B.S.S.) having approximately same volume were filled above the S.S. screen support. Before the start of the activity tests, the catalyst was heated (activated) at $570^\circ C$ in nitrogen atmosphere for 1 h.

The cooling of the catalyst bed to the reaction temperatures was done in a current of nitrogen. After attainment of the desired reaction temperature, the nitrogen flow rate was re-adjusted to the desired value for the reactions. The rate of nitrogen through the catalyst bed was measured by means of the rotameter. Toluene was fed using a peristalic pump. The flow rate was re-confirmed by measuring the volume in a given time.

The conversion versus temperature studies for all the catalysts were done at atmospheric pressure. The toluene flow rate was maintained at 0.3 to 0.45 ml/min and nitrogen flow rate from 0.3 to 0.45 liter/min. The amount of catalyst provided a fixed W/F_{T0} ratio of 7.0 to 12.0 kg.hr/kmol. The nitrogen/toluene feed (N_2/F_{T0}) molal ratio was kept at 4.2-5.0. Several batches of fresh catalyst were used for taking runs at different temperature that varied from $300^\circ C$ to $650^\circ C$.

The product passed through condenser in which product stream was cooled by circulating chilled water in inner circular coiled of glass condenser. Samples were collected after an interval of 10 minutes, which were then analyzed using a gas chromotograph to determine mole composition of components in product.

3.1.6 Run procedure for Kinetic Study

Kinetic studies has been performed on HZSM-5 (SAR-19), 1.756%Cr1.923%Th HZSM-5 (SAR-32) and 3.95% Pb-HY (SAR-3) catalysts. for each cases 2 gm catalyst were taken. Samples were collected at different values of W/F_{T0} at fixed temperature. For verification of the proposed model, runs were taken at different toluene flow rates ranging from 0.52 to 2.05 ml/min corresponding to different W/F_{T0} ratio ranging from 7 to 14 gm of catalyst hr/gmol of toluene.

For 1.756%Cr1.923%Th HZSM-5 (SAR-32) catalyst kinetic was studied at 400 and 550°C, molal ratio of feed of nitrogen to toluene (N_2/F_{T0}) was fixed at 4.15.

For 3.95 wt.% Pb-HY (SAR-3) catalyst the kinetic was studied at 400 and 550°C molal ratio of feed of toluene nitrogen (FT/N_2) was fixed at 1. Kinetic studies of HZSM-5 (SAR-19) was at 450 and 550°C, molal ratio of feed of toluene to nitrogen (N_2/FT) was fixed at 4.334.

The reactor along with catalyst was initially heated at 570°C for PbHY, CrThHZSM-5 catalysts and at 400°C for HZSM-5 (SAR-19) catalyst for one hr. The temperature was choosen as above because at this temperature the zeolite was calcined. After one hr of activation the catalyst was washed for half an hour in a current of nitrogen at reaction temperature. The flow of nitrogen was adjusted at the desired value corresponding to a fixed W/F_{T0} ratio. The feed pump was started and the whole system was allowed to stablized at desired temperature. After stablization for about 10 minutes a product sample was collected which was

analysed by gas chromotograph. This constituted one reading. Similarly different reading were taken for different W/F_{T0} by adjusting the flow of nitrogen and toluene to a fixed value of F_{T0}/N_2.

3.2 ANALYSIS OF SAMPLES

The sample collected during a run contained benzene, toluene, p-xylene, m-xylene and o-xylene. Analysis of the samples was carried out by gas-liquid chromatograph (nucon-5700) using oracle-2 software in our laboratory. Flame ionization detector (FID) was used with nitrogen as the carrier gas, H_2 as fuel gas and O_2 for burning the sample. The gas chromotographic column used for this purpose was celite-545.

The different operating conditions employed for the analysis were as follows :

1.	Sample injected	0.2 micro litre
2.	Injection Port temperature	$180^{\circ}C$
3.	Oven temperature	$90-120^{\circ}C$
4.	Detector temperature	$180^{\circ}C$
5.	Nitrogen pressure	1.2 kg/cm^2
6.	Oxygen pressure	0.8 kg/cm^2
7.	Hydrogen pressure	0.8 kg/cm^2
8.	Sensitivity	10
9.	Attenuation	8

The percentage composition of the different constituents of the samples was then calculated using the data (area) obtained by gas chromotograph. The procedure opted for calculation, composition, conversion are p-xylene selectivity in xylene is represented in Chapter 5.

CHAPTER IV

KINETICS AND THERMODYNAMIC DERIVATIONS

For kinetic study heterogeneous and homogeneous models have been developed and fitted to the experimental results obtained for toluence disproportionation reactions.

4.1. HETEROGENEOUS MODEL FOR TOLUENE DISPORPORTIONATION

The heterogeneous models for catalytic reaction have been developed assuming one of the three steps for catalyst reactions as rate limiting. The three steps are adsorption of reactant on catalysts surface, reaction of reactant on the catalyst, surface and desorption of product from the catalyst surface.

The reaction steps for touluene disproportionation reaction assuming xylene is adsorbed on surface is as below :

Adsoprtion of toluene on the surface of catalysts is represented by reactionn

$$T + S \; \underset{k_T'}{\overset{k_T}{=}} \; T.S. \qquad (4.1)$$

Reaction of toluene on the surface of catalysts., assuming xylene is adsorbed and benzene in gas phase is represented by equation

72

$$T + T.S = \frac{k_s}{k_s'} \ X.S + B \qquad (4.2)$$

Desorption xylene from catalytic surface is given by equation

$$X.S \ \frac{k_d}{k_d'} \ X+S \qquad (4.3)$$

4.1.1 Development of Kinetic Model in terms of Partial pressure

From Eqn. (4.1)

$$r_{AD} = k_T P_T C_v - k_T' C_{T.s}$$

$$r_{AD} = k_T (P_T C_v - C_{T.s}/K_T) \qquad (4.4)$$

Where

$$K_T = k_T/k_T'$$

Rate equation of reaction of toluene on catalytic surface is

$$r_s = k_s P_T C_{T.s} - k_s' P_B C_{X.s}$$

$$r_s = k_s (P_T C_{T.s} - P_B C_{X.s}/K_s) \qquad (4.5)$$

$$K_s = k_s/k_s'$$

Rate equation of desorption of xylene from catallytic surface is

$$r_D = k_D C_{X.s} - k_{D'} \ P_X C_v$$

$$= k_D (C_{X.s} - P_X C_v/K_D) \qquad (4.6)$$

$$K_D = k_D/k_{D'}$$

Total concentration of vacant (active cites) is

$$C_t = C_v + C_{T.S} + C_{x.s} \tag{4.7}$$

4.1.1.1 Kinetic Model for adsorption of toluene is rate limiting step

$$r_{AD} = k_T[P_T C_v - C_{T.S}/K_T] \tag{4.4}$$

For above case k_s and k_D (from equation 4.5 and 4.6) are high therfore,

$$r_s/k_s, \quad r_D/k_D \cong 0$$

From equation 4.5

$$\frac{P_B \cdot C_{xs}}{K_S} = P_T \cdot C_{T.S}$$

$$C_{TS} = \frac{P_B \cdot C_{x.s}}{K_s P_T}$$

or

$$C_{T.S} = \frac{P_B P_x C_v}{K_D K_s P_T} \tag{4.8}$$

From equation 4.6

$$C_{xs} = \frac{P_x.C_v}{K_D} \qquad (4.9)$$

Putting value of $C_{T.S}$ from Eqn. 4.8 in Eqn. 4.4.

$$r_{AD} = k_T.C_v\left[P_T - \frac{P_BP_x}{K_DK_sK_TP_T}\right] \qquad (4.10)$$

Puting $C_{T.S}$, $C_{x.S}$ from eqation 4.8 and 4.9 in Eqn.4.7

$$C_t = C_v + \frac{P_BP_xC_v}{K_DK_sP_T} + \frac{P_x.C_v}{K_D}$$

$$C_v = \frac{C_t}{[1+\frac{P_BP_x}{K_DK_sP_T} + \frac{P_x}{K_D}]} \qquad (4.11)$$

Putting value of C_v from Eqn. 4.11 in Eqn. 4.10.

$$R_{AD} = \frac{k_TC_t[P_T-\frac{P_BP_x}{K_TK_DK_sP_T}]}{[1+\frac{P_BP_x}{K_DK_sP_T} + \frac{P_x}{K_D}]}$$

$$R_{AD} = \frac{k_TC_t[P_T-\frac{P_BP_x}{K_eP_T}]}{[1+\frac{P_BP_x}{K_DK_sP_T} + \frac{P_x}{K_D}]} \qquad (4.12)$$

75

Where,

$K_e = K_T K_S K_D$

K_e = Thermodynamic equilibrium constant of toluene disproportionation reaction

K_D = Desorption equilibrium constant of xylenes

$K_D = \dfrac{1}{K_x}$, Adsorption equilibrium constant of xylenes

$$r_{AD} = \frac{k_1 \ [P_T - \frac{P_B P_x}{K_e P_T}]}{[1 + \frac{P_B P_x K_T}{K_e P_T} + P_x K_x]} \qquad (4.13)$$

$k_1 = k_A C_t$

k_1 is toluene disproportionation reaction rate constant for absorption of toluene is rate limiting step.

Equation 4.13 is rate equation in·terms of partial pressure for adsorption of toluene as rate limiting.

4.1.1.2 Kinetics Model for surface reaction of toluene as rate limiting step

Taking rate equation from Eqn. 4.5

$$r_s = k_s.(P_T C_{T.s} - \frac{P_B \ C_{x.s}}{K_s} \qquad (4.5)$$

From equation 4.4 for above case

$$C_{T.s} = K_A P_T C_v \qquad (4.14)$$

From equation 4.6

$$C_{xS} = \frac{P_x C_v}{K_D} \qquad (4.15)$$

Total concentration of active sites is

$$C_t = [C_v + C_{T.s} + C_{x.s}]$$

From Eqn.4.4

$$C_t = [C_v + K_T P_T C_v + \frac{P_x C_v}{K_D}] \qquad (4.16)$$

ing value of $C_{T.s}, C_{x.s}$ from equation 4.14 and 4.15 in Eqn. 4.5

$$r_s = K_s(P_T^2 K_T C_v - \frac{P_B P_x}{K_s K_D} C_v)$$

$$r_s = \left[\frac{P_T^2 K_T - \dfrac{P_B P_x}{K_s K_D}}{1 + \dfrac{P_x}{K_D} + K_T P_T} \right] k_s C_t$$

$$r_s = \left[\frac{P_T^2 K_T - \dfrac{P_B P_x K_T}{K_e}}{1 + P_X K_x + K_T P_T} \right] = k_s C_t$$

$$r_s = \frac{K_2 K_T [P_T^2 - \dfrac{P_B P_x}{K_e}]}{1 + P_X K_x K_T P_T} \qquad (4.17)$$

77

where

$$K_e = K_T K_s K_D$$

$$\frac{1}{K_D} = K_x$$

$$k_2 = K_s C_t$$

K_2 is ate constant of toluene disproportionation reaction of surface reaction is rate limiting step.

Total vacant active sites is

$$C_t = C_v + C_{T.s} + C_{X.s}$$

$$C_t = C_v[1 + K_T P_T + \frac{P_T^2 K_T K_s}{P_B}]$$

Puting in Eqn.4.19

$$r_d = \frac{k_d C_v (\frac{P_T^2 K_T K_s}{P_B} - \frac{P_x}{K_D})}{P_T^2 K_T K_s}$$

4.1.1.3 Kinetics Model for desorption of xylene as rate limiting step

Taking rate equation 4.6.

$$r_D = k_D \cdot \left[C_{xs} - \frac{P_x \cdot C_v}{K_D} \right] \quad (4.6)$$

From equation 4.4

$$r_{AD}/k_T = 0$$

$$C_{T.s} = K_T P_T C_v$$

From Eq.4.5

$$\frac{P_B . C_{xS}}{K_s} = P_T . C_{T.s}$$

So

$$C_{x.s} \frac{P_T 2 K_A C_v K_s}{P_B} \qquad (4.18)$$

Putting value of $C_{x.s}$ from equation 4.18 in equation 4.6

$$r_d = k_d . C_v \left(\frac{P_T 2 K_T K_s}{P_B} - \frac{P_x}{K_D} \right) \qquad (4.19)$$

$$r_D = \frac{k_3 \left(\frac{P_T 2 \; K_e}{P_B \; K_D} - \frac{P_x}{K_D} \right)}{1 + K_A \; P_T \; + \frac{P_T 2 \; . K_e}{P_B \; K_D}}$$

where,

$$k_3 = k_D C_t$$

k_3 is the toluene disproportionation rate constant for desorption of toluene is rate limiting step.

$$r_D = \frac{k_3 \left(\frac{P_T 2 \; K_e \; K_x}{P_B} - P_x K_x \right)}{1 + K_T \; P_T + \frac{P_T 2 \; . K_e K_x}{P_B}} \qquad (4.20)$$

4.1.2 Development of kinetics model in terms of converrsion (x) of toluene :

Rate of reaction of toluene in terms of mole of toluene converted per unit time per gm of catalysts can be represented by equation

$$r_T = \frac{dF_T}{dw} = \frac{d}{dw} [F_{To}(1-x)]$$

From equations

$$2T = B + X$$

$$T = \frac{B}{2} + \frac{X}{2}$$

$$P_T = P_{TO}(1-x)$$

$$P_B = P_{TO}(\phi/B + x/2) = P_{TO}.x/2$$

$$P_x = P_{TO}(\phi X + x/2) = P_{TO}.x/2$$

where,

$$\phi B = P_{BO}/P_{TO} = 0$$

$$\phi X = P_{xo}/P_{TO} = 0 \quad \text{(because no benzene and xylenes are present initially in feed)}$$

At steady state

$$r_{AD} = r_s = r_D$$

From equation 4.13

$$r_{AD} = \frac{dx}{dw} = \cfrac{K_1[P_{TO}(1-x)- \cfrac{P_T^2 \, x^2}{4K_e \, P_{TO}} \quad \cfrac{}{(1-x)}]}{F_{To}[1+ \cfrac{P_{TO}^2 \, x^2 \, K_T}{4 \, K_e \, P_{TO}(1-x)} + \cfrac{P_{TO} \, x}{2} K_x]}$$

$$r_{AD} = \frac{dx}{dw} = \frac{K_1 P_{TO}[(1-x) - \frac{x^2}{4K_e(1-x)}]}{F_{TO}[1 + \frac{P_{TO} \, x^2 \, K_T}{4 \, K_e \, (1-x)} + \frac{P_{TO} \, x}{2} K_x]} \qquad (4.21)$$

Equation 4.21 is rate equation in terms of partial pressure of toluene fed in the reactor and its conversion for adsorption of toluene is rate limited step. From Eqn. 4.17

$$r_s = \frac{dx}{dw} = \frac{K_2 K_T P_{TO}^2 (1-X)^2 - \frac{x^2}{4K_e}]}{F_{TO}[1 + \frac{P_{TO} \, x \, K_x}{2} + K_T P_{TO}(1-x)]} \qquad (4.22)$$

where,

$$k_2 = k_s C_t$$

Equation 4.22 is the rate Eqn. for disproportionation of toluene considering surface reaction as controlling step.

From equation 4.20.

$$r_D = \frac{dx}{dw} = \frac{k_3 P_{TO}[2(1-x)^2 K_e K_x/x - xK_x/2]}{F_{TO}[1 + K_T P_{TO}(1-x) + 2K_e K_x P_{TO}(1-x)^2/x]} \qquad (4.23)$$

Equation 4.23 is rate equation for toluene disproportionation, desorption of xylene as rate limiting step.

4.1.2.1 Solution of rate equation for adsorption of toluene as rate limiting step

Equation 4.21 may be further solved as

$$\frac{dx}{dw} = \frac{k_1 P_{TO}}{F_{TO}} \left[\frac{4\,K_e(1\text{-}2x)}{4K_e(1\text{-}x) + P_{To}K_T\,x^2 + 2K_e(x\text{-}x^2)} \right]$$

Assuming $K_x = K_T$;Rate of adsorption of toluene = Rate of desorption of xylenes

$$\frac{dx}{dw} = \frac{k_1 P_{TO}}{F_{TO}} \cdot \left[\frac{4\,K_e(1\text{-}2x)}{4K_e + (\text{-}4K_e + 2P_{TO}K_e \cdot K_T)x + (1\text{-}2K_e)P_{TO}K_T x^2} \right]$$

$$\int_0^x \left[\frac{4K_e + (2P_{TO}K_eK_T\text{-}4K_e)x + (1\text{-}2K_e)P_{To}K_T x^2)}{1\text{-}2x} \right] dx = \int_0^w \frac{4K_e k_1 P_{T}^{o}}{F_{TO}} dw$$

Integrating on both sides

$$4K_e \int_0^x \frac{dx}{1\text{-}2x} + (2P_{TO}K_eK_T\text{-}4K_e) \int_0^x \frac{x}{1\text{-}2x}\, dx + (1\text{-}2K_e)P_{TO}K_T \int_0^x \frac{x^2}{1\text{-}2x}\, dx$$

$$= \int_0^w \frac{4K_e k_1 P_T}{F_{TO}}\, dw$$

Solving by synthetics division method

$$4K_e \frac{\log(1\text{-}2x)}{-2} + (2P_{TO}K_eK_T\text{-}4K_e)\int_0^x \frac{-1}{2} + \frac{0.5}{1\text{-}2x}dx + (1\text{-}2K_e)P_{TO}K_T \int_0^x (\text{-}\frac{x}{2} - \frac{-1}{4} + \frac{0.25}{1\text{-}2x})dx$$

$$= \frac{4K_e k_1 P_{To}}{F_{TO}}$$

$$-2K_e.\log(1\text{-}2x) + (2P_{TO}K_eK_T\text{-}4K_e)\left[\frac{-1}{2}x + \frac{\log(1\text{-}2x)}{-2x^2}\right] + 1(1\text{-}2K_e)P_{TO}K_T[\frac{-x2}{4} + \frac{-x}{4} +$$

$$\frac{\log(1\text{-}2x)}{4.(-2)} = \frac{4K_ek_1P_{T^0}}{F_{TO}}$$

$$\frac{1}{4K_eP_{To}}[-2K_e\log(1\text{-}2x) + (2P_{TO}K_eK_T\text{-}4K_e)[\frac{-1}{2}x + \frac{\log(1\text{-}2x)}{-4}] + 1(1\text{-}2K_e)P_{TO}K_T[\frac{-x2}{4} +$$

$$\frac{-x}{4} + \frac{\log(1\text{-}2x)}{4.(-2)}] = \frac{k_1W}{F_{TO}} \tag{4.24}$$

By plotting value of L.H.S of equation 4.24 against W/F_{TO} the toluene disproportionation constant k_1 (adsorption of toluene rate limiting) may be determined.

4.1.2.2 Solution of rate equation for surface reaction of toluene as rate limiting step

Equation (4.22) may further be solved as

$$r_s = \frac{dx}{dw} = \frac{k_2K_TP_{TO^2}[(1\text{-}x)^2 - \frac{x^2}{4K_e}]}{F_{To}[1 + \frac{P_{TO}.xK_x}{2} + K_TP_{TO}(1\text{-}x)} \tag{4.22}$$

$$\frac{dx}{dw} = \frac{k_2K_TP_{TO}^2[4K_e(1\text{-}2x+x^2)\text{-}x^2}{4K_eF_{To}[1 + \frac{P_{To}xK_T}{2} + K_TP_{TO}\text{-}K_T\text{-}K_TP_{TO}x}$$

$K_T = K_x$ as assumed previously

$$\frac{dx}{dw} = \frac{k_2K_TP_{TO^2}[x^2(4K_e\text{-}1)\text{-}8K_ex+4K_e}{4K_eF_{TO}[(1+K_TP_{TO}) + (K_TP_{To}/2)x]}$$

$$\int_{0}^{x} \frac{[(1+K_T P_{TO})-(K_T P_{TO}/2)x]}{[x^2(4K_e-1)-8K_e x+4K_e)} \, dx = \frac{k_2 K_T P_{TO}^2}{4K_e F_{TO}} \int_{0}^{w} dw$$

$$\int_{0}^{x} \frac{[(1+K_T P_{TO})]}{[x^2(4K_e-1)-8K_e x+4K_e)} \, dx - \int_{0}^{x} \frac{(K_T P_{TO}/2)x}{[x^2(4K_e-1)-8K_e x+4K_e)} \, dx \frac{k_2 K_T P_{TO}^2 W}{4K_e F_{TO}}$$

$$\underbrace{\int_{0}^{x} \frac{(1+K_T P_{TO})}{x^2 - \frac{8K_e x}{(4K_e-1)} + \frac{4.K_e}{(4K_e-1)}} \, dx}_{I} - \underbrace{\int_{0}^{x} \frac{(K_T P_{TO}/2)x}{x^2 - \frac{8K_e x}{(4K_e-1)} + \frac{4.K_e}{(4K_e-1)}} \, dx}_{II} = \frac{k_2 K_T P_{To}^2 W(4K_e-1)}{4K_e F_{To}}$$

Taking (I) part of L.H.S of above equation

$$I = \int_{0}^{x} \frac{(1+K_T P_{TO})}{(x - \frac{4K_e x}{(4K_e-1)})^2 + (\frac{2\sqrt{K_e}}{(4K_e-1)})^2} dx$$

Let $1 = \dfrac{K_e}{4K_{e-1}}$

$$I = (1+K_T P_{TO}) \int_{0}^{x} \frac{1}{(x-4l)^2 - 16l^2 + 4l}$$

$$= 1+K_T P_{TO} \int_{0}^{x} \frac{1}{-[(16l^2-4l)-(x-4l)^2]}$$

$$= \frac{(-1)(1+K_T P_{To})}{2\sqrt{16l^2-4l}} \Big[\log \frac{\sqrt{16l^2-4l} + x - 4l}{\sqrt{16l^2-4l} - x + 4l}\Big]_{0}^{x}$$

Taking limits of above equation

$$= \frac{-(1+K_T P_{To})}{2\sqrt{16l^2-4l}} \left[\log\left(\frac{\sqrt{16l^2-4l} + x - 4l}{\sqrt{16l^2-4l} - x + 4l}\right) - \log\left(\frac{\sqrt{16l^2-4l} - 4l}{\sqrt{16l^2-4l} + 4l}\right)\right]$$

Taking II part of L.H.S above eauation

$$\int_o^x \frac{x\ (1+K_T P_{To}/2)}{x^2-8xl+4l}\ dx = \int_o^x \frac{x\ (1x+0)dx}{x^2-8xl+4l}$$

$$x+0 = K_1 \frac{d}{dx}(x^2-8xl+4l) + K_2$$

$$x+0 = k_1\ (2x-8l) + K_2 \qquad\qquad (*)$$

$$x+0 = (2K_1)x + (-8lk_1+K_2)$$

comparing x coefficient on both sides & constants

$$2K_1 = 1$$

$$K_1 = 1/2$$

$$-8lK_1+K_2 = 0$$

$K_2 = 4l$, putting K_1 & K_2 in equation *

$$(1+K_T P_{To}/2)\int_o^x \frac{x}{x^2-8xl+4l}\ dx = (1+K_T P_{To}/2)\int_o^x \frac{1/2\ (2x-8l)+4l}{x^2-8xl+4l}\ dx$$

$$= 1/2\ (1+K_T P_{To}/2)\left[\int_o^x \frac{(2x-8l)}{x^2-8xl+4l}\ dx + 4l\int_o^x \frac{1}{x^2-8xl+4l}\ dx\right]$$

$$= 1/2(1+K_T P_{To}/2)\left[\log\ (x^2-8xl+4l)\Big|_o^x + 4l\int_o^x \frac{1}{x^2-8xl+4l}\ dx\right]$$

$$II = 1/2(1+K_T P_{To}/2)[[\log\ (x^2-8xl+4l)-1/2\ \log\ (4l)$$

85

$$+4I(-1/2) \; \frac{1}{2 \; \sqrt{16I^2-4I}} \; [\log \; (\frac{\sqrt{16I^2-4I} + x - 4I}{\sqrt{16I^2-4I} - x + 4I}) \; -\log \; (\frac{\sqrt{16I^2-4I} \;\; - 4I}{\sqrt{16I^2-4I} \;\; +4I})]]$$

$$I+II \; = \; \frac{k_2 K_T P_{To}^2 W(4K_e-1)}{4K_e F_{To}}$$

$$I+II \; = \; \frac{k_2 K_T P_{To}^2 W}{I \, F_{To}}$$

$$\frac{(I+II)I}{K_T P_{To}^2} \; = \; \frac{k_2}{F_{To}} \; W \tag{4.25}$$

By plotting L.H.S. of equation .4.25 against W/F_{TO} the disportionation reaction constant k_2 of surface reaction control may be dterrmined.

4.1.2.3 Solution of rate equation for desorption of xylene as rate limiting step

the rate equation (4.23) for desorption of xylene as controlling step may be further solves as

$$r_D \; = \; \frac{dx}{dw} \; = \; \frac{k_3 P_{T^o}}{F_{T_o}} \; \frac{[\frac{2(1-X)^2 K_e \cdot K_x}{x} - \frac{P_{T_o} x K_x}{2}]}{1+K_T P_{T_0}(1-x) + \frac{2P_{To}(1-x)^2}{x} K_e K_x}$$

Considering,

$K_x = K_T$ (as assumed previously)

$$\frac{dx}{dw} \; = \; \frac{k_3 P_{To} \; [2(1-X)^2 K_e K_T - 0.5 P_{To} x^2 K_T]}{F_{To} \; [x + x K_T P_{T_0}(1-x) + 2P_{T_0}(-x)^2 K_e K_T]}$$

86

$$\int_0^x \frac{x + xK_TP_{T_o}(1-x) + 2P_T(1-x)^2K_eK_T]}{[2(1-x)^2K_eK_T - 0.5P_{T_o}x^2K_T} \, dx = \int_0^w \frac{K_3P_{T_o}}{F_{T_o}} \, dw$$

$$= \frac{x + xK_TP_{T_o}-x^2K_TP_{T_o}+(2P_{T_o}-4P_{T_o}x+2P_{T_o}x^2)K_eK_T]}{(1-2x+x^2)2K_eK_T - 0.5P_Tx^2K_T} = \frac{K_3P_{T_o}W}{F_{T_o}}$$

$$= \frac{\overset{a}{x^2[[2K_eK_TP_{T_o}-K_TP_{T_o}]} + \overset{b}{x(1+K_TP_{T_o}-4P_{T_o}K_eK_T)} + \overset{c}{2P_{T_o}K_eK_T]}}{\underset{d}{x^2(2K_eK_T-0.5P_{T_o}K_T)} - \underset{e}{(4K_eK_T)x} + \underset{g}{2K_eK_T}}$$

define g = f/2

or f = $4K_eK_T$

$$\Rightarrow \int \left(\frac{ax^2+bx+c}{dx^2+ex+f} \right) dx = \int \frac{K_3P_{T_o}W}{F_{T_o}}$$

This is improper fraction (x degree in both numerator and denominator is same)

Further it will be made proper by synthetic division. converting the improper fraction (from the above) as proper function by synthetic division.

$$
\begin{array}{r}
a/d \\
dx^2+ex+f \overline{) ax^2 + bx + c} \\
\underline{ax^2+e.a/(d).x+a.f/d} \\
(b-\frac{e.a}{b}) x + (c-\frac{a.f}{d})
\end{array}
$$

$$\left(\frac{ax^2+bx+c}{dx^2+ex+f} \right) = \frac{a}{b} + \frac{\overset{A}{(b-e.a/d)x} + \overset{B}{(c-af/d)}}{dx^2+ex+f} \qquad (4.26)$$

87

Above function is of the type $\left[\dfrac{ax+b}{lx^2+mx+c}\right]$ (4.27)

where,

$$a = 2K_eK_{To} - K_TP_{To}$$

$$b = 1 + K_TP_{To} - 4P_{To}K_eK_T$$

$$c = 2P_{To}K_eK_T$$

$$d = 2K_eK_T - 0.5P_{To}K_T$$

$$e = -4K_eK_T$$

$$f = 4K_eK_T$$

Equation 4.27 can be expressed as

$$Ax+B = K_1 \frac{d}{dx}(lx^2+mx+c) + K_2$$

Here K_1 & K_2 are to be calculated

Further dx^2+ex+f is to be made in to the form x^2+a^2

or x^2-a^2 or a^2-x^2 whichever it gives on simplification

Taking equation 4.27

$$Ax +B = K_1[2xd+e] +K_2 = (2dK_1)x+ (eK_1+K_2)$$

because $lx^2+mx+c = dx^2+ex+f$

Comparing the coefficients of x and constants separately on both sides

$$A = 2.dK_1$$

where,

$$K_1 = A/(2d)$$

$$B = eK_1+K_2$$

$$B = eA/(2d) + K_2$$

and

$K_2 = B - Ae/(2.d)$

so,

$Ax + B = A/(2d) (2xd + e) + B - A.e/(2d)$

Equation 4.26 becomes

$$\int_0^x \frac{a}{d}\, dx + \frac{A}{2d}\, [\log\,(dx^2 + ex + f)]_0^x + \int_0^x \frac{B - Ae/(2d)}{dx^2 + ex + f}\, dx = \int_0^w \frac{k_3 P_{T^0}}{F_{T_0}}\, dw \qquad (4.28)$$

$(dx^2 + ex + f)$ may be written as

$dx^2 + ex + f = d[x^2 + (e/d)x + f/d] = d[(x + (e/(2d))^2 - e^2/4d^2) + f/d]$

$= d[(x + e/(2d))^2 + (\sqrt{f/d - e2/4d^2})^2]$

Equation 4.28 yield

$$\frac{1}{P_{T_0}}\, [\frac{a}{d}\, x + [\, \frac{A}{2d}\, \log\,(dx^2 + ex + f) + (B - \frac{A.e}{2d})\, \frac{1}{d}\, \frac{1}{\sqrt{(f/d - e^2/4d_2}}\, \tan^{-1} \frac{x + e/(2d)}{\sqrt{(f/d - e^2\,/4d^2)}}$$

$$-[\frac{A}{2d}\, \log\,(f) + (B - \frac{A.e}{2d})\, \frac{1}{d}\, \frac{1}{\sqrt{(f/d - e^2/4d^2)}}\, \tan^{-1}(\frac{e/(2d)}{\sqrt{(f/d - e^2/4d^2)}})]] = \frac{k_3\, W}{F_{T_0}} \qquad (4.29)$$

where

$A = b - ea/d$

$B = c - af/d$

By plotting L.H.S. of equation 4.29 against W/F_{T_0}, the k_3, (rate constant of disproportionation reaction) in term of desorption of xylene may be calculated.

4.2 HOMOGENEOUS MODEL OF TOLUENE DISPORPORTIONATION

For kinetic study . considering a catalyst without any side reaction, disproportonation of volume to benzene and xylens is represented by the reaction.

$$\text{Rate} = -r_T = -\frac{dF}{dw} = kp(p_T^2 - \frac{P_B P_X}{K_p}) \tag{4.31}$$

Since total pressure through reactor was constant,

$$P_{To} + P_{No} = P_B + P_T + P_x + P_{No}$$

Since nitrogen is not taking part in the reaction, total number of moles at the inlet and outlet are to same

$$P_{To} = P_B + P_T + P_X \tag{4.32}$$

$$P_{To} = \frac{nT_o}{V} RT \quad \text{and } P_T = \frac{nT}{V}.RT \tag{4.33}$$

Since X = mole fraction conversion

$$n_T = n_{To} (1-x)$$

The number of moles of benzene (n_B) number of moles of xylene, at the outlet can be written as

$$n_B = n_{To} \frac{x}{2} \quad \text{,and} \quad n_X = n_{To} \frac{x}{2}$$

$$P_T = \frac{n_{To}}{V} (1-x)RT \quad = (1-x)P_{To} \tag{4.34}$$

$$P_B = \frac{n_{To}}{v} \frac{x}{2} RT \quad = \frac{x}{2} P_{To} \tag{4.35}$$

$$P_X = \frac{n_{To}}{v} \frac{x}{2} RT \quad = \frac{x}{2} P_{To} \tag{4.36}$$

Eqn. 4.30 can now be written as

$$-r_T = kp \; P_{To}^2 \left[(1-x)^2 - \frac{\frac{x}{2} \cdot \frac{x}{2}}{K_p} \right]$$

$$-\frac{dF}{dw} = k_P \cdot P_{To}^2 \left[(1-x)^2 - \frac{x^2}{4K_p} \right]$$

(4.37)
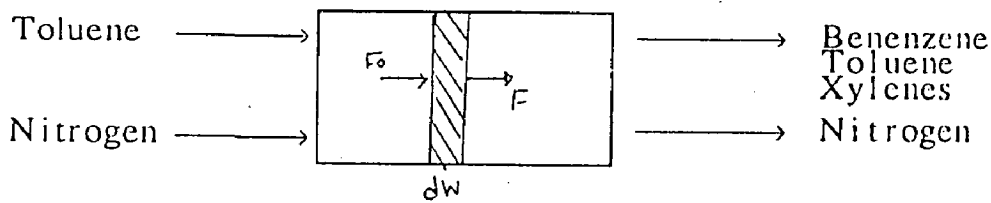
The mole fraction conversion of toluene is

$$x = \frac{F_o - F}{Fo}$$

$$F_o x = F_o - F$$

$$F = F_o(1-x)$$

$$dF = -F_o dx$$

substituting value of dF in Eqn. 4.37

$$\frac{F_o dx}{dw} = kpP_{T0}^2 \left[(1-x)^2 - \frac{x^2}{4Kp} \right]$$

$$\frac{F}{1-x} \frac{dx}{dw} = kpP_{T0}^2 \left[(1-x)^2 - \frac{x^2}{4Kp} \right]$$

$$\frac{K_P P_{To}^2}{F_o} \int_0^w dw = \int_0^x \frac{dx}{(1-x)^2 - \frac{x^2}{4K_P}}$$

$$\frac{w}{F_o} = \frac{1}{K_P P_{To}^2} \int_0^x \frac{dx}{(1-x)^2 - \frac{x^2}{4K_P}}$$

$$\frac{w}{F_0} = \frac{1}{k_P P_{To}^2} 4K_P \int_0^x \frac{dx}{4K_P(1-x)^2 - x^2}$$

$$\frac{w}{F_0} = \frac{1}{k_P P_{To}^2} 4K_P \int_0^x \frac{dx}{4K_P - 8K_P x + 4K_P x^2 - x^2}$$

$$\frac{w}{F_0} = \frac{1}{k_P P_{To}^2} 4K_P \int_0^x \frac{dx}{(4K_P - 1)x^2 - 8K_P x + 4K_P}$$

$$\frac{w}{F_0} = \frac{k_P}{k_P P_{To}^2} \int_0^x \frac{dx}{x^2 - \dfrac{8K_P x}{4K_P - 1} + \dfrac{4K_P}{4K_P - 1}} \tag{4.48}$$

The Eqn. 4.38 is in $x^2 - bx + c$ from, which can be written in a $x^2 + a^2$ or $a^2 - x^2$ or $x^2 - a^2$ which ever is obtained.

$$= \frac{4K_P}{k_P P_{To}^2 (4K_P - 1)} \int_0^x \frac{dx}{x^2 - 2\dfrac{4K_P x}{4K_P - 1} + \left(\dfrac{4K_P}{4K_P - 1}\right)^2 - \left(\dfrac{4K_P}{4K_P - 1}\right)^2 + \dfrac{4K_P}{4K_P - 1}}$$

$$= \frac{4K_P}{k_P P_{To}^2 (4K_P - 1)} \int_0^x \frac{dx}{\left(x - \dfrac{4K_P}{4K_P - 1}\right)^2 - \dfrac{(4K_P)^2 - 4K_P(4K_P - 1)}{(4K_P - 1)^2}}$$

$$= \frac{4K_P}{(4K_P - 1)k_P P_{To}^2} \int_0^x \frac{dx}{\left(x - \dfrac{4K_P}{4K_P - 1}\right)^2 - \left(\dfrac{\sqrt{4K_P}}{(4K_P - 1)^2}\right)^2}$$

$$\frac{\sqrt{K_P}}{k_P P_{To}^2} \left[\ln \frac{(4K_P - 1)x - 4K_P - \sqrt{4K_P}}{(4K_P - 1)x - 4K_P + \sqrt{4K_P}} \right]_0^x$$

Dividing the numerator and denominator by $2 K_P$

$$\frac{\sqrt{K_P}}{k_P P_{To}{}^2}\left[\ln\frac{2(1-\frac{1}{4K_P})x-2-\frac{1}{\sqrt{K_P}}}{2(1-\frac{1}{4K_P})x-2+\frac{1}{\sqrt{K_P}}}\right]_0^x$$

$$=\frac{\sqrt{K_P}}{k_P P_{To}{}^2}\left[\ln\frac{2Ax-2-\frac{1}{\sqrt{K_P}}}{2Ax-2+\frac{1}{\sqrt{K_P}}}-\ln\frac{-(2+\frac{1}{\sqrt{K_P}})}{(-2+\frac{1}{\sqrt{K_P}})}\right]$$

where, $A=1-\dfrac{1}{4K_p}$

$$=\frac{\sqrt{K_P}}{k_P P_{To}{}^2}\left[\ln\frac{(2Ax+(-2-\frac{1}{\sqrt{K_p}}))\ (-2+\frac{1}{\sqrt{K_p}})}{(2Ax+(-2+\frac{1}{\sqrt{K_P}})(-2-\frac{1}{\sqrt{K_P}})}\right]$$

$$=\frac{\sqrt{K_P}}{k_P P_{To}{}^2}\left[\ln\frac{(2Ax+(-2+\frac{1}{\sqrt{K_p}})+4-\frac{1}{K_P})}{(2Ax(-2-\frac{1}{\sqrt{K_P}})+4-\frac{1}{K_P})}\right]$$

$$\frac{w}{F_{To}}=\frac{\sqrt{K_P}}{k_P P_{To}{}^2}\left[\ln\ \frac{2ACx+4A}{2ADx+4A}\right] \tag{4.39}$$

where, $C=(-2+\dfrac{1}{\sqrt{K_P}})$

93

$$D = \left(-2 - \frac{1}{\sqrt{K_P}} \right)$$

$$\frac{W}{F_{To}} = \frac{\sqrt{K_P}}{k_P P_{To}{}^2} \cdot \ln \frac{Cx + 2}{Dx + 2} \qquad (4.40)$$

P_{To} = Partial Pr of toluence in feed streem.

x = Toluene conversion.

by plotting graph between W/F_{To} against

the Toluene disporportionation rate constant K_p can be determined.

4.3 THERMODYNAMIC RELATIONSHIPS FOR CALCUATION OF EQUILIBRIUM CONSTANTS

Equilibrium constant K_e was determined by using the deductions gtiven by Smith and Van Ness [26]

The equilibrium constant, K_e for a chemical reaction aA + bB == cC + dD can

be defined as $K_e = \dfrac{a_C^c \cdot a_D^d}{a_A^a \cdot a_B^b}$ where a_A, a_B, a_C and a_D are the activities of the

components A,B,C, and D respectively. This equilibrium constant, K_e is related to the free energy chage of the chemical reaction by

$$\Delta F_T^0 = -RT \text{ in } K_e \qquad (4.42)$$

where ΔF_T^0 = Standard free energy change at any temperature $T^0 K$ and R = gas constant

Again, this equilibrium constant, (K_e) is related to the standard heat of reaction at any temperature, H_T^0 by the expression

$$\frac{d(\ln Ke)}{dT} = \frac{\Delta H_T^0}{RT^2}$$

or $\quad \ln K_e = \dfrac{\Delta H_T^0}{RT^2} dT + C$ (4.43)

The standard heat of reaction at any temperature, H_T^0, is given by the expression

$$\Delta H_T^0 = \Delta H_R^0 + \Delta H_{298}^0 + \Delta H_P^0$$ (4.44)

where, ΔH_{298}^0 = Standard heat of reaction at 298^0K

ΔH_R^0 = chage in enthalpy of reactants

$$= \sum_{React} (n \int_T^{298} C_p^0 dT)$$

ΔH_P^0 = change in enthalpy of the products

$$= \sum_{Prod} (n \int_{298}^T C_p^0 dT)$$

Therefore, $\Delta H_T^0 = \Delta H_{298}^0 + \sum_{Prod.} (n \int_{298}^T c_p^0 dT) - \sum_{React.} (n \int_{298}^T c_p^0 dT)$

or $\quad \Delta H_T^0 = \Delta H_{298}^0 + \int_{298}^T \Delta c_p^0 dT$ (4.45)

where $\Delta c_p^0 = \sum_{Prod.} n c_p^0 - \sum_{React.} n c_p^0$ (4.46)

If the c_p^0 value of each of the reactants and products are expressed as a function of temperature, i.e.,

$c_p^0 = \alpha + \beta T + \gamma T^2$, eqn. 4.46 becomes

$\Delta c_p^0 = \Delta \alpha + (\Delta \beta)T + (\Delta \gamma)T^2$

where, $\Delta \alpha = \sum_{Prod.} n\alpha - \sum_{React.} n\alpha$

$\Delta \beta = \sum_{Prod.} n\beta - \sum_{React.} n\beta$

$$\Delta \gamma = \sum_{Prod.} n\gamma - \sum_{React.} n\gamma$$

Substituting in Eq. 4.45

$$\Delta H_T^0 = \Delta H_{298}^0 + \int_{298}^{T}[\Delta \alpha + (\Delta \beta)T + (\Delta \gamma)T^2]dT$$

or $\quad \Delta H_T^0 = \Delta H_{298}^0 + \Delta \alpha(T - 298) + \dfrac{\Delta \beta}{2}(T^2 - 198^2) + \dfrac{\Delta \gamma}{3}(T^3 - 198^3)$

If all the constant terms in this equation are collected and lumped together in a constant ΔH_0 ,

$$\Delta H_T^0 = \Delta H_0 + \Delta \alpha T + \dfrac{\Delta \beta}{2}T^2 + \dfrac{\Delta \lambda}{3}T^3 \qquad (4.47)$$

Now, combining eqn. 4.43 and eqn. 4.47 and integrating

we get,

$$\text{Ink} = -\dfrac{\Delta H_0}{RT} + \dfrac{\Delta \alpha}{R}\text{InT} + \dfrac{\Delta \beta}{2R}T + \dfrac{\Delta \gamma}{6R}T^2 + C \qquad (4.48)$$

where, C is a constant.

From eqn. 4.42 and eqn. 4.48 we get

$$\Delta F_T^0 = -RT[-\dfrac{\Delta H_0}{RT} + \dfrac{\Delta \alpha}{R}\text{InT} + \dfrac{\Delta \beta}{2R}T + \dfrac{\Delta \gamma}{6R}T^2 + C]$$

$$\Delta F_T^0 = \Delta H_0 - \Delta \alpha.T.\text{InT} - \dfrac{\Delta \beta}{2}T^2 - \dfrac{\Delta \gamma}{6}T^3 - CRT \qquad (4.49)$$

By knowing the value of ΔH_0 form eqn. 4.47 and the value of ΔF_T^0 at 298^0K, we can calculate the value of C from eqn. 4.49, where the value of K at any temperature T^0K can be calculated by eqn. 4.48. $\Delta \alpha$, $\Delta \beta$, $\Delta \gamma$ may be determined by heat capacity

4.3.1 Calculation of Average α, β, γ, ΔH_{298}^0 and ΔF_{298}^0 for Mixed Xylenes

At equalibrium the compositon of p, m and 0-xylene into product was reported by P. Beltrame [7] as,

p-xylene = 0.23 - 0.24 = 0.235 mole fraction

m-xylene = 0.54 - 0.56 = 0.55   mole fraction

o-xylene = 0.21 - 0.22 = 0.215   mole fraction

values of α, β, γ, ΔH_{298}^0 ΔF_{298}^0 for benzene, toluene and xylenes as obtained from literature is presented in Table 4.1 and Table 4.2.

Table 4.1   Heat Capacity Data

$$C_p^0 = \alpha + \beta T + \gamma T^2 \, Cal \, / \, mole \, {}^0K$$

S.No.	Compound	α	$\beta \times 10^3$	$\gamma \times 10^7$
1.	Benzene (g)	-0.409	77.621	-264.29
2	Toluene (g)	0.576	93.493	-312.27
3	p-xylene (g)	1.846	108.594	-352.00
4	m-xylene (g)	107.956	107.147	-355.83
5	o-xylene (g)	4.603	104.476	-336.16

Table 4.2 Standard Heat of Formation and Standard Free Energy of Formation Data [28]

S.No.	Compound	ΔH_{f298}^0 kcal/g mole	ΔF_{f298}^0 kcal/g mole
1.	Benzene (g)	19.820	30.989
2	Toluene (g)	11.950	29.228
3	p-xylene (g)	4.290	28.952
4	m-xylene (g)	4.120	28.405
5	o-xylene (g)	4.540	29.177

Calculations : α_{av} = [(0.235)x 1.846 + (0.55)x 1.956 + 0.215 x 4.603]

$\qquad$ = 2.499

β_{av} = [0.235 x 108.594 + 0.55 x 107.147 + 0.215 x 104.476]10^{-3}

$$= 106.912 \times 10^{-3}$$

$$\gamma_{av} = [0.235 \times -352.00) + 0.55 \times (-355.83) + 0.215 \times (-336.16)] \, 10^{-7}$$

$$= -350.701 \times 10^{-7}$$

$$\Delta H^0_{f298 \, av} = [0.235 \times 4.290 + 0.55 \times 4.120 + 0.215 \times 4.540]$$

$$= 4.250 \, (\text{kcal/g mole})$$

$$\Delta F_{298 \, av} = [0.235 \times 28.952 + 0.55 \times 28.405 + 0.215 \times 29.177]$$

$$= 28.670 \, (\text{kcal/gmol})$$

4.3.2 Calculation of Heat of Reacton at different Temperature (k) [29]

Considering the disproportionation reaction, the values of $\Delta\alpha$, $\Delta\beta$, $\Delta\gamma$ and ΔH^0_{298} were calculated as shown below.

$$\Delta\alpha = (\alpha_X + \alpha_B) - 2(\alpha_T) = (4.499 - 0.409) - (2 \times 0.576) = 0.938$$

$$\Delta\beta = (\beta_X + \beta_B) - 2(\beta_T) = (106.913 - 77.621) - (2 \times 93.493) \times 10^{-7} = -2.452 \times 10^{-3} \text{ and}$$

$$\Delta\gamma = [(\gamma_X + \gamma_B) - 2(\gamma_T) = (-350.701 - 264.29) - 2(-312.27)] \, 10^{-7} = 9.549 \times 10^{-7}$$

where B, T and X represent benzene, toluene and xylenes respectively.

$$\Delta H^0_{298} = \sum_{Prod.} \Delta H^0_{f298} - \sum_{React.} \Delta H^0_{f298}$$

$$= (19.820 + 4.250) - (2 \times 11.950)$$

$$= 0.170 \, \text{kcal}$$

$$= 170 \, \text{cal}.$$

Substituting the above values of $\Delta\alpha$, $\Delta\beta$, $\Delta\gamma$ in eqn. 4.45, we get

$$\Delta H^0_T = \Delta H_0 + 0.938T - \frac{2.452 \times 10^{-3}}{2} T^2 + \frac{9.549 \times 10^{-7}}{3} T^3$$

At 298^0K, $\Delta H^0_T = \Delta H^0_{298} = 170 \, \text{cal}.$

Therefore, the above expression becomes

$$170 = \Delta H_0 + 0.938 \times 298 - \frac{2.452 \times 10^{-3}}{2} \times 298^2 + \frac{9.549 \times 10^{-7}}{3} \times 298^3$$

where $\Delta H_0 = -9.02$ cal.

Hence, the eqn. 4.45 can be written as

$$\Delta H_T^0 = -9.07 + 0.938T - \frac{2.452 \times 10^{-3}}{2}T^2 + \frac{9.549 \times 10^{-7}}{3}T^3 \qquad (4.45)$$

The standard heat of reaction at any temperature, T^0K can be calculated at different values of T^0K in eqn. 4.48.

4.3.3 Calculation of Equilibrium Constant, K_e at different Temperature (K) [29]

Standard free energy change for the toluence disproportionation can be calculated by considering the disproportionation reaction and ΔF_{298}^0 values for benzene, toluene and xylenes.

ΔF_{298}^0 for toluene disproportionation $= \sum_{Prod.} \Delta F_{298}^0 - \sum_{React.} \Delta F_{298}^0$

$= (30.989 + 28.723) - (2 \times 29.228)$

$= 1.201$ kcal

$= 1201$ cal.

Hence, substituting the values of ΔF_{298}^0 and ΔH_0 in eqn. 4.19, we get

$$\Delta F_{T0}^0 = \Delta H_0 - \Delta\alpha T \ln T - \frac{\Delta P}{2}T^2 - \frac{\Delta\gamma}{6}T^3 - CRT$$

$$1256 = -9.07 - 0.938 \times (298)\ln(298) - \frac{2.45 \times 10^{-3}}{2} \times (298)^2$$

$$- \frac{9.549 \times 10^{-7}}{6} \times (298)^3 - C \times 1.987 \times 298$$

R = 1.987

C = -4.924

Hence Eqn. 4.48 becomes

$$\ln K = \frac{4.565}{T} + 0.472 \ln T - 0.617 \times 10^{-3}T + 0.801 \times 10^{-7}(T^2) - 4.924$$

Above Eqn. was used to calculate the values of K at different temperatures T^0K.

Results are shown in Table 4.3

Table 4.3 Calculated Values of Eulibrium Constant

Temp(^{0}C)	K_e
300	0.0166
350	0.1020
400	0.1083
450	0.1092
500	0.1099
550	0.1104
600	0.1108
650	0.1111

CALCULATION METHOD AND RESULTS

By using the data obtained from gas chromatograph the compositions in product conversion of toluene p-selectivity was calculated by using the following form of computer programme in C language. The result is tabulated for difference catalysts.

$$\text{Mole of Toluene } (m_T) = \frac{V_F A_T \rho_T}{S\text{-}A_B M_B}$$

$$\text{Mole of Benzene } (m_B) = \frac{V_F A_B \rho_B}{S\text{-}A_B M_B}$$

$$\text{Mole of Para-Xylene } (m_{p}\text{-}X) = \frac{V_F A_B \rho_{p\text{-}x}}{S\text{-}A_{p\text{-}x} M_{p\text{-}x}}$$

$$\text{Mole of ortho-Xylene}(m_{p}\text{-}X) = \frac{V_F A_{px} \rho_{p\text{-}x}}{S\text{-}A_{o\text{-}x} M_{p\text{-}x}}$$

$$\text{Mole of meta-Xylene}(m_{m}\text{-}X) = \frac{V_F A_{m\text{-}X} \rho_{p\text{-}X}}{S\text{-}A_{m\text{-}X} \times M_{m\text{-}X}}$$

where $V_F = 0.002$

$\rho_T = 0.867$

$\rho_B = 0.8731$

$\rho_{p}\text{-}X = 0.860$

$\rho_{o}\text{-}X = 0.88$

$\rho_{m\text{-}x} = 0.86417$

$M_T = 92.14$

$M_B = 78.066$

$M_{p-x} = M_{oX} = M_{m-x} = 107.088$

Total mole of xylene

Total mole of xylene

$(m_{xs}) = m_{p-x} + m_{o-x} + m_{m-x}$

Total mole of feed

$m_{tl} = m_B + m_{xs} + m_T$

Conversion of toluene (CVN) $= \dfrac{mtl-m_T}{m_t}$

p-Xylene selectivity in xylenes

$s_{p-X} = \dfrac{m_{p-X}}{m_{xs}}$

Yield of p-xylene $\dfrac{m_{p-x}}{mtl}$

Benzene to xylenes ratio (BRX) $= \dfrac{m_B}{m_{xs}}$

102

Table 5.1   Performance of HZSM-5 (SAR-19) Catalyst

Reactor pressure = 1 atmosphere

$$\frac{W}{F_{T0}} = 8.856 \ \frac{kg\ of\ catalyst.h}{kmol\ toluene}$$

$$\frac{N_2}{F_{T0}} = 4.796\ (molal)$$

$$P_{T0} = 0.1776\ bar$$

Calcination temp. = 400°C,
& duration   5h

Activation temp. = 400°C,
& duration   1h

N_2 = 0.40 lpm.

F_{T0} = 0.40 ml.min^{-1}

Temp., °C	Product (mole)					B/X	Conversion, %	p-X Selectivity, %	p-X yield, %
	B x 10^7	T x10^4	p-X x 10^7	m,o-X x 10^7	Total-X x 10^7				
350	0.0	0.21	0.0	0.0	0.0	--	0.46	0.0	0.0
400	1.55	0.198	0.0	0.0	0.0	--	0.776	0.0	0.0
450	5.20	0.203	0.0	0.0	0.0	--	2.493	0.0	0.0
500	12.14	0.198	1.15	4.41	5.56	2.184	8.212	20.741	0.536
550	30.07	0.191	3.86	11.66	15.53	1.94	19.253	24.891	1.94
600	180.37	0.180	7.48	22.01	29.48	1.89	32.089	25.358	1.99

Table 5.2 Performance of HY (SAR-3) Catalyst

Reactor pressure   =   1 atmosphere   Calcination temp. = 570°C,
                                                   & duration   5 h

$\dfrac{W}{F_{T0}}$ = 8.856 $\dfrac{\text{kg catalyst.h}}{\text{kmol toluene}}$ Activation temp. = 570°C
                                                   & duration   1 h

$\dfrac{N_2}{F_{T0}}$ = 4.796 (molal) N_2 = 0.40 lpm.

P_{T0} = 0.177 bar F_{T0} = 0.40 ml.min^{-1}

Temp., °C	Product (mole)					B/X	Conversion, %	p-X Selectivity, %	p-X yield, %
	B x 10^7	T x10^4	p-X x 10^7	m,o-X x 10^7	Total-X x 10^7				
350	1.48	0.176	0.0	0.0	0.0	--	0.835	0.0	0.0
400	1.58	0.177	0.0	0.0	0.0	--	0.885	0.0	0.0
450	2.13	0.178	0.0	0.0	0.0	--	1.184	0.0	0.0
500	2.15	0.178	0.0	0.0	0.0	--	1.192	0.0	0.0
550	11.59	0.179	1.42	3.93	5.35	2.165	8.608	26.55	0.724
600	30.95	0.178	3.97	11.31	15.28	2.026	20.556	25.958	1.770
650	59.39	0.165	4.32	23.94	28.26	2/101	34.65	15.285	1.710

Table 5.3 Performance of HMordenite (SAR-13) Catalyst

Reactor pressure = 1 atmosphere

Calcination temp. = 570°C, & duration 5 h

$$\frac{W}{F_{T0}} = 8.856 \quad \frac{kg\ catalyst.h}{kmol\ toluene}$$

Activation temp. = 570°C, & duration 1 h

$$\frac{N_2}{F_{T0}} = 4.794\ (molal) \qquad N_2 = 0.40\ lpm.$$

$$P_{T0} = 0.1776\ bar \qquad F_{T0} = 0.40\ ml.min^{-1}$$

Temp., °C	Product (mole)					B/X	Conversion, %	p-X Selectivity, %	p-X yield, %
	B x 10^7	T x10^4	p-X x 10^7	M,o-X X 10^7	Total-X x 10^7				
350	0.41	0.174	0.0	0.0	0.0	--	0.34	0.0	0.0
400	0.52	0.174	0.0	0.0	0.0	--	0.296	0.0	0.0
450	0.62	0.175	0.0	0.0	0.0	--	0.352	0.0	0.0
500	0.90	0.174	0.0	0.0	0.0	--	0.414	0.0	0.0
550	2.72	0.172	0.0	0.71	0.71	3.825	1.952	0.0	0.0
600	3.75	0.168	0.38	1.18	1.18	2.404	3.056	24.13	0.22
650	5.37	0.175	0.67	1.82	1.82	2.151	4.294	26.94	0.41

Table 5.4   Performance of 3.95%PbY (SAR-3) Catalyst

Reactor pressure   =   1 atmosphere   Calcination temp. = 570°C, & duration 5 h

$$\frac{W}{F_{T0}} = 8.856 \ \frac{\cdot kg\ catalyst.h}{kmol\ toluene}$$

Activation Temp. = 570°C, & duration 1 h

$$\frac{N_2}{F_{T0}} = 4.794\ (molal) \qquad N_2 = 0.40\ lpm.$$

$$P_{T0} = 0.1776\ bar \qquad F_{T0} = 0.40\ ml.min^{-1}$$

Temp., °C	Product (mole)					B/X	Conversion, %	p-X Selectivity, %	p-X yield, %
	B x 10^7	T x10^4	p-X x 10^7	m,o-X x 10^7	Total-X x 10^7				
350	2.19	0.182	0.0	0.72	0.72	3.055	1.571	0.0	0.0
400	2.04	0.169	0.0	0.0	0.0	--	1.192	0.0	0.0
450	4.44	0.173	0.61	1.57	2.19	2.029	3.692	28.00	0.34
500	12.89	0.171	2.0	5.95	7.96	1.622	10.857	25.17	1.04
550	51.15	0.157	4.22	23.60	27.82	1.839	33.425	15.16	1.79
600	15.19	0.174	2.10	5.55	7.66	1.894	111.57	27.47	1.06
650	4.40	0.171	0.79	2.20	2.99	1.147	4.138	26.37	0.443

Table 5.5   Performance of   1.46%CuHZSM-5 (SAR-32) Catalyst

Reactor pressure =   1 atmosphere   Calcination temp. = 570°C,
                                                        & duration   5 h

$\dfrac{W}{F_{T0}}$ = 8.856 $\dfrac{\text{kg catalyst.h}}{\text{kmol toluene}}$ Activation Temp. = 570°C,
                                                        & duration   1 h

$\dfrac{N_2}{F_{T0}}$ = 3.597 (molal) N_2 = 0.3 lpm.

P_{T0} = 0.211 bar F_{T0} = 0.4 ml.min^{-1}

Temp., °C	Product (mole)					B/X	Conversion, %	p-X Selectivity, %	p-X yield, %
	B x 10^7	T x10^4	p-X x 10^7	m,o-X x 10^7	Total-X x 10^7				
350	0.16203	0.45	0.0	0.0	0.0	-	0.274	0.0	0.0
400	0.71	0.189	0.0	0.0	0.0	-	0.372	0.0	0.0
450	1.29	0.183	0.0	0.0	0.0	-	0.699	0.0	0.0
500	1.81	0.182	0.0	0.0	0.0	-	0.988	0.0	0.0
550	6.03	1.814	1.58	3.71	5.29	1.141	5.871	29.890	0.086
600	6.75	1.778	3.79	9.75	13.55	0.498	10.25	27.948	0.21

N_2 = 0.1 lpm

Temp., °C	Product (mole)					B/X	Conversion, %	p-X Selectivity, %	p-X yield, %
	B x 10^7	T x10^4	p-X x 10^7	m,o-X x 10^7	Total-X x 10^7				
550	5.67	0.17651	1.58	3.64	5.21	1.088	5.808	30.226	0.84
600	7.61	0.18385	1.61	3.33	4.94	1.541	6.587	32.574	0.83

Contd....... 2

$N_2 = 0.6$ lpm

Temp., °C	Product (mole)					B/X	Conversion, %	p-X Selectivity, %	p-X yield, %
	B x 10^7	T x10^4	p-X x 10^7	m,o-X x 10^7	Total-X x 10^7				
550	4.97	0.181	1.26	3.02	4.28	1.161	4.882	29.399	0.66
600	8.26	0.178	2.87	6.68	17.81	0.864	9.091	30.031	1.41

Table 5.6 Performance of 0.59%NiHZSM-5 (SAR-32) Catalyst
(Particle Size 0.955 mm)

Reactor pressure = 1 atmosphere   Calcination temp. = 570°C, & duration 5 h

$$\frac{W}{F_{T0}} = 10.121 \frac{\text{kg catalyst.h}}{\text{kmol toluene}}$$

Activation temp. = 570°C, & duration 1 h

$$\frac{N_2}{F_{T0}} = 4.196 \text{ (molal)} \qquad N_2 = 0.35 \text{ lpm.}$$

$$P_{T0} = 0.1977 \text{ bar} \qquad F_{T0} = 0.40 \text{ ml.min}^{-1}$$

Temp., °C	Product (mole)					B/X	Conversion, %	p-X Selectivity, %	p-X yield, %
	$B \times 10^7$	$T \times 10^4$	$p\text{-}X \times 10^7$	$m,o\text{-}X \times 10^7$	$\text{Total-}X \times 10^7$				
350	1.70	0.185	0.0	1.14	1.14	1.494	1.513	0.0	0.0
400	1.71	0.175	0.0	0.46	0.46	3.734	1.221	0.0	0.0
450	2.11	0.178	0.0	0.0	0.0	-	1.173	0.0	0.0
500	2.14	0.173	0.0	0.0	0.0	-	1.221	0.0	0.0
550	3.19	0.181	0.0	0.69	0.69	4.615	2.106	0.0	0.0
600	7.63	0.178	0.78	2.40	3.18	2.395	5.720	24.547	0.41
650	14.39	0.174	1.69	5.12	6.82	2.111	10.860	24.847	0.66

Table 5.7 — Performance of 0.59%NiHZSM-5 (SAR-32) Catalyst
(Particle size 0.604 mm)

Reactor pressure = 1 atmosphere

Calcination temp. = 570°C, & duration 5 h

$$\frac{W}{F_{T0}} = 10.121 \frac{kg \ catalyst. \ h}{kmol \ toluene}$$

Activation temp. = 570°C, & duration 1 h

$$\frac{N_2}{F_{T0}} = 4.196 \ (molal) \qquad N_2 = 0.35 \ lpm.$$

$$P_{T0} = 0.1977 \ bar \qquad F_{T0} = 0.40 \ ml.min^{-1}$$

Temp., °C	Product (mole)					B/X	Conversion, %	p-X Selectivity, %	p-X yield, %
	B x 10^7	T x10^4	p-X x 10^7	m,o-X x 10^7	Total-X x 10^7				
350	2.69	0.168	0.0	1.36	1.36	1.554	2.565	21.668	0.0
400	1.94	0.168	0.0	0.57	0.57	3.410	1.472	0.0	0.0
450	2.10	0.175	0.0	0.55	0.55	3.798	1.489	0.0	0.0
500	2.41	0.172	0.0	0.55	0.55	4.371	1.692	0.0	0.0
550	4.74	0.178	0.35	1.32	1.67	2.845	3.486	21.234	0.19
600	4.81	0.175	0.41	1.40	1.82	2.65	3.640	22.784	0.23
650	19.15	0.172	2.28	4.76	7.06	9.34	14.19	24.415	0.32

**Table 5.8   Performance of 0.59%Ni HZSM-5 (SAR-32) Catalyst
(Particle size 1.302 mm)**

Reactor pressure   =   1 atmosphere   Calcination temp. = 570°C,
                                                & duration   5 h

$$\frac{W}{F_{T0}} = 8.856 \ \frac{kg\ catalyst.h}{kmol\ toluene}$$

Activation temp. = 570°C,
& duration   1 h

$$\frac{N_2}{F_{T0}} = 4.196 \ (molal) \qquad N_2 = 0.35\ lpm.$$

$$P_{T0} = 0.1977\ bar \qquad F_{T0} = 0.40\ ml.min^{-1}$$

| Temp., °C | Product (mole) | | | | | B/X | Conversion, % | p-X Selectivity, % | p-X yield, % |
	$B \times 10^7$	$T \times 10^4$	$p\text{-}X \times 10^7$	$m,o\text{-}X \times 10^7$	$Total\text{-}X \times 10^7$				
350	1.76	0.178	0.0	0.03	0.03	62.81	0.995	0.0	0.0
400	1.59	0.169	0.0	0.0	0.0	0.0	0.930	0.0	0.0
450	1.70	0.168	0.0	0.0	0.0	-	1.0	0.0	0.0
500	1.92	0.169	0.0	0.0	0.0	-	1.221	0.0	0.0
550	2.44	0.171	0.0	0.0	0.0	-	1.221	0.0	0.0
600	4.98	0.176	0.42	1.21	1.63	3.062	3.621	25.885	0.30
650	9.30	0.173	1.01	2.79	0.380	2.446	7.041	26.528	0.54

Table 5.9   Performance of 3.805%ThHZSM-5 (SAR-32) Catalyst

Reactor pressure   =   1 atmosphere   Calcination temp. = 570°C,
                                                   & duration   5 h

$\dfrac{W}{F_{T0}}$ =   8.856 $\dfrac{\text{kg catalyst. h}}{\text{kmol toluene}}$ Activation temp. = 570°C,
                                                   & duration   1 h

$\dfrac{N_2}{F_{T0}}$ =   4.796 (molal) N_2 =   0.4 lpm.

P_{T0} =   0.1776 bar F_{T0} =   0.4 ml.min^{-1}

Temp., °C	Product (mole)					B/X	Conversion, %	p-X Selectivity, %	p-X yield, %
	B x 10^7	T x10^4	p-X x 10^7	m,o-X x 10^7	Total-X x 10^7				
350	0.64	0.195	0.0	0.0	0.0	-	0.329	0.0	0.0
400	0.60	0.190	0.0	0.0	0.0	-	0.314	0.0	0.0
450	0.7	0.196	0.0	0.0	0.0	-	0.392	0.0	0.0
500	1.37	0.191	0.0	0.0	0.0	-	0.711	0.0	0.0
550	3.14	0.204	0.0	0.0	0.0	3.203	1.981	0.0	0.0
600	6.29	0.189	0.64	2.41	3.05	2.06	4.697	21.098	0.32
650	14.30	0.184	1.93	6.09	8.02	1.784	10.83	24.095	0.94

Table 5.10   Performance of 3.71%CeHZSM-5 (SAR-32) Catalyst

Reactor pressure   =   1 atmosphere

$\dfrac{W}{F_{T0}}$ =   8.856 $\dfrac{\text{kg catalyst.h}}{\text{kmol toluene}}$

$\dfrac{N_2}{F_{T0}}$ =   4.796 (molal)

P_{T0} =   0.1776 bar

Calcination temp. = 570°C, & duration   5 h

Activation Temp. = 570°C, & duration   1 h

N_2 =   0.4 lpm.

F_{T0} =   0.4 ml.min^{-1}

Temp., °C	Product (mole)					B/X	Conversion, %	p-X Selectivity, %	p-X yield, %
	B x 10^7	T x10^4	p-X x 10^7	m,o-X x 10^7	Total-X x 10^7				
350	1.53	0.1894	0.0	1.950	1.950	0.593	2.118	24.079	0.0
400	1.19	0.1746	0.0	0.94	0.94	1.266	1.206	0.0	0.0
450	1.55	0.1795	0.0	0.80	0.80	1.930	1.293	0.0	0.0
500	2.05	0.187	0.0	0.95	0.95	2.154	1.578	0.0	0.0
550	3.90	0.186	0.43	1.59	2.03	1.994	3.088	21.0285	0.22
600	9.33	0.177	1.15	3.93	5.08	1.838	7.514	22.559	0.61
650	19.71	0.182	2.70	8.89	11.59	1.700	14.64	23.319	1.27

Table 5.11   Performance of   2.97%LaHZSM-5(SAR-32) Catalyst

Reactor pressure = 1 atmosphere   Calcination temp. = 570°C,
                                           & duration   5 h

$\dfrac{W}{F_{T0}}$ = 8.856 $\dfrac{\text{kg catalyst.h}}{\text{kmol toluene}}$ Activation temp. = 570°C,
                                           & duration   1 h

$\dfrac{N_2}{F_{T0}}$ = 4.796 (molal) N_2 = 0.4 lpm

P_{T0} = 0.1776 bar F_{T0} = 0.4 ml.min^{-1}

Temp., °C	Product (mole)					B/X	Conversion, %	p-X Selectivity, %	p-X yield, %
	B x 10^7	T x10^4	p-X x 10^7	m,o-X x 10^7	Total-X x 10^7				
350	1.20	0.179	0.0	1.770	1.770	0.532	1.88	21.331	0.0
400	1.50	0.179	0.0	0.89	0.89	1.696	1.316	0.0	0.0
450	1.70	0.176	0.0	0.75	0.75	2.271	1.371	0.0	0.0
500	2.05	0.187	0.0	0.95	0.95	2.154	1.578	0.0	0.0
550	3.42	0.179	0.0	0.71	0.71	4.791	2.260	0.0	0.0
600	7.40	0.176	0.0	4.15	4.15	1.783	6.144	24.229	0.60
650	17.24	0.176	2.12	6.95	9.07	1.901	13.001	23.367	1.05

Table 5.12   Performance of   1.76%Cr1.92%ThHZSM-5 (SAR-32) Catalyst

Reactor pressure   =   1 atmosphere

$$\frac{W}{F_{T0}} = 8.856 \ \frac{kg\ catalyst.\ h}{kmol\ toluene}$$

$$\frac{N_2}{F_{T0}} = \cdot 4.796 \ (molal)$$

P_{T0} =   0.1776 bar

Calcination temp. = 570°C,
& duration   5 h

Activation temp. = 570°C,
& duration   1 h

N_2 =   0.4 lpm.

F_{T0} =   0.4 ml.min^{-1}

Temp., °C	Product (mole)					B/X	Conversion, %	p-X Selectivity, %	p-X yield, %
	B x 10^7	T x10^4	p-X x 10^7	m,o-X x 10^7	Total-X x 10^7				
350	0.73	0.113	0.0	0.20	0.20	3.656	0.815	0.0	0.0
400	1.27	0.180	0.0	0.50	0.50	2.541	0.972	0.0	0.0
450	1.91	0.180	0.0	0.0	0.0	-	1.046	0.0	0.0
500	2.08	0.156	0.0	0.63	0.63	3.324	1.697	0.0	0.0
550	10.26	0.167	1.39	4.48	5.82	1.764	8.776	22.985	0.73
600	21.22	0.177	2.85	9.40	12.25	1.732	15.885	23.23	1.39
650	29.70	0.81	5.53	23.84	53.54	1.245	22.861	23.18	2.31

Table 5.13   Performance of 1.249%PbHZSM-5 (SAR-32) Catalyst

Reactor pressure	=	1 atmosphere	Calcination temp. = 570°C, & duration 5 h
$\dfrac{W}{F_{T0}}$	=	$8.856 \dfrac{\text{kg catalyst. h}}{\text{kmol toluene}}$	Activation temp. = 570°C, & duration 1 h
$\dfrac{N_2}{F_{T0}}$	=	4.796 (molal)	N_2 = 0.4 lpm.
P_{T0}	=	0.1776 bar	F_{T0} = 0.4 ml.min^{-1}

Temp., °C	Product (mole)					B/X	Conversion, %	p-X Selectivity, %	p-X yield, %
	B x 10^7	T x10^4	p-X x 10^7	m,o-X x 10^7	Total-X x 10^7				
350	1.90	0.186	0.0	2.93	2.93	0.513	2.92	0.0	0.0
400	1.51	0.202	0.0	0.85	0.85	1.781	1.151	0.0	0.0
450	1.75	0.185	0.0	0.63	0.63	2.753	1.267	0.0	0.0
500	2.20	0.189	0.0	0.67	0.67	3.287	1.493	0.0	0.0
550	3.64	0.194	0.0	1.07	1.07	3.383	2.371	0.0	0.0
600	6.01	0.187	0.72	2.58	3.31	1.824	4.73	21.739	0.35
650	14.22	0.186	1.80	6.06	7.86	1.809	10.607	22.94	0.87

Table 5.14 Performance of 3.34%CrHZSM-5 (SAR-19) Catalyst

Reactor pressure $=$ 1 atmosphere

$\dfrac{W}{F_{T0}} = 8.856 \ \dfrac{\text{kg catalyst.h}}{\text{kmol toluene}}$

$\dfrac{N_2}{F_{T0}} = 3.597$ (molal)

$P_{T0} = 0.224$ bar

Calcination temp. = 570°C, & duration 5 h

Activation temp. = 570°C, & duration 1 h

$N_2 = 0.30$ lpm.

$F_{T0} = 0.40$ ml.min^{-1}

Temp., °C	Product (mole)					B/X	Conversion, %	p-X Selectivity, %	p-X yield, %
	B $\times 10^7$	T $\times 10^4$	p-X $\times 10^7$	m,o-X $\times 10^7$	Total-X $\times 10^7$				
350	1.79	0.169	0.0	0.0	0.0	--	1.046	0.0	0.0
400	2.15	0.169	0.0	0.0	0.0	--	1.25	0.0	0.0
450	3.33	0.173	0.0	0.79	0.79	4.208	2.326	0.0	0.0
500	8.95	0.172	1.17	3.84	5.01	1.785	7.51	23.373	0.62
550	9.38	0.169	1.20	3.95	5.16	1.809	7.936	23.353	0.64
600	20.71	0.168	2.67	8.85	11.52	1.798	16.03	14.610	0.66
650	47.96	0.161	4.34	24.81	29.15	81.64	32.423	14.87	1.96

Table 5.15   Performance of 2.33%CrHZSM-5 (SAR-43) Catalyst

Reactor pressure = 1 atmosphere   Calcination temp. = 570°C, & duration 5 h

$$\frac{W}{F_{T0}} = 8.856 \frac{kg\ catalyst.h}{kmol\ toluene}$$

Activation temp. = 570°C, & duration 1 h

$$\frac{N_2}{F_{T0}} = .4.796\ \text{(molal)} \qquad N_2 = 0.40\ lpm.$$

$$P_{T0} = 0.1776\ bar \qquad F_{T0} = 0.40\ ml.min^{-1}$$

Temp., °C	Product (mole)					B/X	Conversion, %	p-X Selectivity, %	p-X yield, %
	$B \times 10^7$	$T \times 10^4$	$p\text{-}X \times 10^7$	$m,o\text{-}X \times 10^7$	$Total\text{-}X \times 10^7$				
350	1.45	0.157	0.0	0.0	0.0	--	0.915	0.0	0.0
400	1.51	0.157	0.0	0.0	0.0	--	0.952	0.0	0.0
450	1.53	0.156	0.0	0.0	0.0	--	0.967	0.0	0.0
500	1.83	0/160	0.0	0.0	0.0	--	1.129	0.0	0.0
550	1.83	0.160	0.0	0.0	0.0	--	1.129	0.0	0.0
600	3.65	0.168	0.39	1.14	1.53	2.382	2.99	25.281	0.592
650	8.17	0.161	1.04	2.75	3.79	2.155	6.70	27.487	0.601

Table 5.16   Performance of 2.71%CrHZSM-5 (SAR-40) Catalyst

Reactor pressure   =   1 atmosphere

$\dfrac{W}{F_{T0}}$ =   8.335 $\dfrac{\text{kg catalyst. h}}{\text{kmol toluene}}$

$\dfrac{N_2}{F_{T0}}$ =   4.28   (molal) N_2 =   3.8 lpm.

P_{T0} =   0.195 bar F_{T0} =   0.40 ml.min^{-1}

Calcination temp. = 570°C,
& duration   5 h
Activation temp. = 570°C,
& duration   1 h

Temp., °C	Product (mole)					B/X	Conversion, %	p-X Selectivity, %	p-X yield, %
	B x 10^7	T x10^4	p-X x 10^7	m,o-X x 10^7	Total-X x 10^7				
350	3.73	0.161	0.68	2.81	2.81	1.327	3.89	24.35	0.405
400	1.33	0.160	0.61	2.41	2.41	0.551	2.281	25.08	0.373
450	5.17	0.159	0.99	2.98	3.97	1.301	5.417	24.85	0.589
500	7.58	0.159	3.11	9.67	12.79	0.593	11.361	24.35	1.72
550	19.93	0.155	3.99	12.41	16.40	1.215	18.982	24.33	2.07
600	23.89	0.152	9.55	30.77	40.39	0.592	29.374	23.68	3.71
650	19.62	0.144	16.04	53.12	69.16	0.284	38.10	23.17	6.89

Table 5.17   Performance of   1.756%Cr1.923%ThHZSM-5 (SAR-32) Catalyst
At different space time *(Kinetic Study)*

Reactor pressure   =   .1 atmosphere   Calcination temp. = 570°C,
                                                    & duration   5 h

P_{T0} =   0.1776 bar   Activation temp. =   570°C,
                                                   & duration   1 h

Temperature   =   400°C   Weight of catalyst = 2 g

| W/F_{T0}, kg.h. kmol^{-1} | Product (mole) | | | | | B/X | Conversion, % | p-X Selectivity, % | p-X yield, % |
	B x 10^7	T x10^4	p-X x 10^7	m,o-X x 10^7	Total-X x 10^7				
6.81	1.81	0.164	0.07	0.09	0.16	13.24	1.30	45.495	0.04
5.45	1.93	0.1647	0.09	0.09	0.18	13.78	1.267	51.067	0.044
4.47	1.82	0.163	0.08	0.081	0.161	17.10	1.25	50.00	0.048
3.728	2.03	0.172	0.09	0.031	0.121	16.69	1.238	76.88	0.051
3.373	1.97	0.171	0.09	0.03	0.12	16.74	1.21	77.668	0.052

Temperature   =   550°C

| W/F_{T0}, kg.h. kmol^{-1} | Product (mole) | | | | | B/X | Conversion, % | p-X Selectivity, % | p-X yield, % |
	B x 10^7	T x10^4	p-X x 10^7	m,o-X x 10^7	Total-X x 10^7				
6.44	5.82	0.17	2.36	3.57	5.93	1.631	5.228	33.80	1.30
5.20	3.91	0.161	1.29	2.53	3.82	0.565	4.610	33.843	0.77
4.60	4.42	0.167	1.06	1.97	3.03	1.458	4.282	34.922	0.602
3.37	3.37	0.159	0.60	0.93	1.54	2.319	3.09	39.31	0.365

Table 5.18 Performance of HZSM-5 (SAR-19) Catalyst at different space time (Kinetic Study)

Reactor pressure = 1 atmosphere
P_{TO} = 0.1776 bar
Temperature = 550°C

Calcination temp. = 570°C, & duration 5 h
Activation temp. = 570°C, & duration 1 h
Weight of catalyst = 2 g

W/F$_{TO}$, kg.h. kmol^{-1}	Product (mole)					B/X	Conversion, %	p-X Selectivity, %	p-X yield, %
	B x 10^7	T x10^4	p-X x 10^7	m,o-X x 10^7	Total-X x 10^7				
6.88	29.34	0.1641	4.41	28.40	32.81	0.894	29.44	13.434	1.95
5.65	31.21	0.158	3.97	23.57	27.53	0.133	27.10	14.410	1.83
4.90	2.40	0.163	3.32	18.92	22.24	1.232	23.30	14.930	1.57
4.268	23.39	0.157	3.15	15.63	18.78	1.126	21.00	18.77	1.52
3.542	18.10	0.155	2.65	8.32	10.97	1.10	18.19	24.19	1.48

Temperature = 450°C

W/F$_{TO}$, kg.h. kmol^{-1}	Product (mole)					B/X	Conversion, %	p-X Selectivity, %	p-X yield, %
	B x 10^7	T x10^4	p-X x 10^7	m,o-X x 10^7	Total-X x 10^7				
6.11	8.17	0.163	1.38	4.50	5.58	1.389	7.96	23.44	0.78
5.45	6.73	0.161	1.05	3.26	4.11	1.528	6.471	23.83	0.61
4.27	5.68	0.162	0.96	2.99	3.95	1.437	5.59	24.25	0.56
3.94	4.59	0.167	0.86	2.69	3.54	1.294	5.657	24.16	0.49
3.54	3.54	0.163	0.83	2.33	3.17	1.119	3.938	26.26	0.48

Table 5.19 Performance of 3.95%PbHY (SAR-3) Catalyst at different space time *(Kinetic Study)*

Reactor pressure = 1 atmosphere

P_{T0} = 0.1776 bar

Temperature = 400°C

Calcination temp. = 570°C, & duration 5 h

Activation temp. = 570°C, & duration 1 h

Weight of catalyst = 2 g

W/F$_{T0}$, kg.h. kmol^{-1}	Product (mole)					B/X	Conversion, %	p-X Selectivity, %	p-X yield, %
	B x 10^7	T x10^4	p-X x 10^7	m,o-X x 10^7	Total-X x 10^7				
6.81	1.10	0.194	0.130	0.31	0.440	2.23	0.87	32.335	0.15
5.45	1.17	0.184	0.140	0.28	0.420	2.828	0.856	33.414	0.12
4.80	1.15	0.181	0.130	0.25	0.380	3.018	0.84	34.058	0.11
3.60	1.14	0.196	0.140	0.27	0.410	2.779	0.785	33.566	0.11
3.37	1.09	0.181	0.115	0.19	0.305	3.205	0.765	35.15	0.10
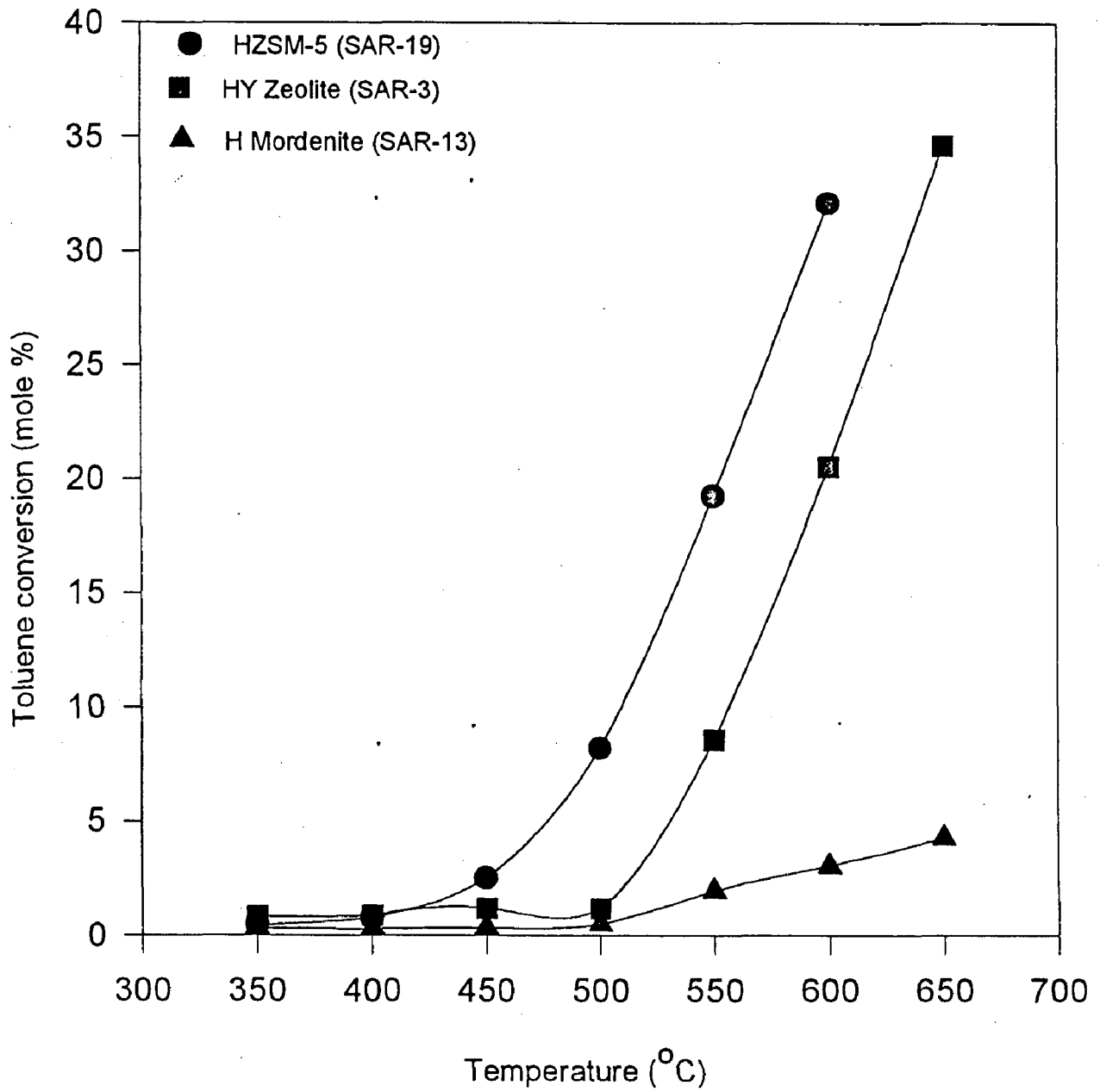
Fig. 5.1 EFFECT OF REACTION TEMPERATURE ON TOLUENE CONVERSION
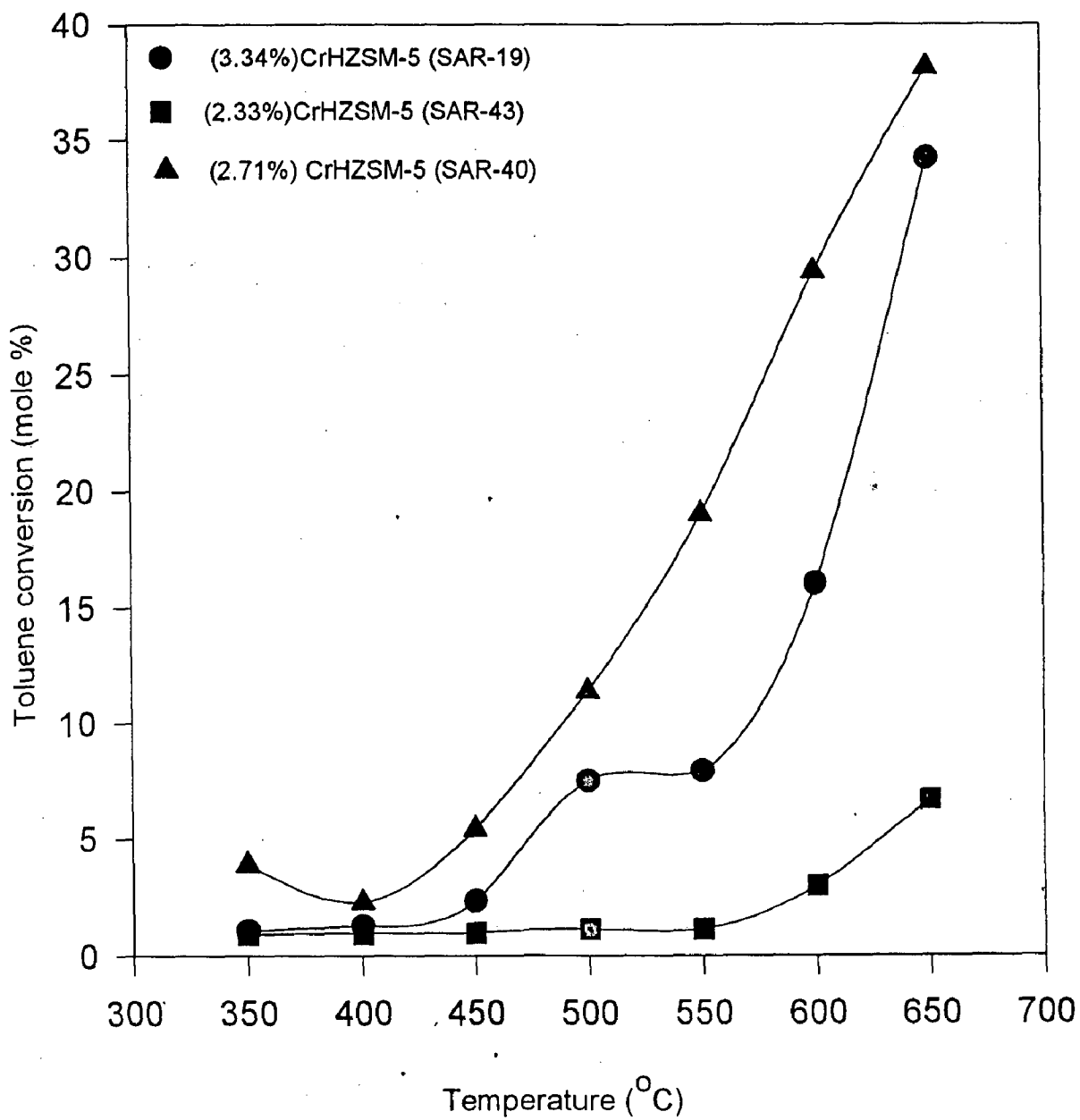
Fig. 5.2 EFFECT OF REACTION TEMPERATURE ON TOLUENE CONVERSION
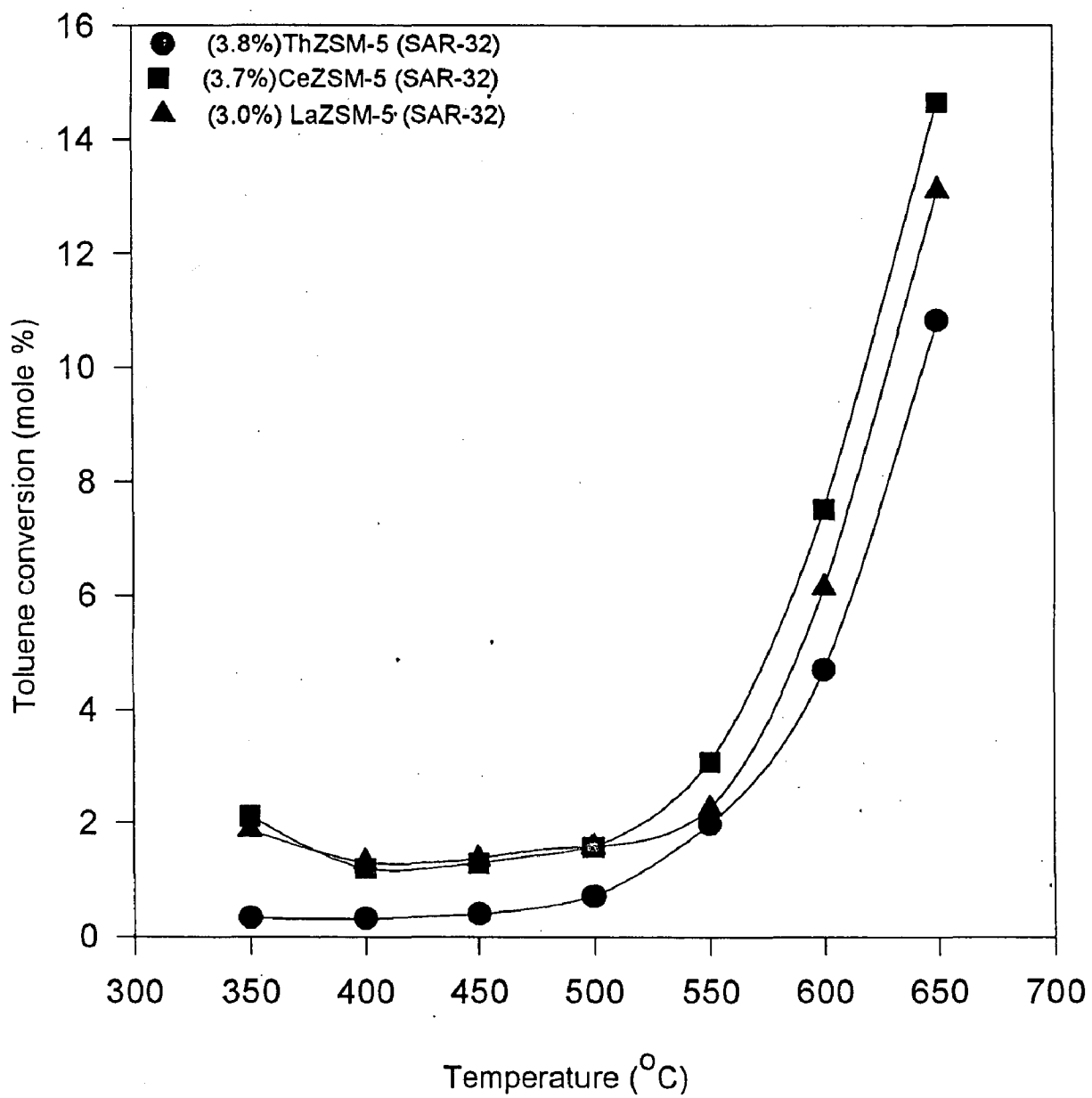
Fig. 5.3 EFFECT OF REACTION TEMPERATURE ON TOLUENE CONVERSION
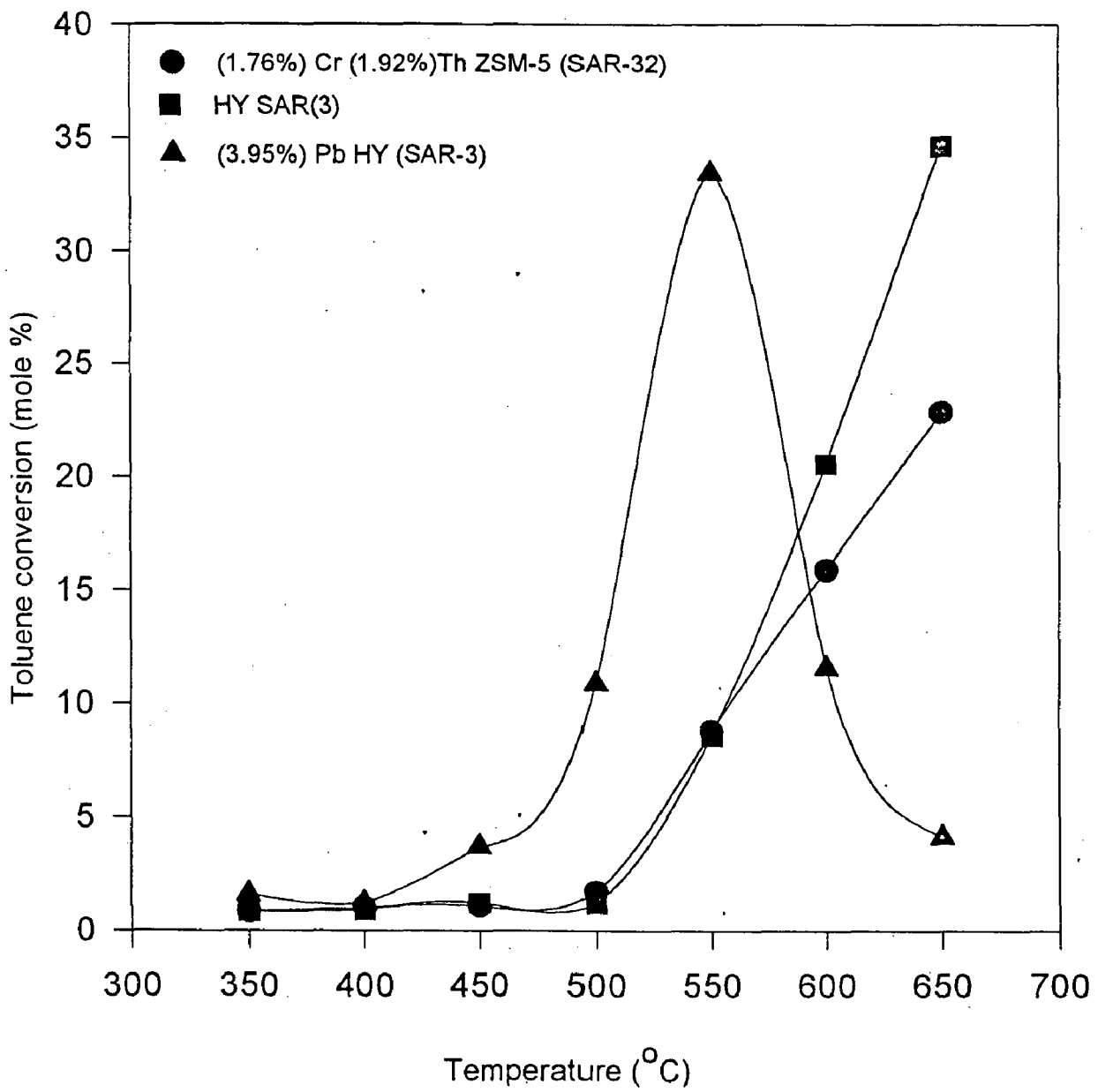
Fig. 5.4 EFFECT OF REACTION TEMPERATURE ON TOLUENE CONVERSION
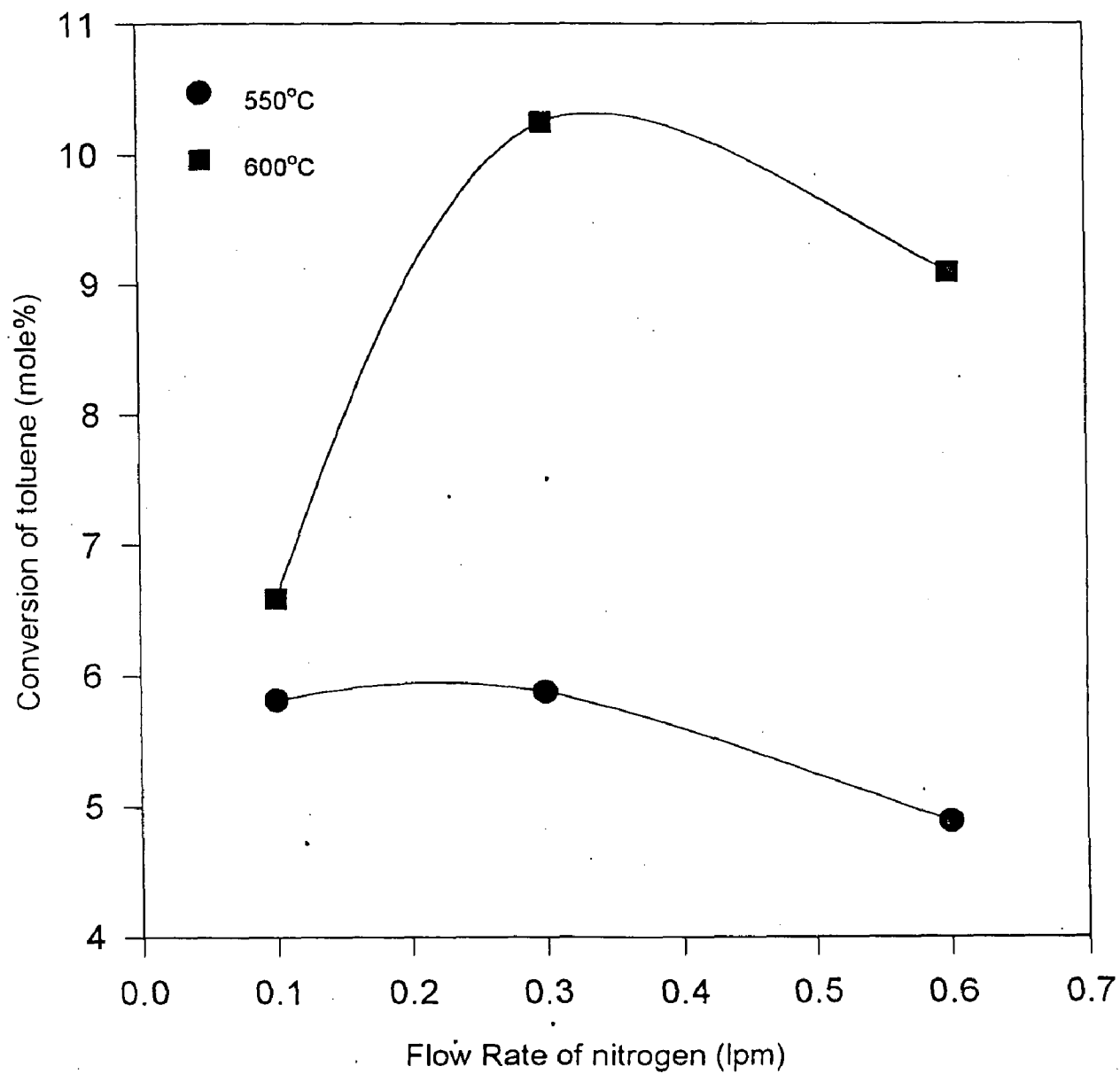
FIG. 5.5   EFFECT OF NITROGEN FLOW RATE ON TOLUNE CONVERSION
FOR (1.46%)CuHZSM-5 (SAR-32)
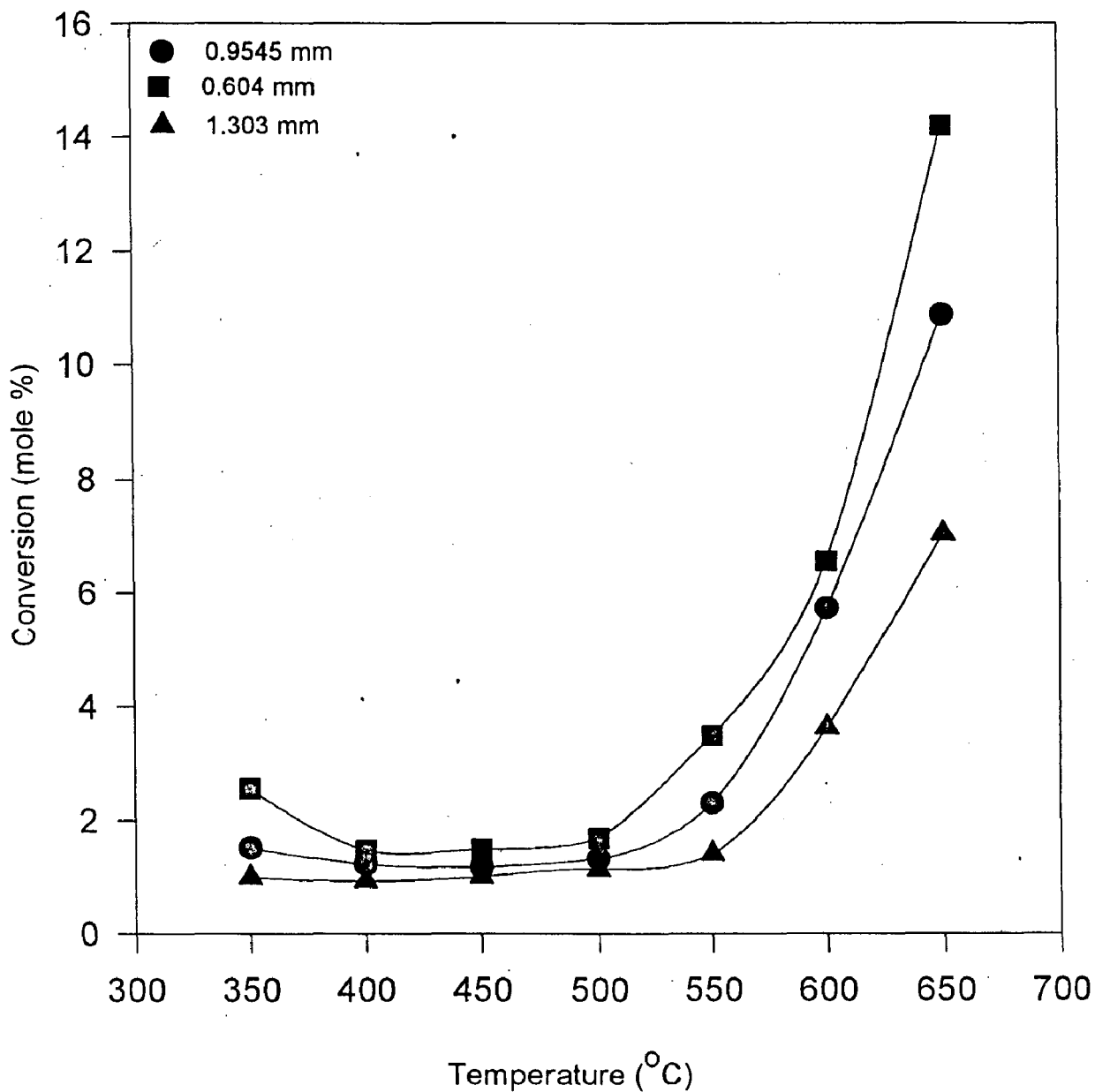
Fig. 5.6 EFFECT OF TEMPERATURE ON TOLUENE CONVERSION FOR DIFFERENT CATALYST PARTICLE SIZE OF (0.59 %) Ni HZSM-5 (SAR-32)
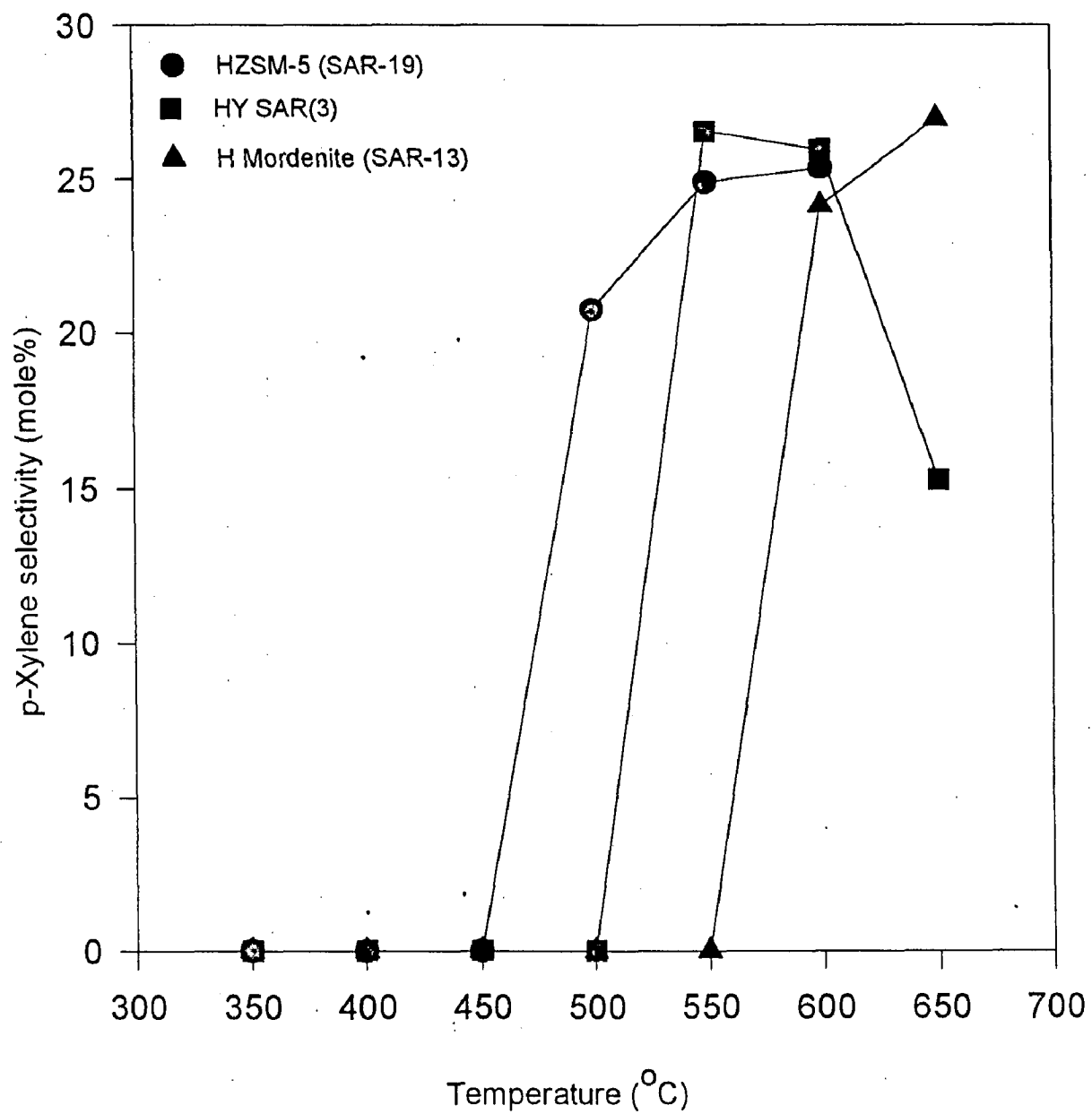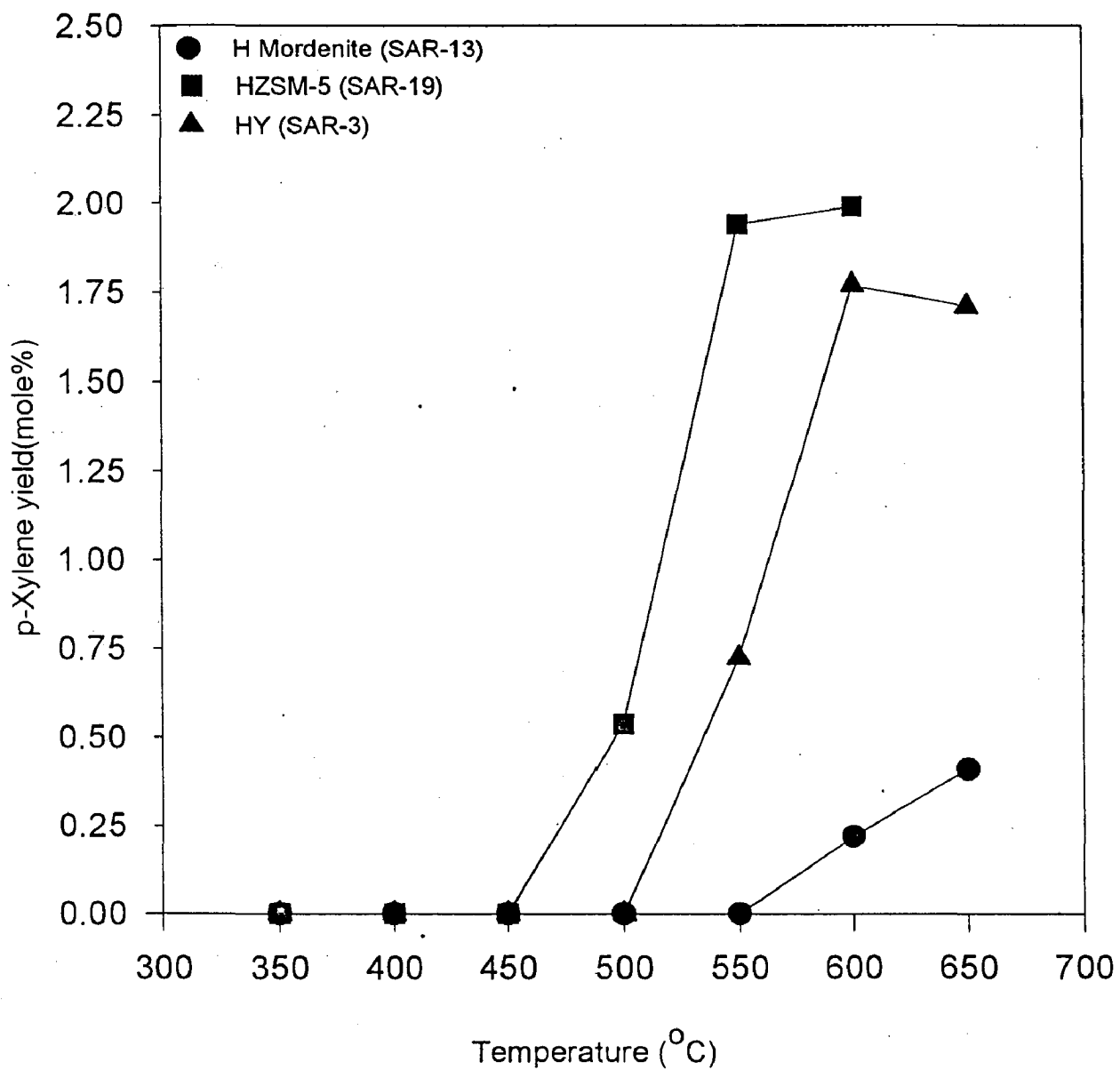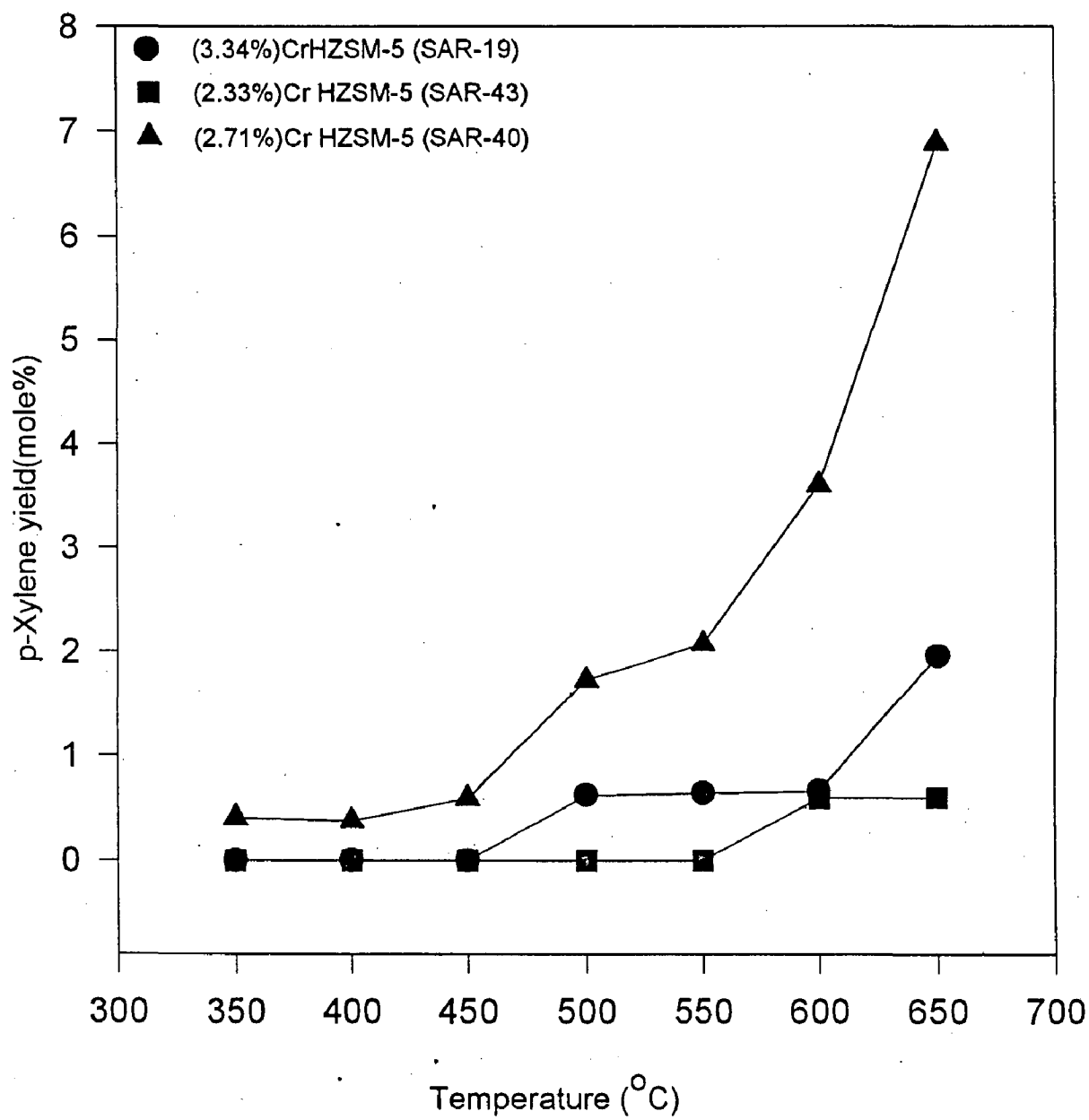
Fig. 5.7 EFFECT OF REACTION TEMPERATURE ON p-XYLENE SELECTIVITY
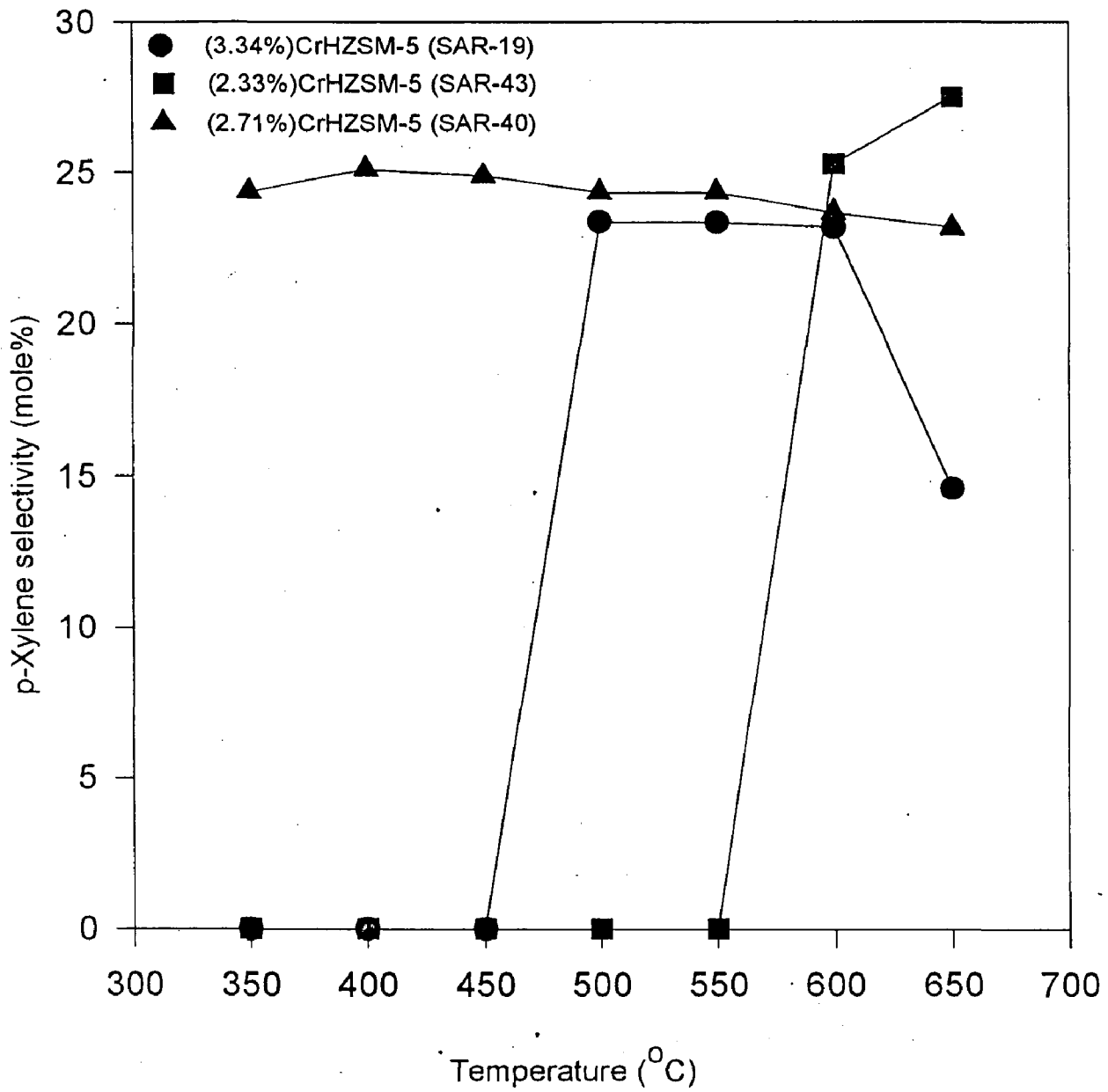
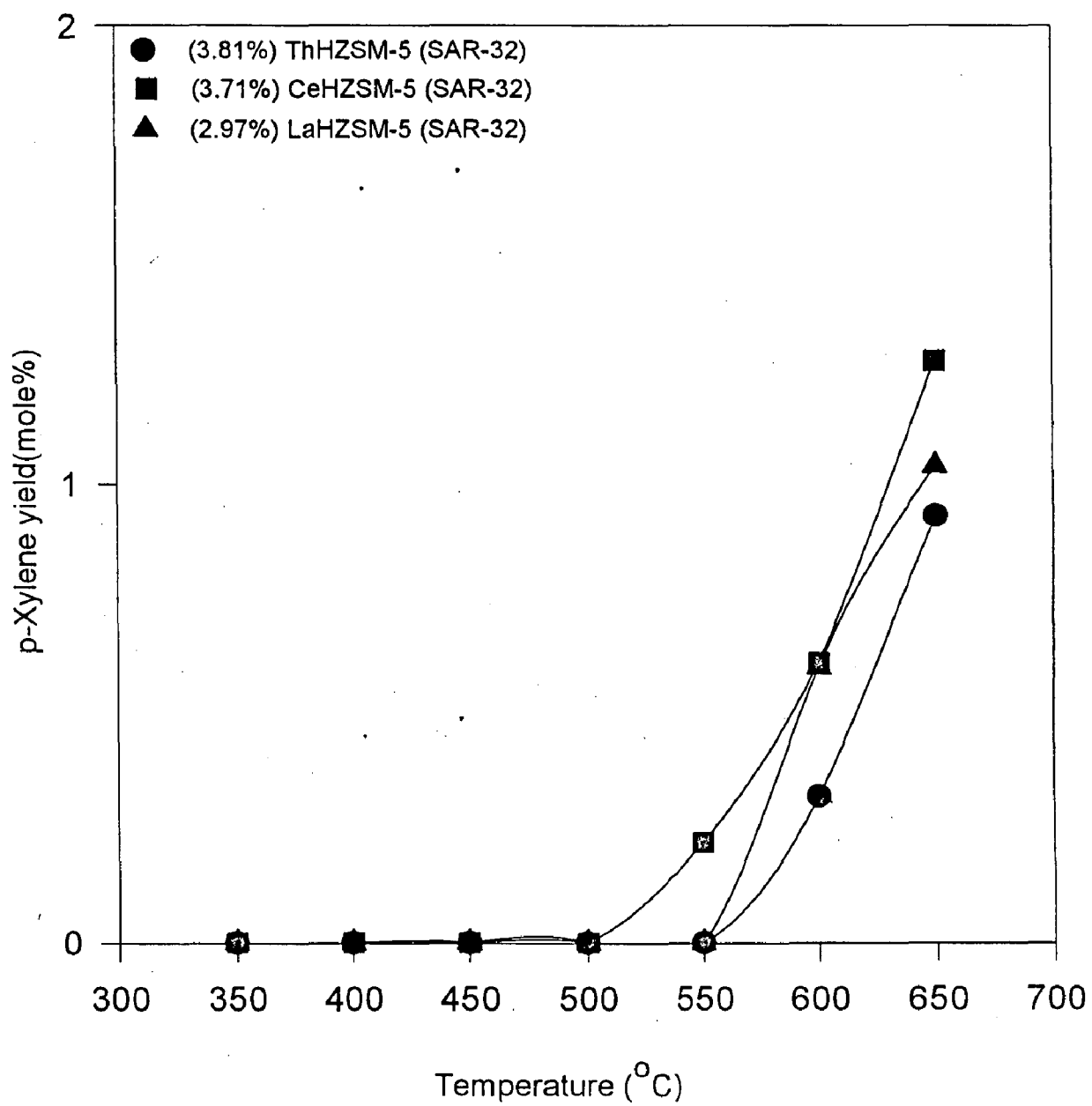Fig. 5.8   EFFECT OF REACTION TEMPERATURE ON p-XYLENE SELECTIVITY
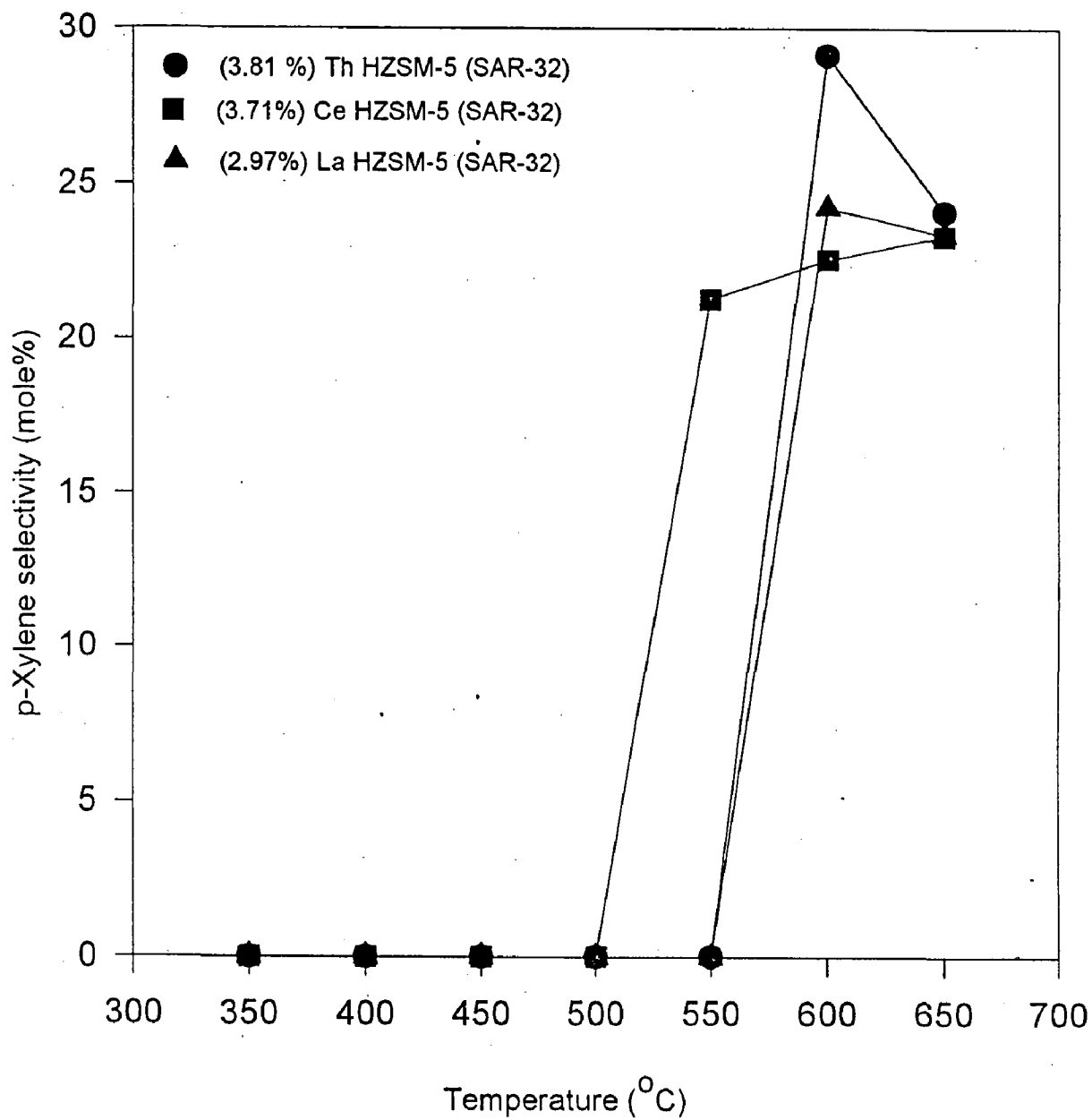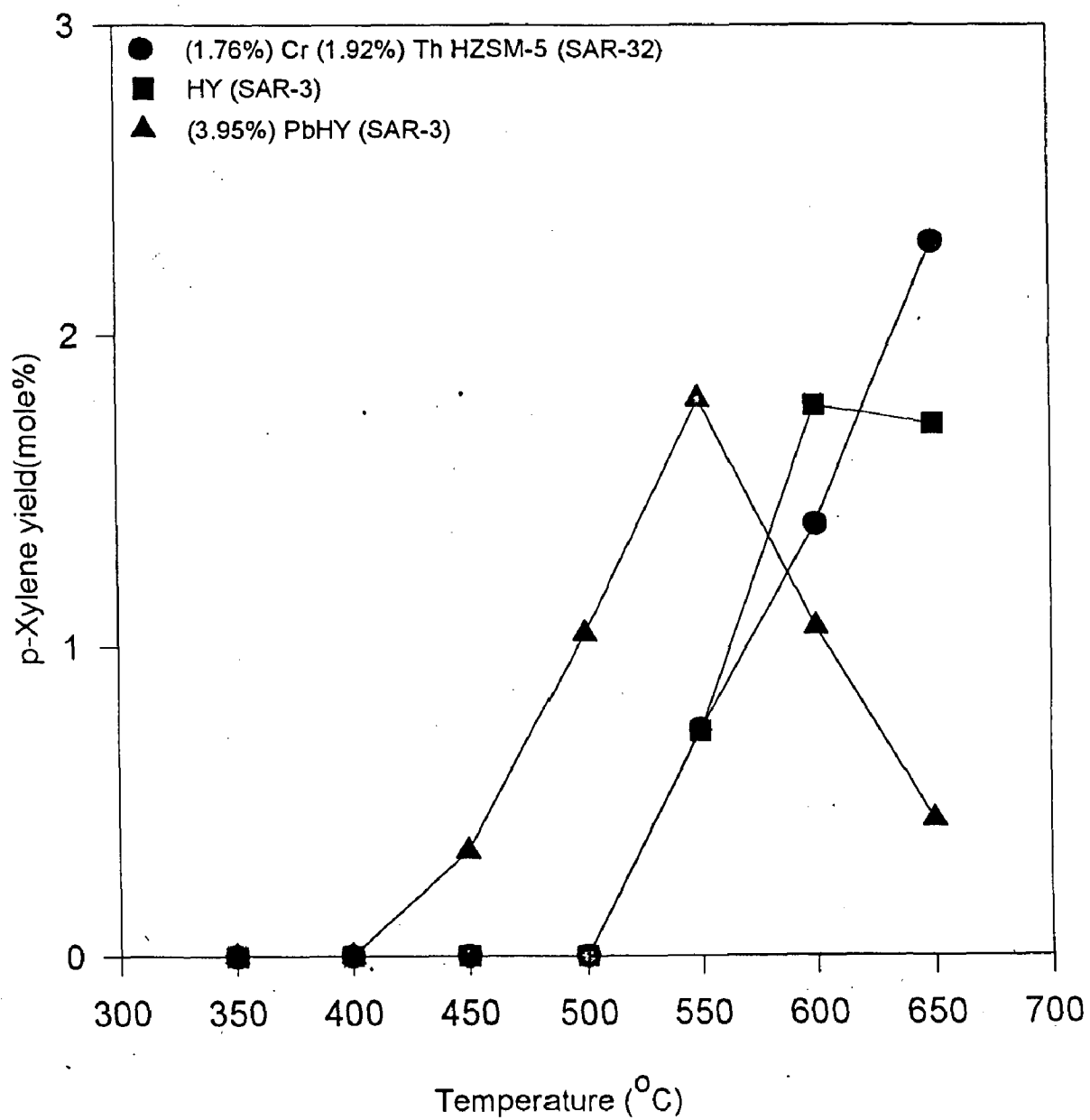
Fig. 5.9 EFFECT OF REACTION TEMPERATURE ON p-XYLENE SELECTIVITY
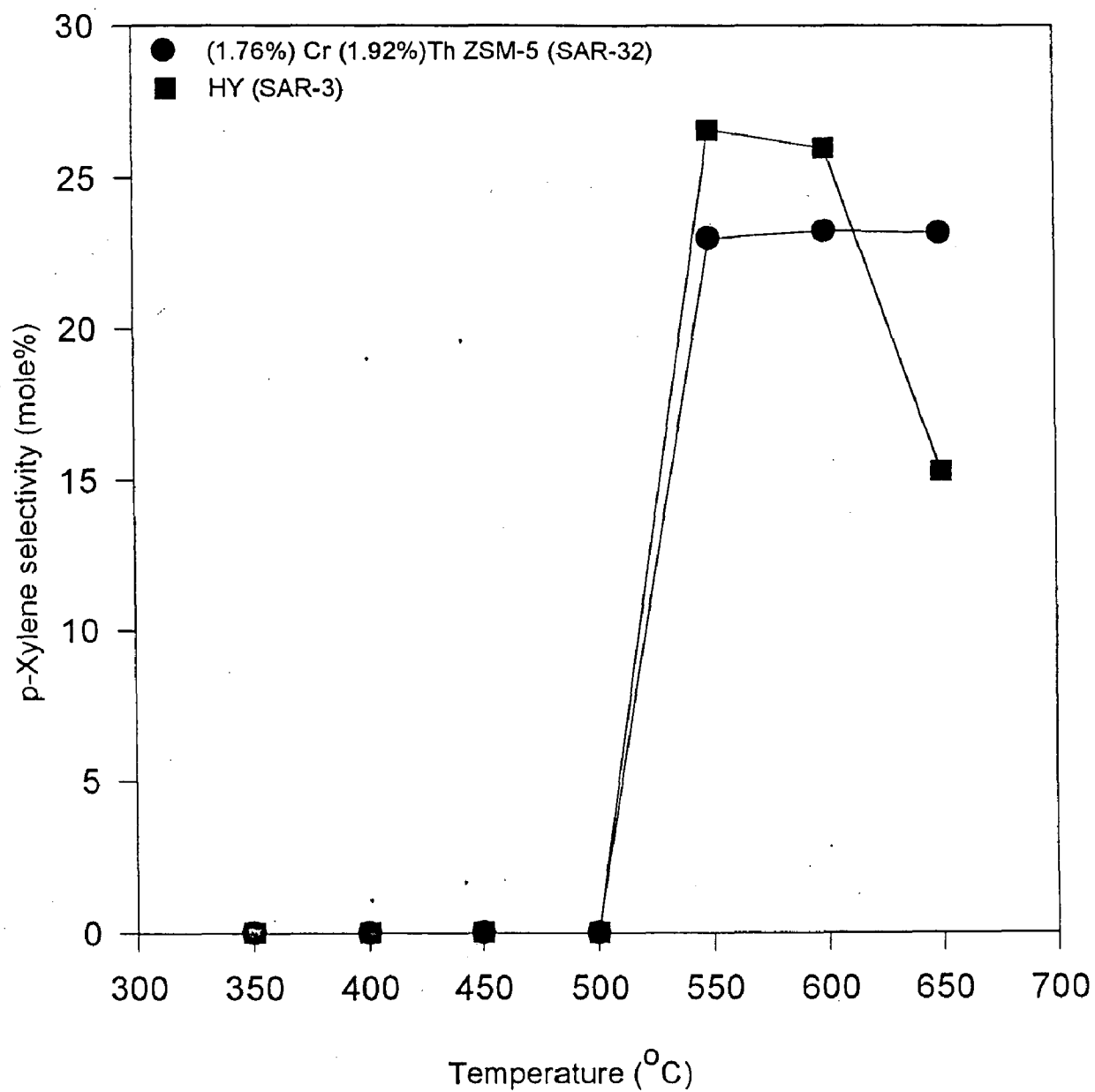
Fig. 5.10 EFFECT OF REACTION TEMPERATURE ON p-XYLENE SELECTIVITY
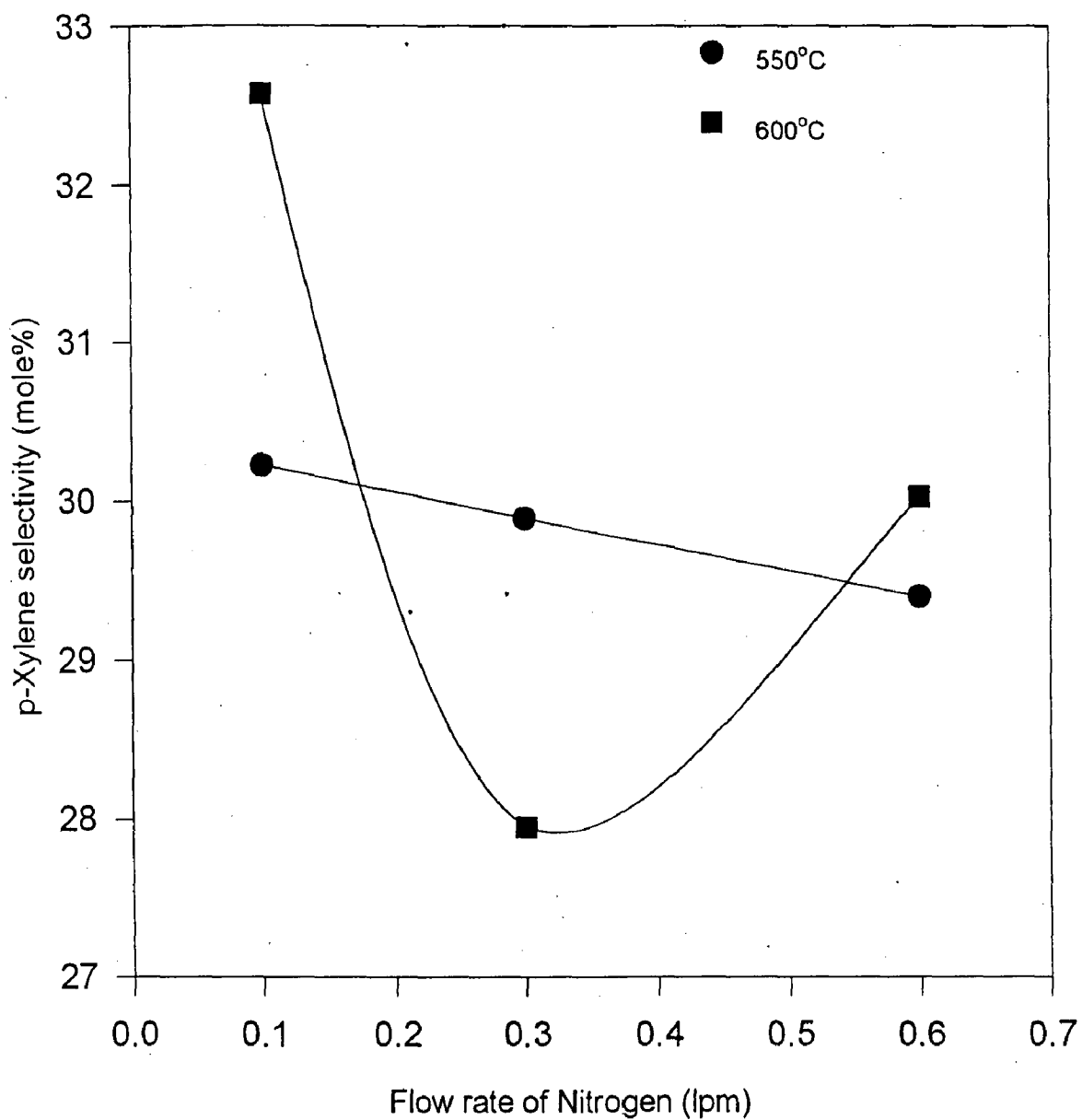
FIG. 5.11 EFFECT OF NITROGEN FLOW RATE ON p-XYLENE SELECTIVITY
FOR (1.46%) CuHZSM-5 (SAR-32)
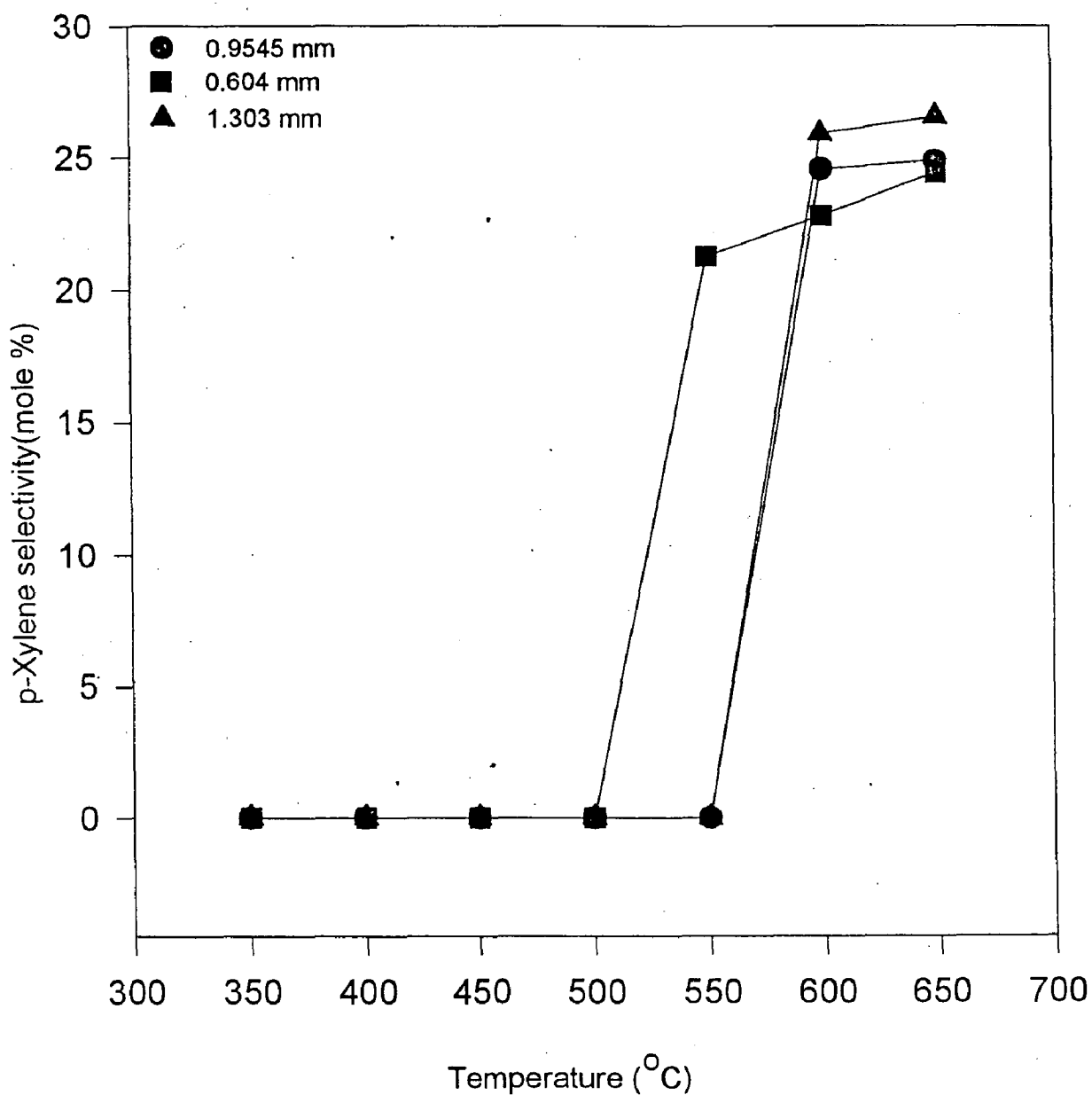
Fig. 5.12 EFFECT OF TEMPERATURE ON p-XYLENE SELECTIVITY FOR DIFFERENT CATALYST PARTICLE SIZE OF (0.59%)Ni HZSM-5 SAR(32)

Fig. 5.13 EFFECT OF RECTION TEMPERATURE ON p-XYLENE YIELD

Fig. 5.14 EFFECT OF REACTION TEMPERATURE ON p-XYLENE YIELD

Fig. 5.15 EFFECT OF REACTION TEMPERATURE ON p-XYLENE YIELD

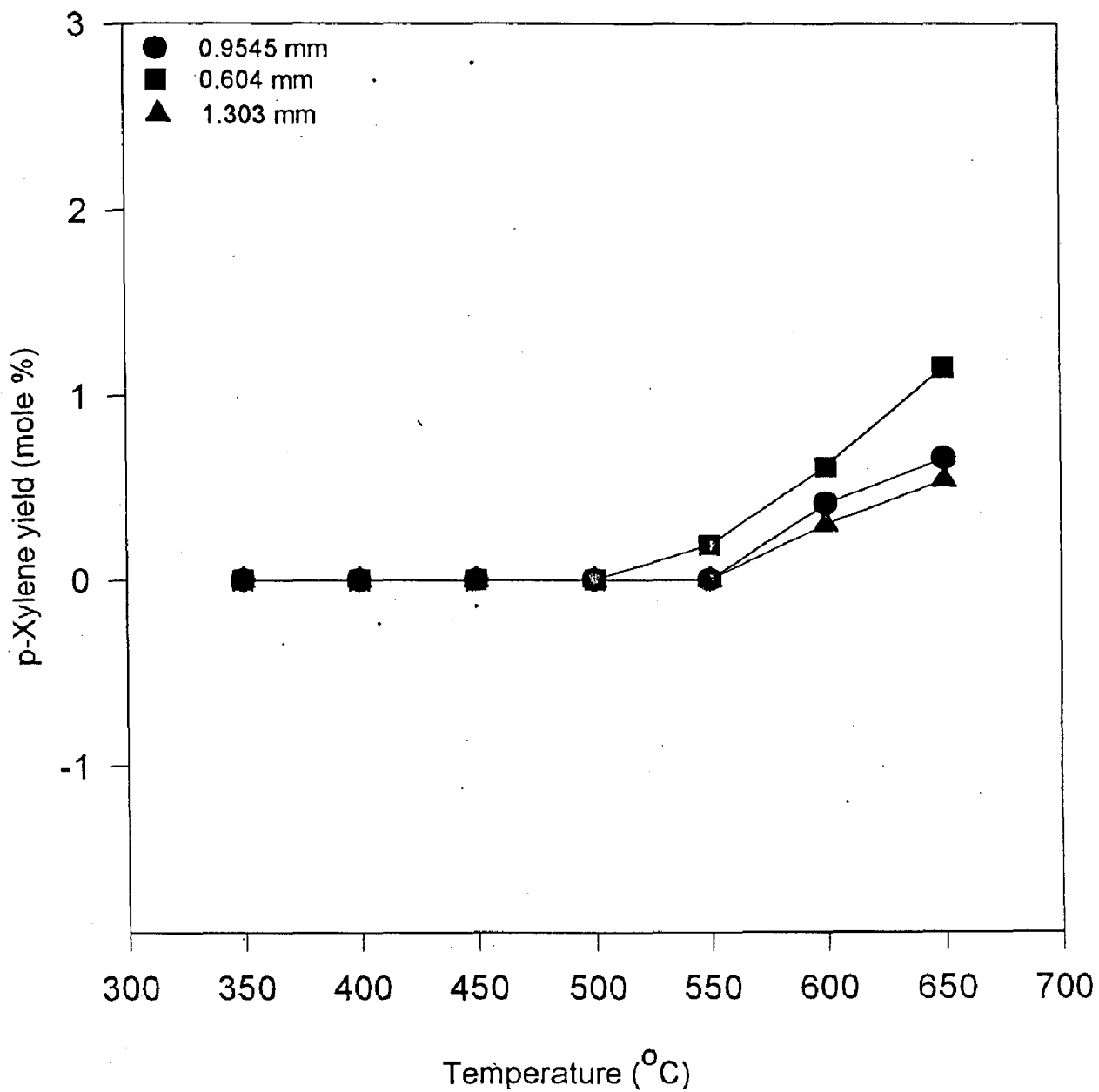Fig. 5.16   EFFECT OF REACTION TEMPERATURE ON p-XYLENE YIELD

Fig. 5.17 EFFECT OF TEMPERATURE ON p-XYLENE YIELD FOR DIFFERENT
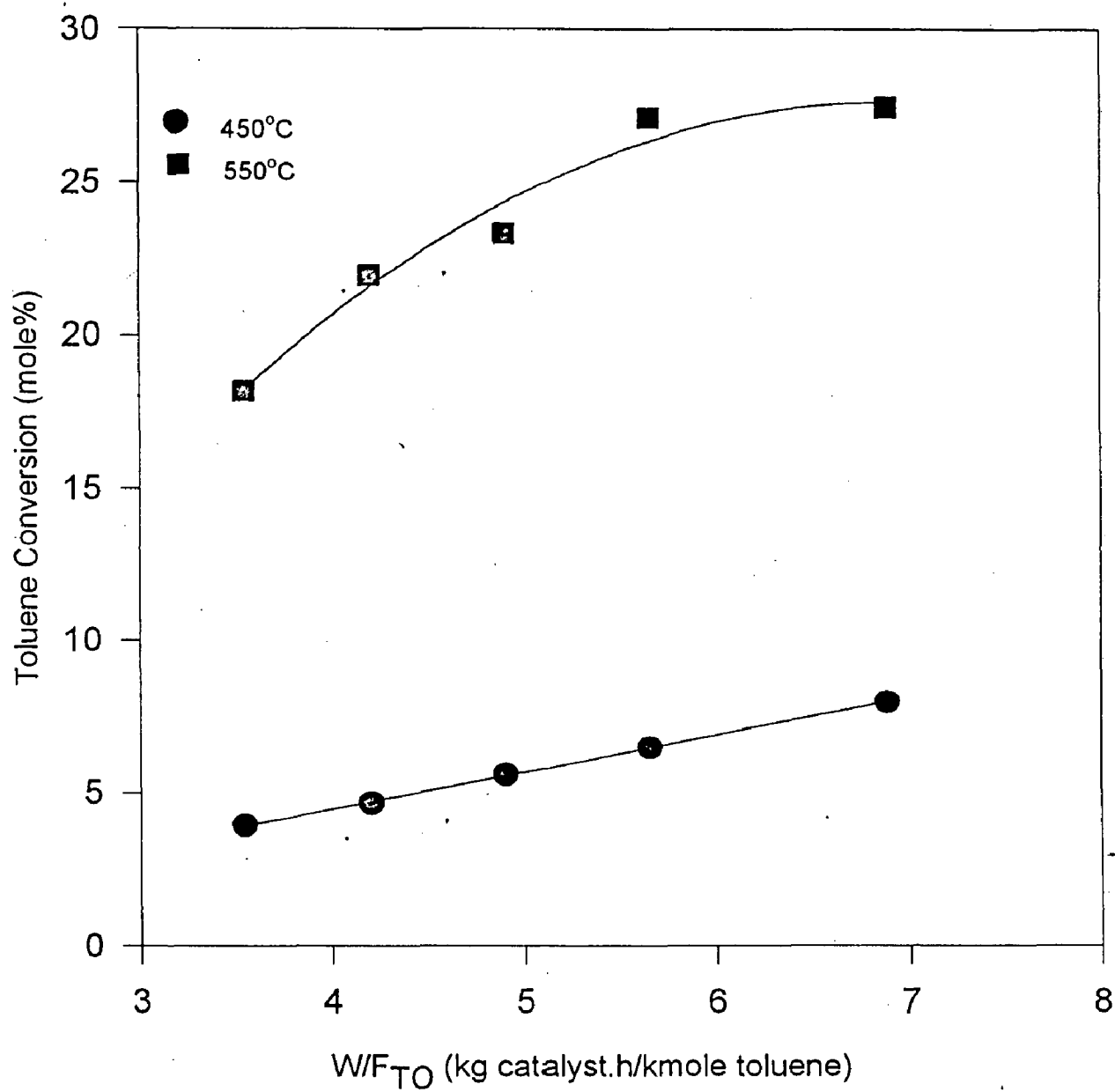CATALYST PARTICLE SIZE OF (0.59%)Ni HZSM-5 SAR(32)

FIG. 5.18 EFFECT OF SPACE TIME ON TOLUENE CONVERSION
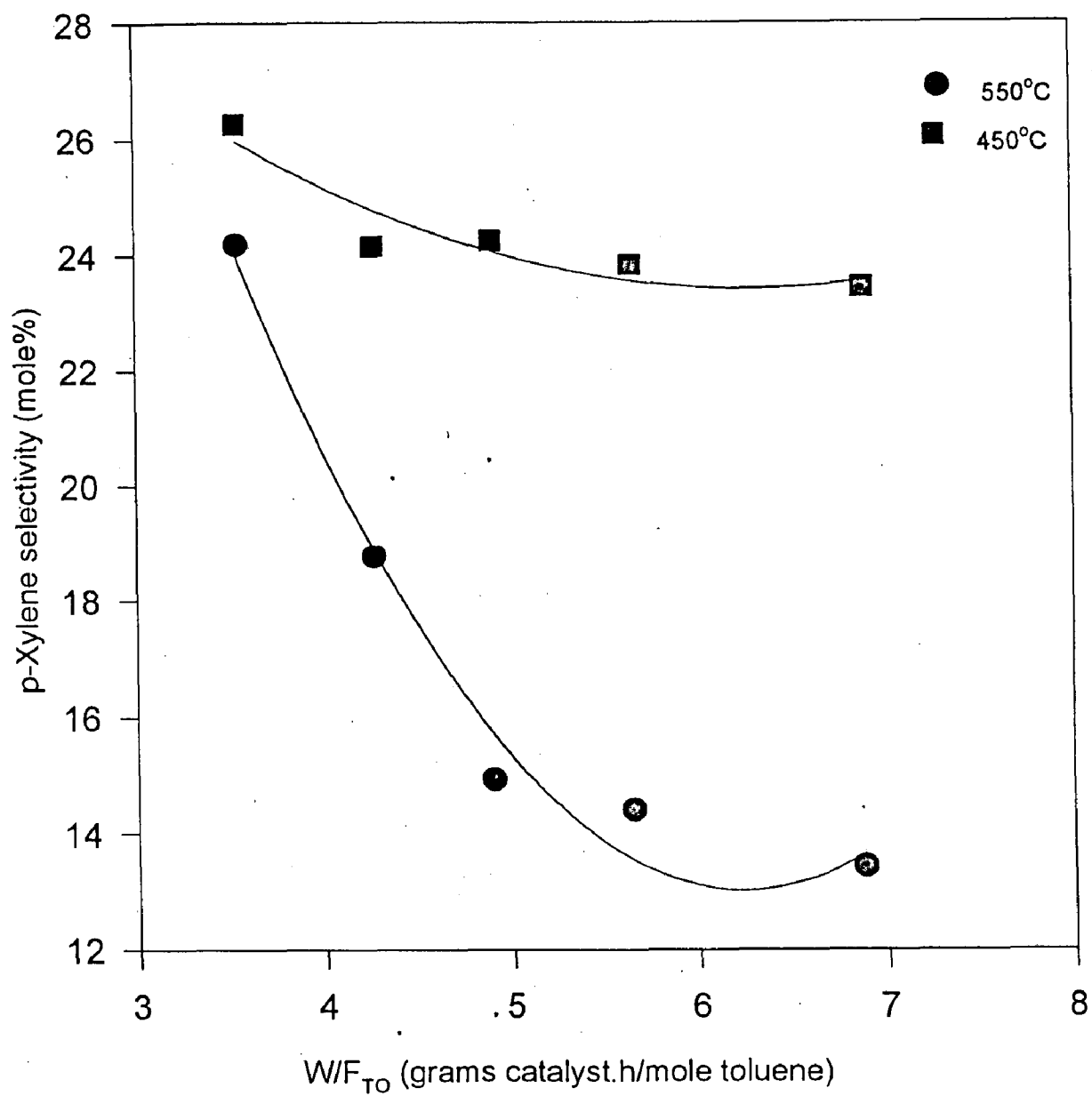OVER HZSM-5 (SAR-19)

FIG. 5.19 EFFECT OF SPACE TIME ON p-XYLENE SELECTIVITY
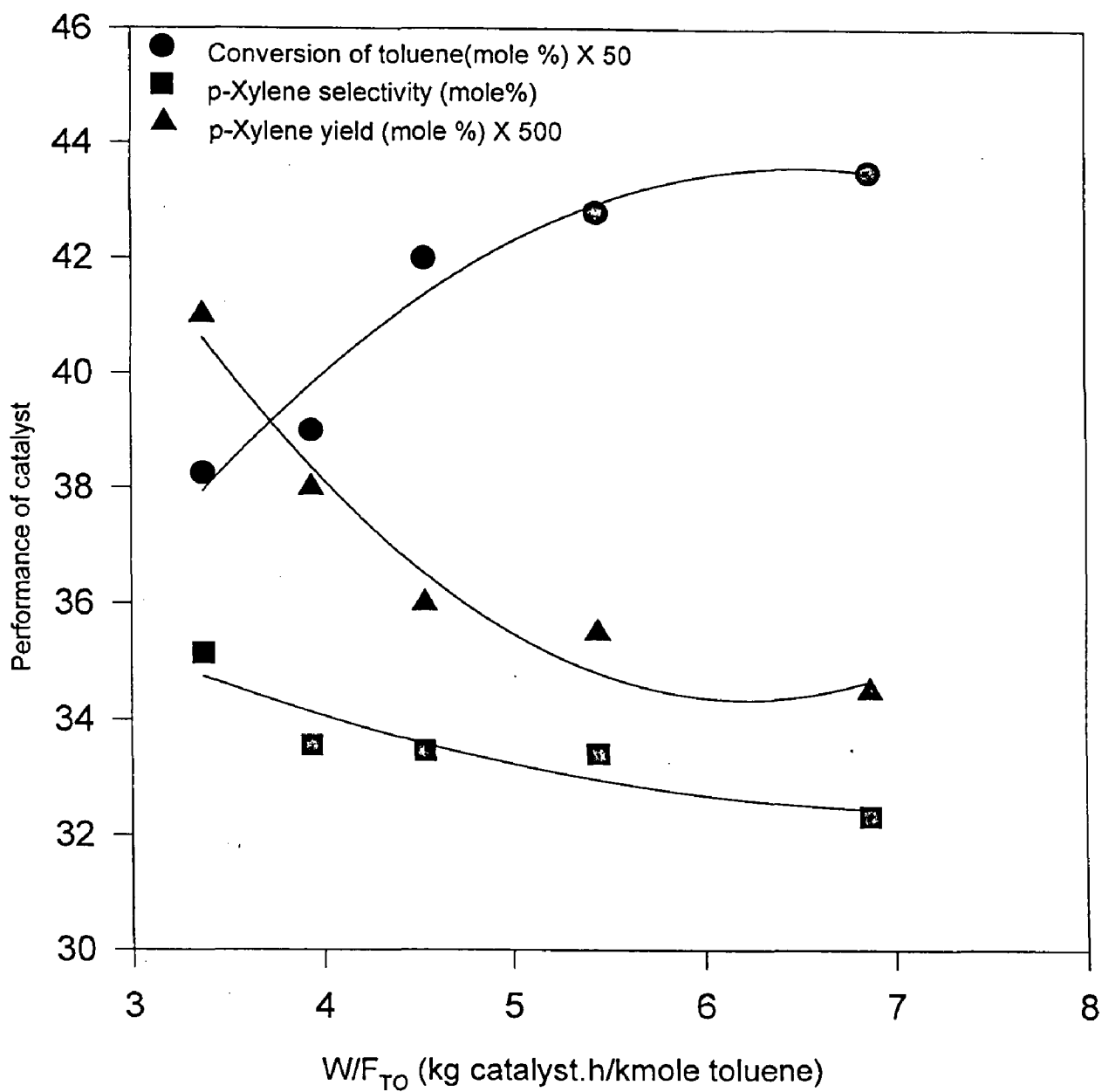OVER HZSM-5 (SAR-19)

FIG. 5.20 EFFECT OF SPACE TIME ON PERFORMANCE OF
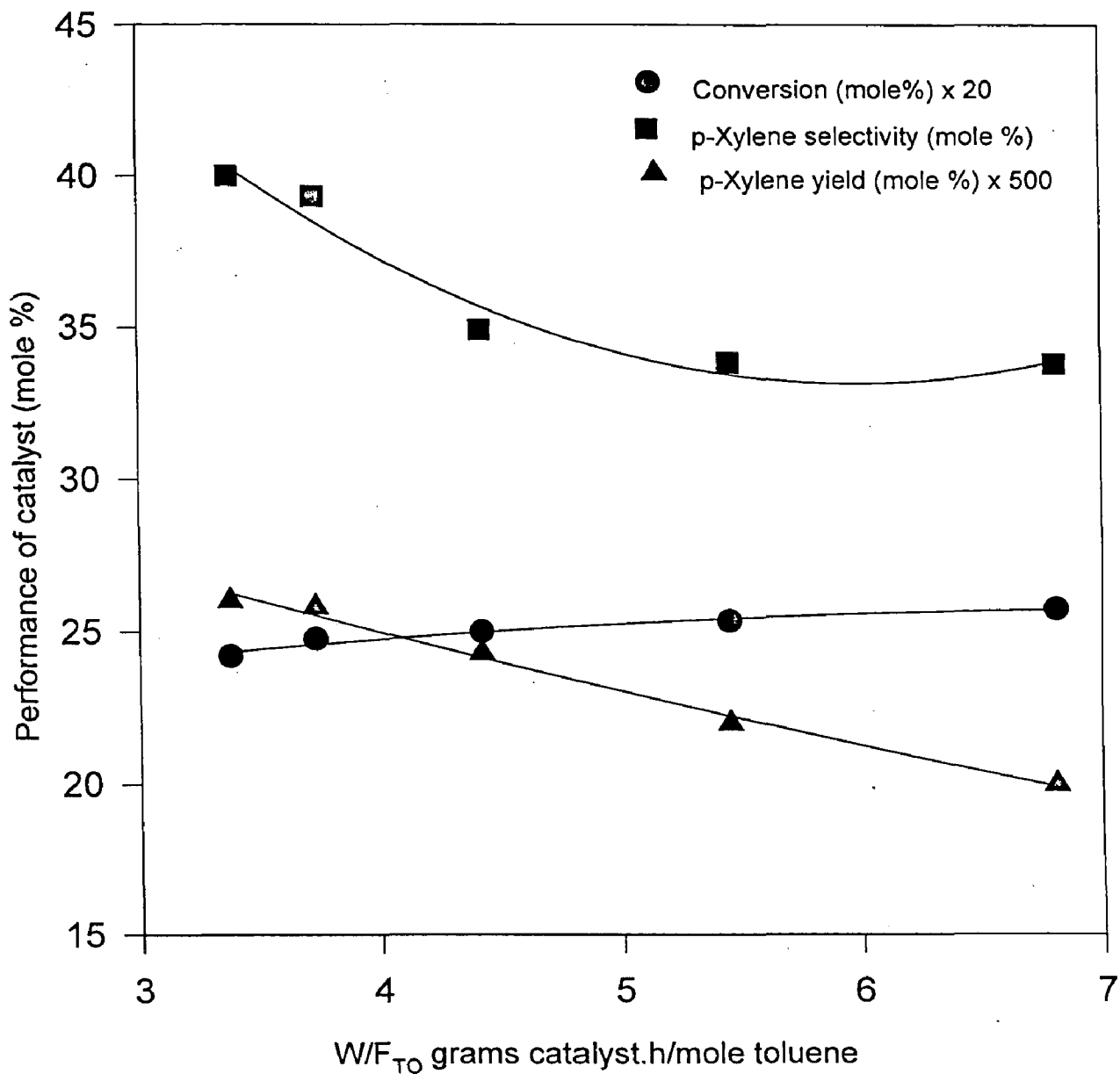(3.95%)PbHY (SAR-3) CATALYST AT 400°C

FIG. 5. 21 EFFECT OF SPACE TIME ON PERFORMANCE OF
(1.92%) Th(1.76%)Cr HZSM-5 (SAR-32) AT 550°C
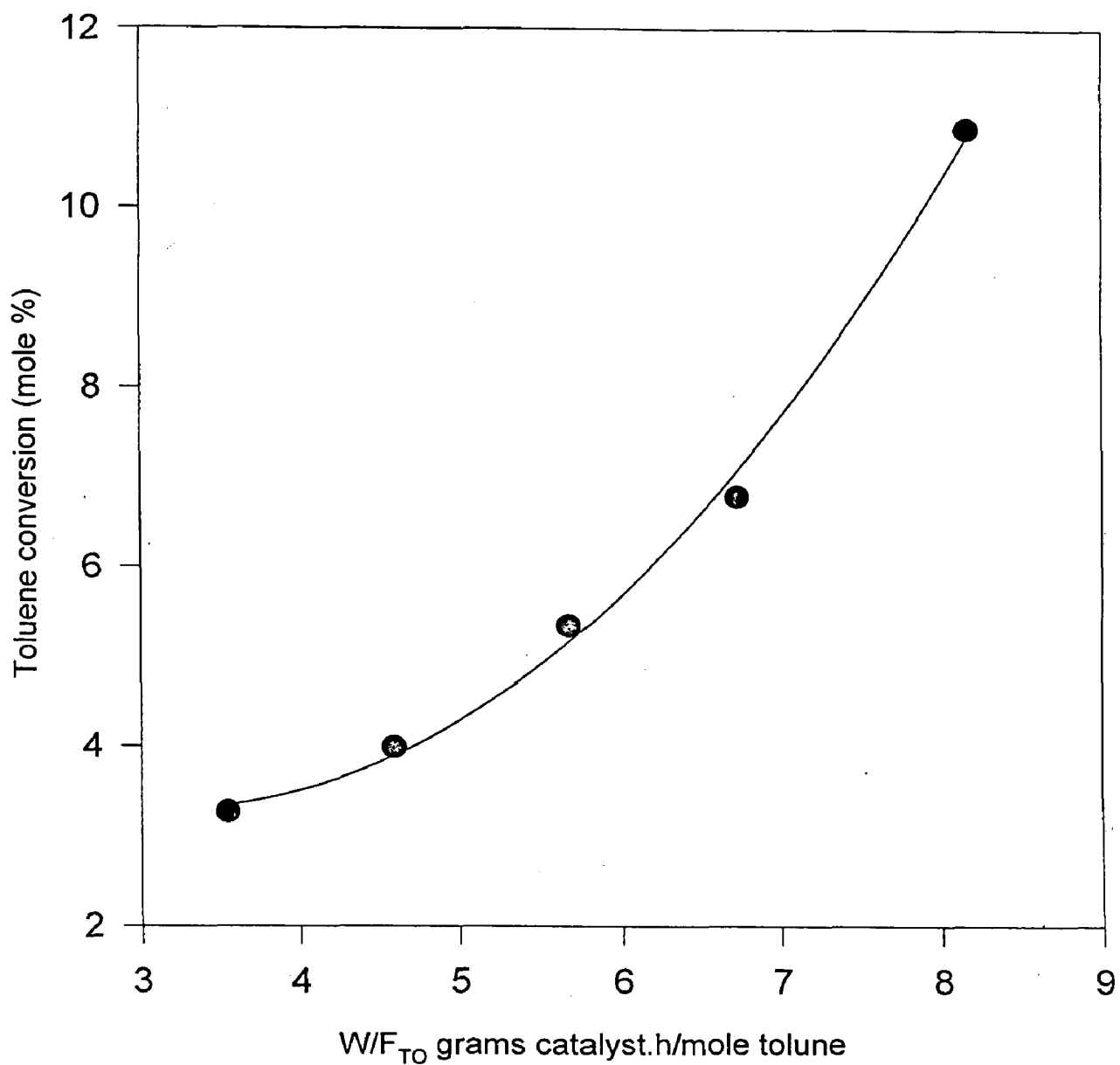
FIG. 5.22 EFFECT OF SPACE TIME ON TOLUENE CONVERSION FOR HZSM-5 (SAR-19) AT 450°C

FIG. 5.23 TEST FOR REVERSIBLE SECOND ORDER HOMOGENEOUS
REACTION MODEL FOR HZSM-5 (SAR-19)
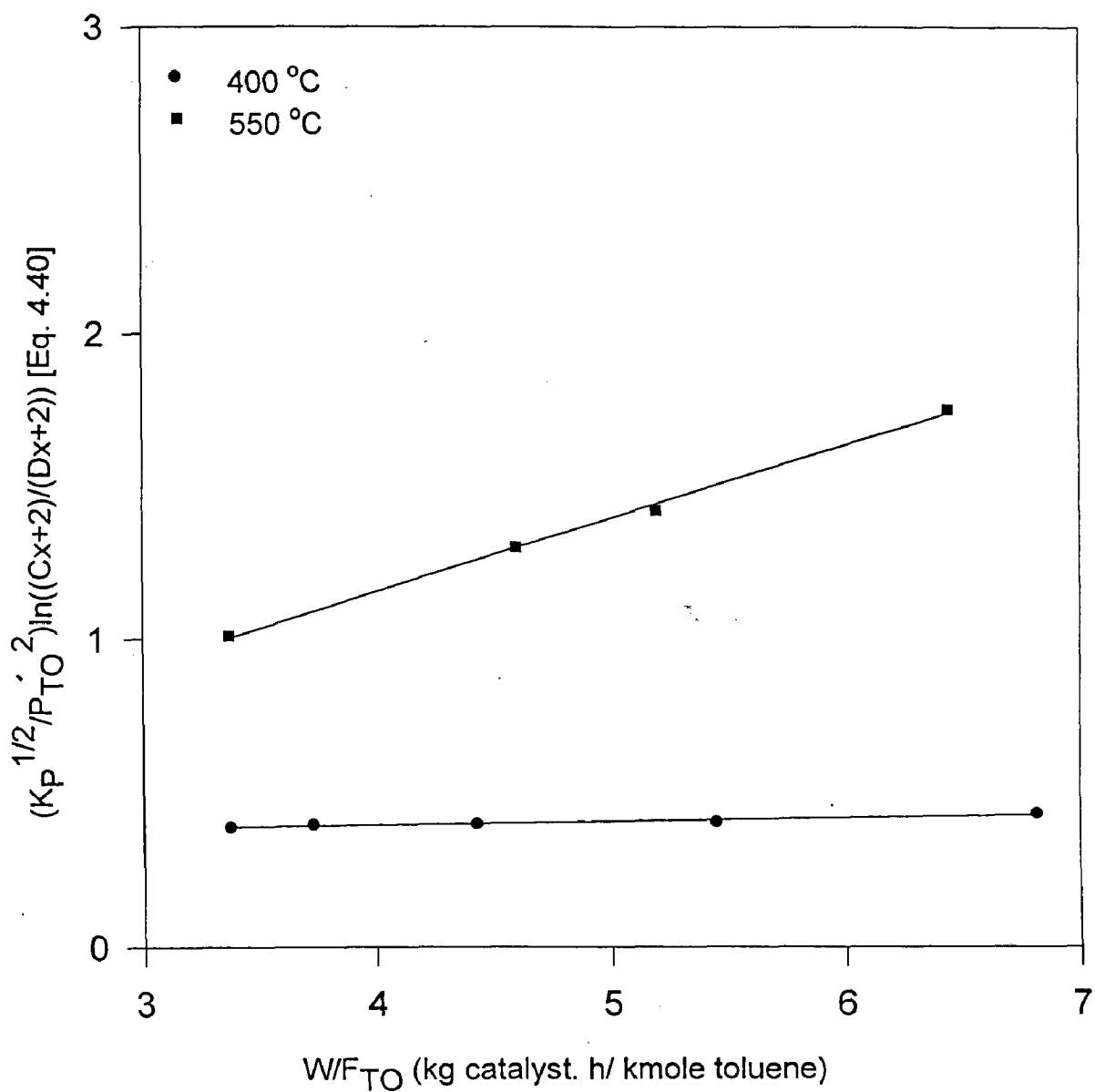
FIG. 5.24 TEST FOR REVERSIBLE SECOND ORDER HOMOGENEOUS
REACTION MODEL FOR (1.76%)Cr (1/92%) Th HZSM-5 (SAR-32)
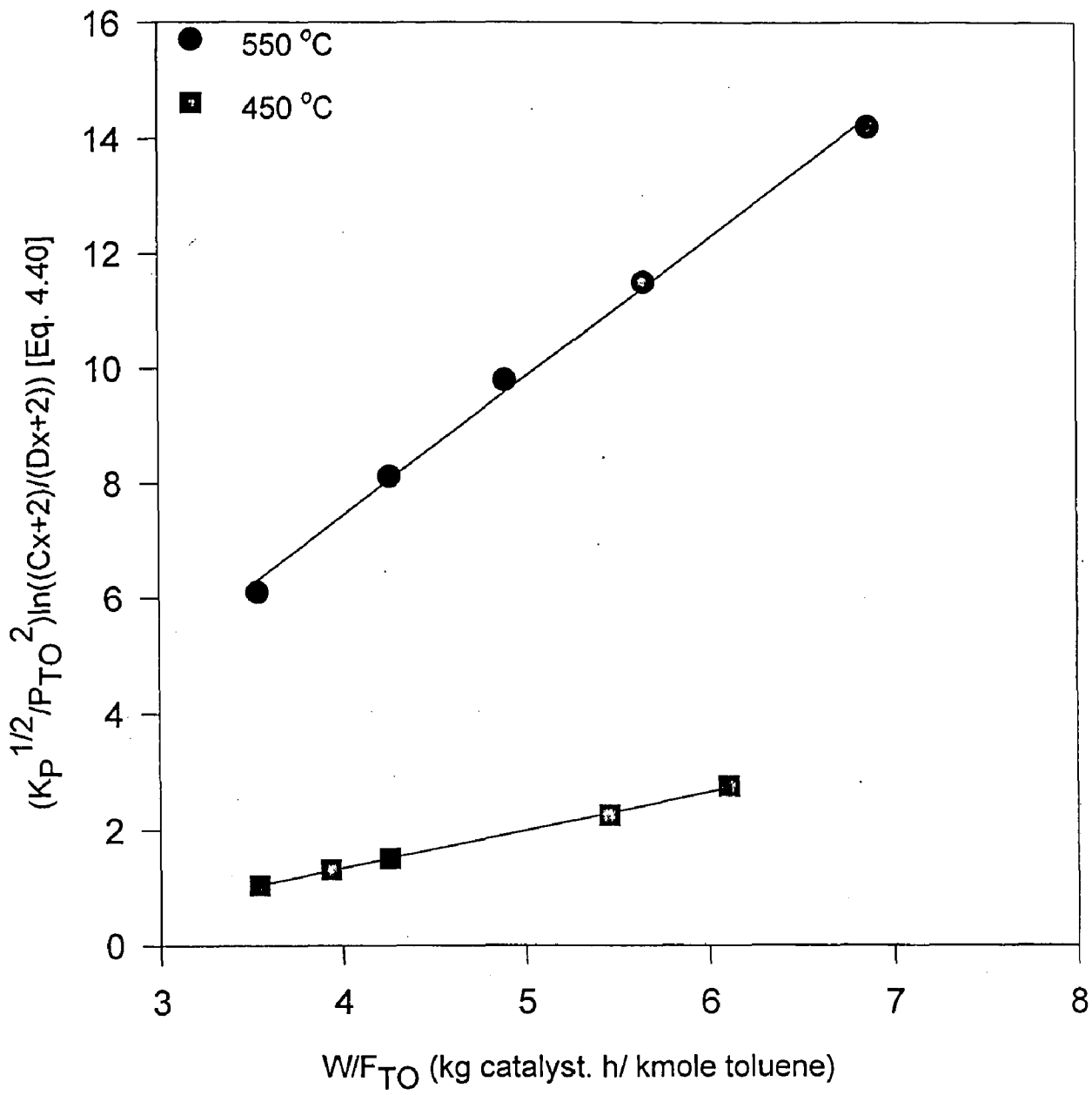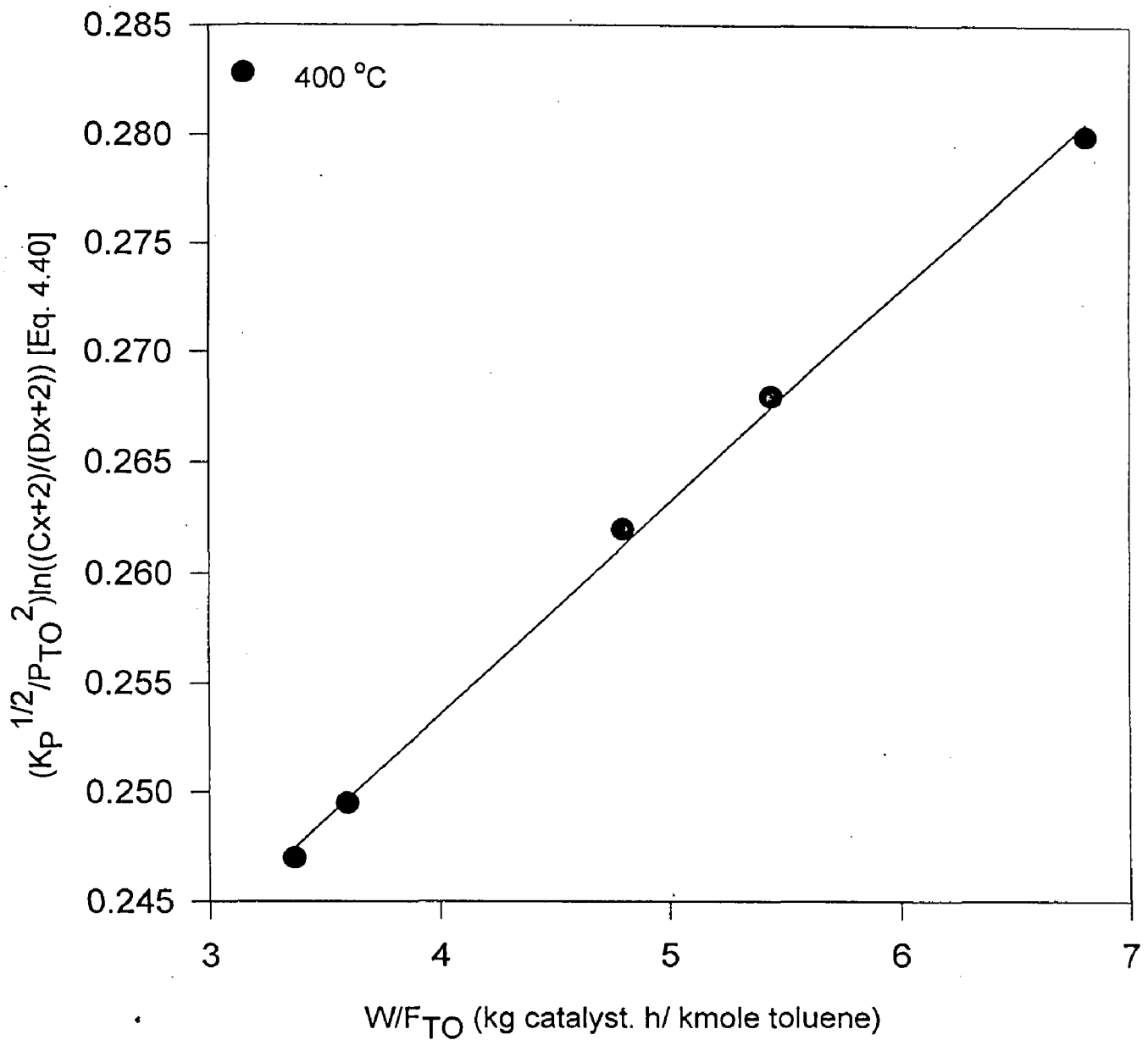
FIG. 5.25 TEST FOR REVERSIBLE SECOND ORDER HOMOGENEOUS
REACTION MODEL FOR (3.95%)Pb HY (SAR-3)

FIG. 5.26 TEST FOR REVERSIBLE SECOND ORDER HETROGENEOUS
REACTION MODEL FOR HZSM-5 (SAR-19)
(ADSORPTION OF TOLUENE RATE LIMITING)
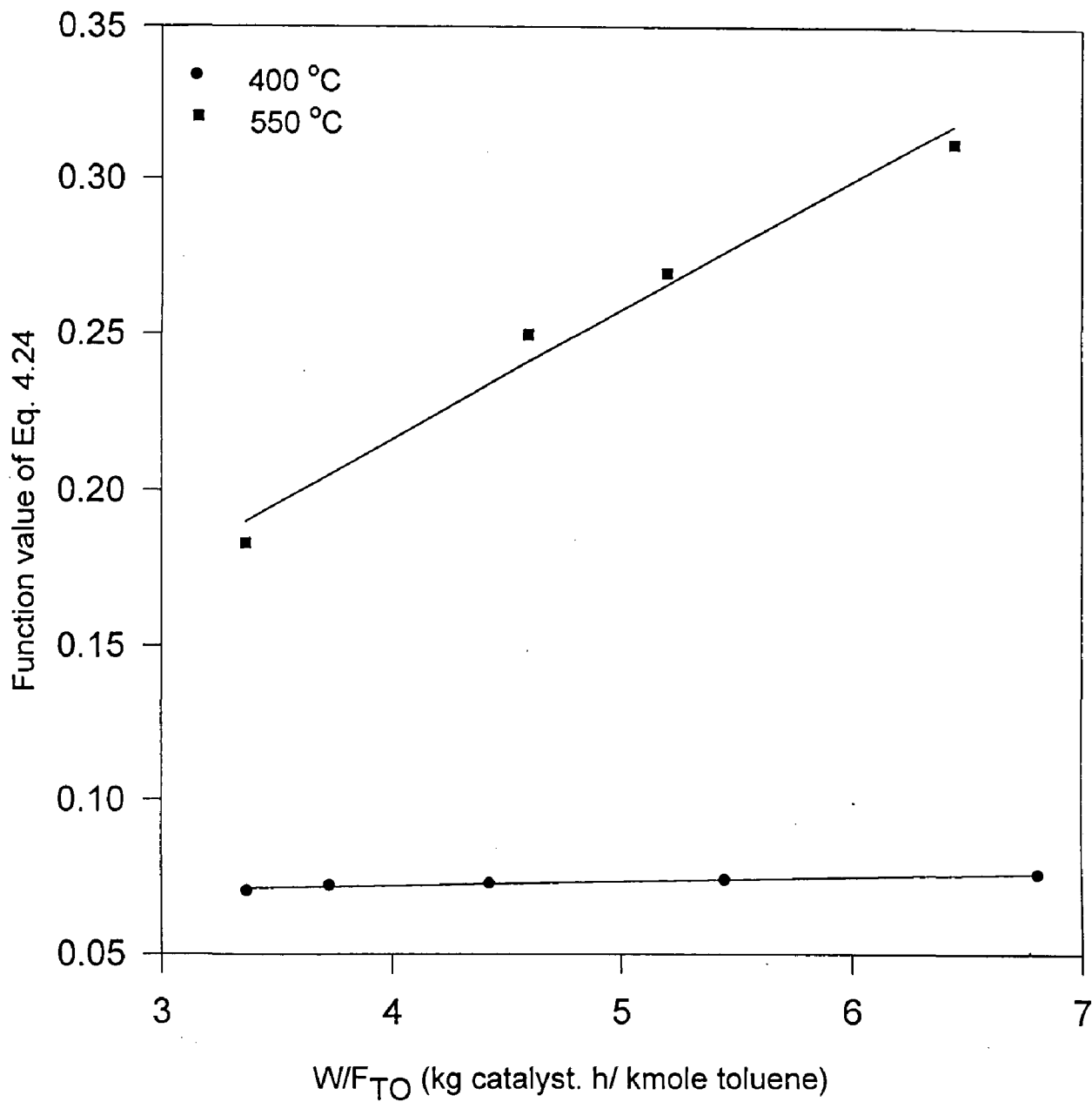
FIG. 5.27 TEST FOR REVERSIBLE SECOND ORDER HETROGENEOUS REACTION MODEL FOR (1.76%)Cr (1/92%) Th HZSM-5 (SAR-32) *(ADSORPTION OF TOLUENE RATE LIMITING)*
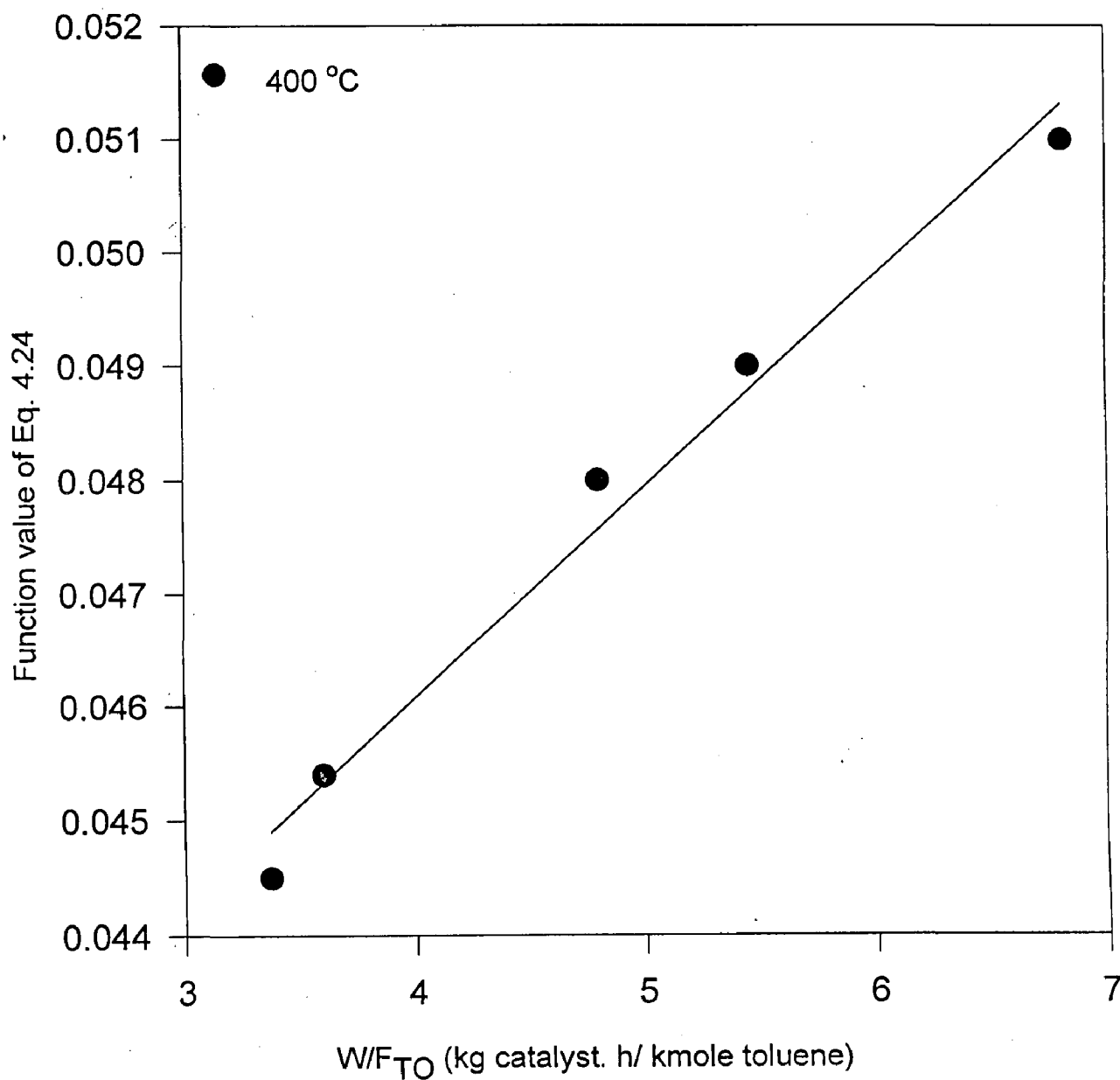
FIG. 5.28 TEST FOR REVERSIBLE SECOND ORDER HETROGENEOUS
REACTION MODEL FOR (3.95%)Pb HY (SAR-3)
(ADSORPTION OF TOLUENE RATE LIMITING)

FIG. 5.29 TEST FOR REVERSIBLE SECOND ORDER HETROGENEOUS
REACTION MODEL FOR HZSM-5 (SAR-19)
(DESORPTION OF XYLENES RATE LIMITING)

FIG. 5.30 TEST FOR REVERSIBLE SECOND ORDER HETROGENEOUS
REACTION MODEL FOR (1.76%)Cr(1.92%)Th HZSM-5 (SAR-32)
(DESORPTION OF XYLENES RATE LIMITING)

FIG. 5.31 TEST FOR REVERSIBLE SECOND ORDER HETROGENEOUS
REACTION MODEL FOR (3.95%)Pb HY (SAR-3)
(DESORPTION OF XYLENES RATE LIMITING)

153

FIG. 5.32 TEST FOR REVERSIBLE SECOND ORDER HETROGENEOUS
REACTION MODEL FOR HZSM-5 (SAR-19)
(SURFACE REACTION CONTROLLING)

FIG. 5.33 TEST FOR REVERSIBLE SECOND ORDER HETROGENEOUS
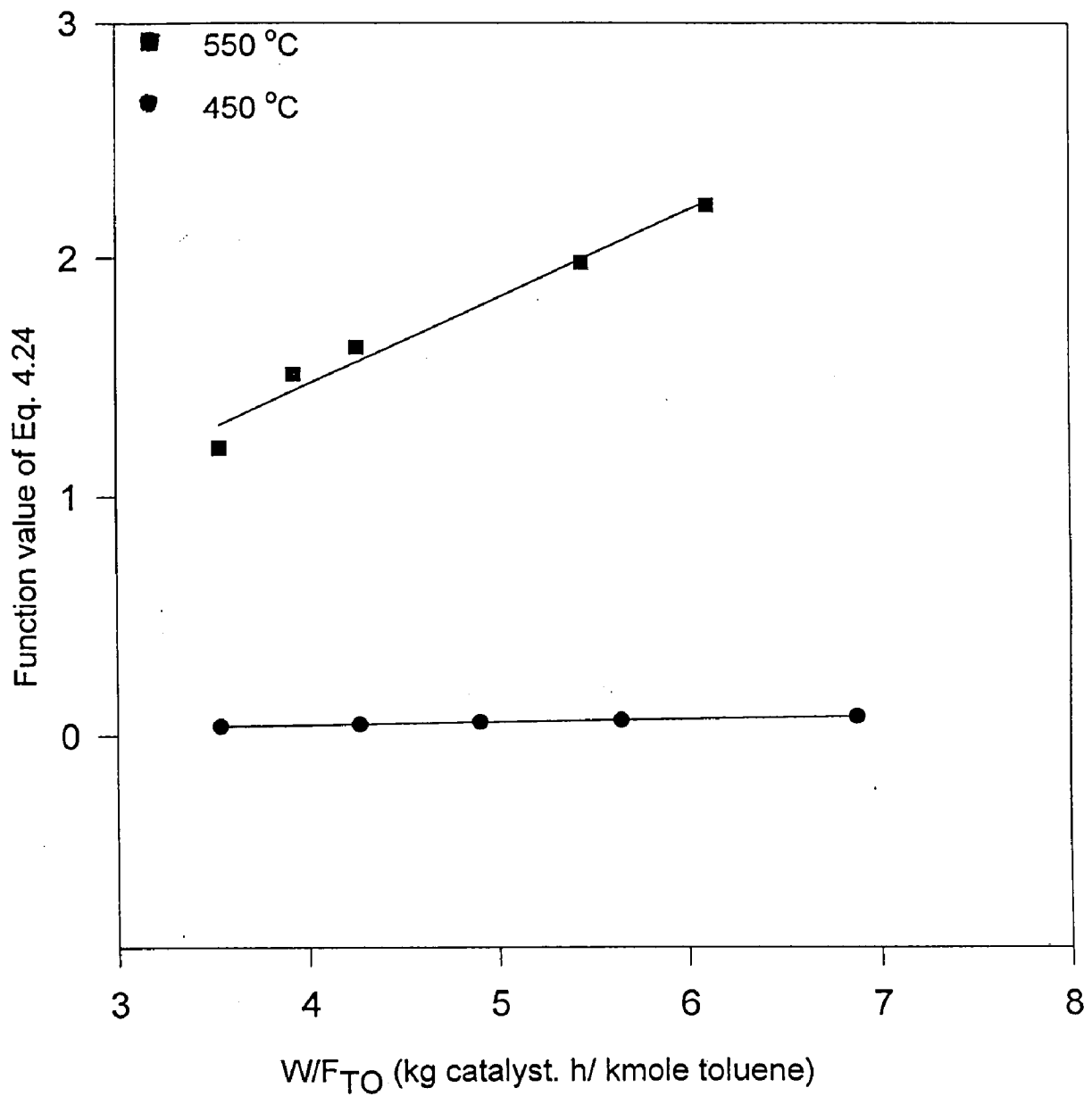REACTION MODEL FOR (2.76%)Cr(1.92%)Th HZSM-5 (SAR-32)
(SURFACE REACTION CONTROLLING)

155

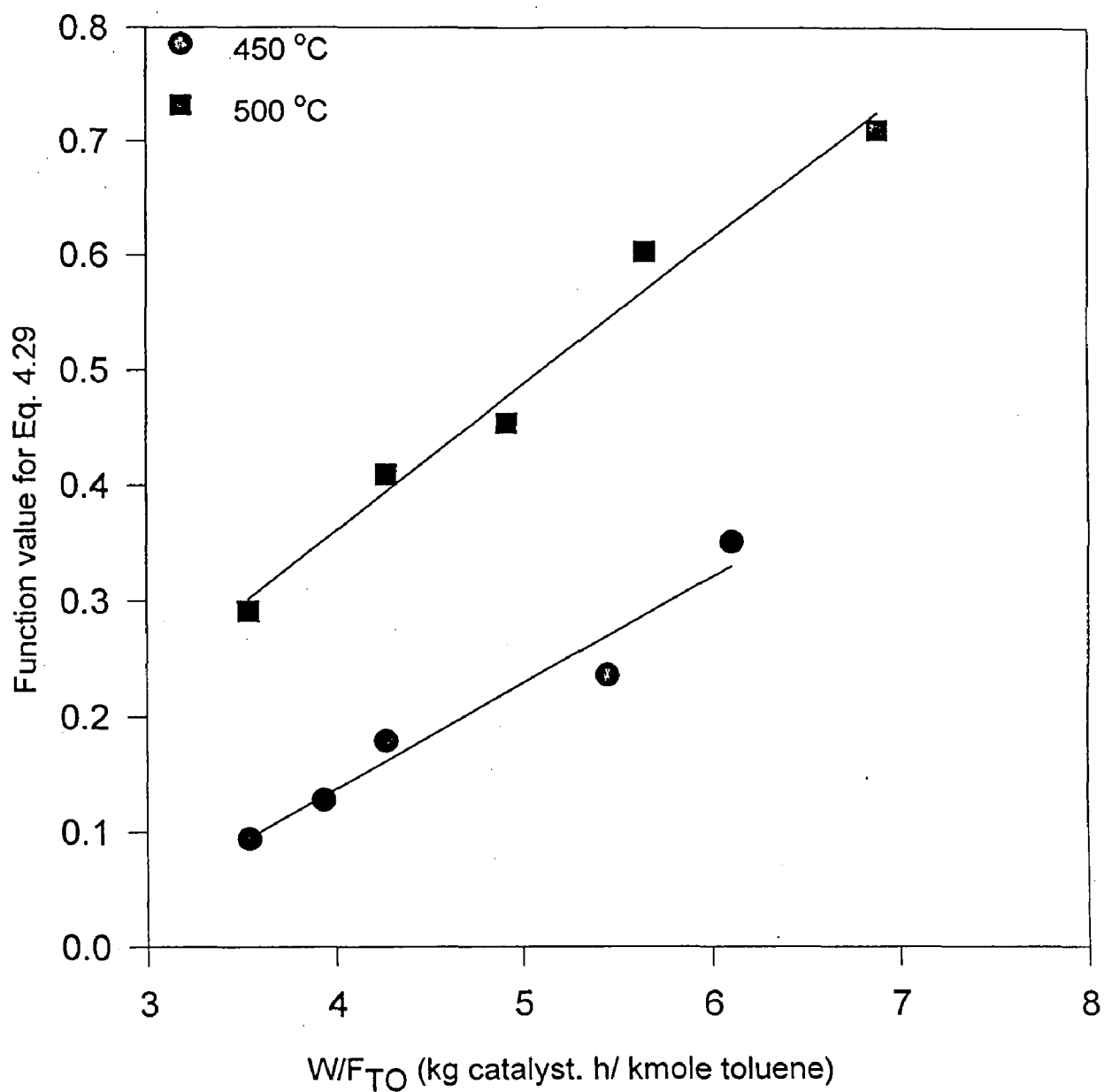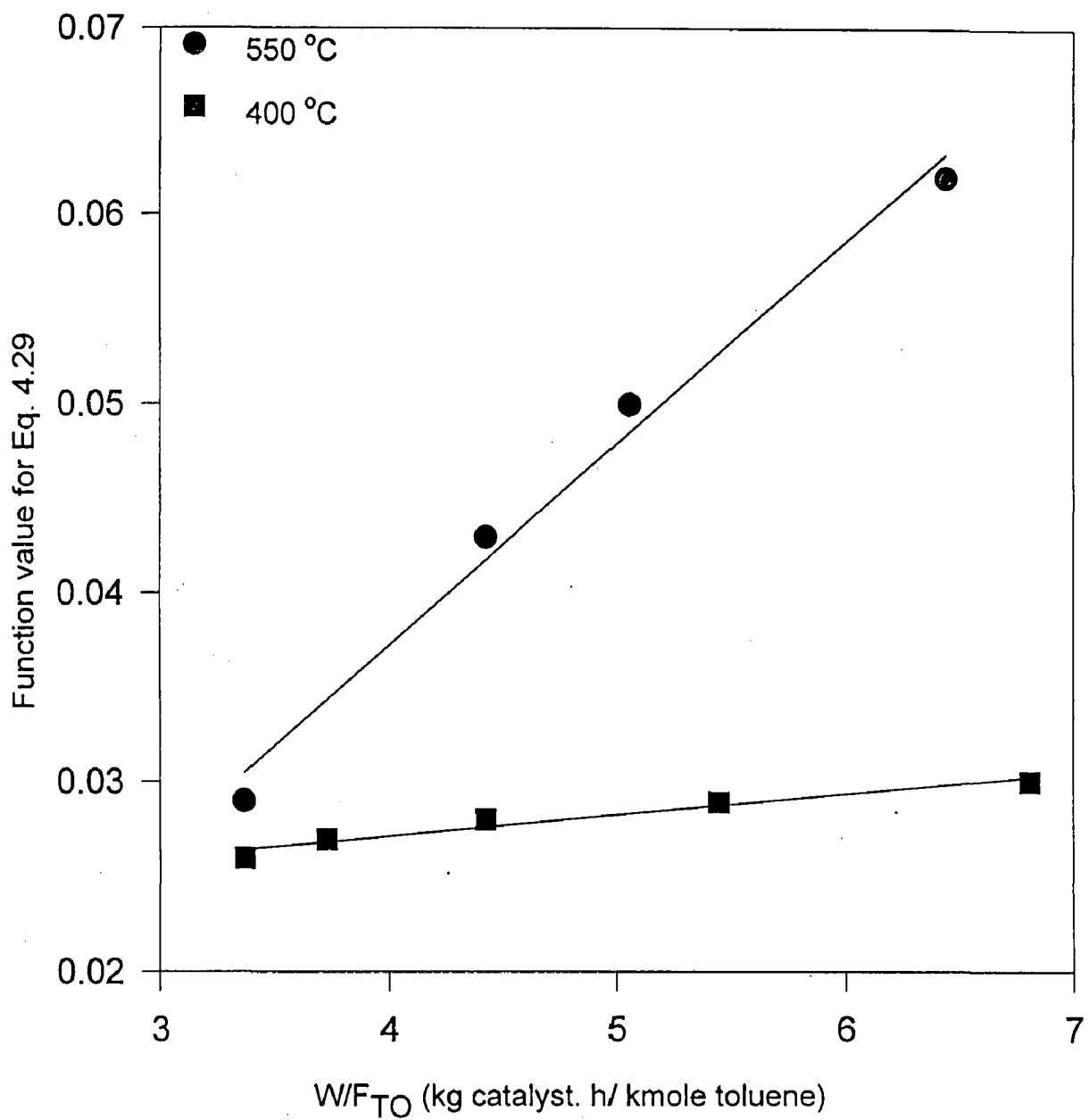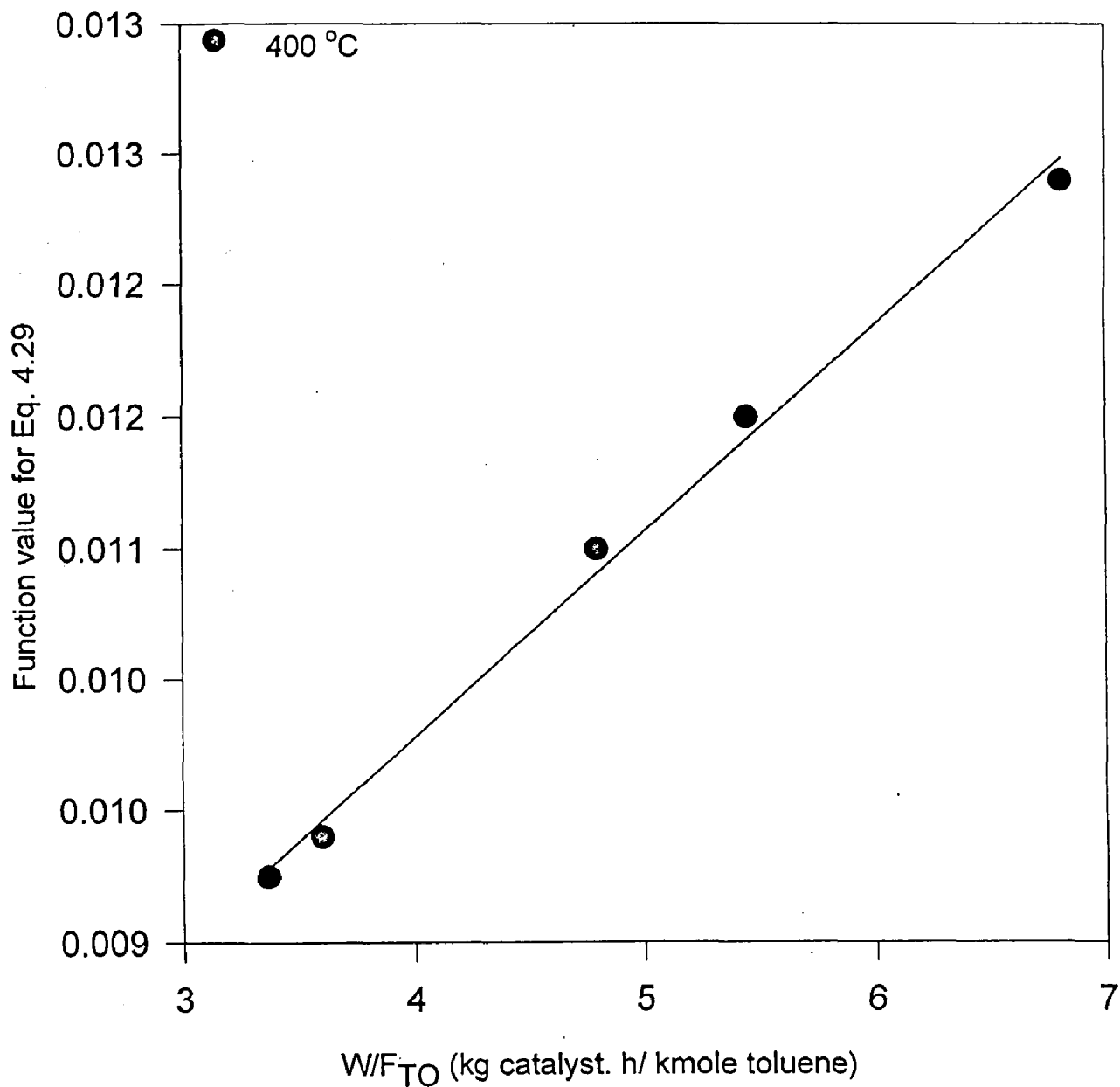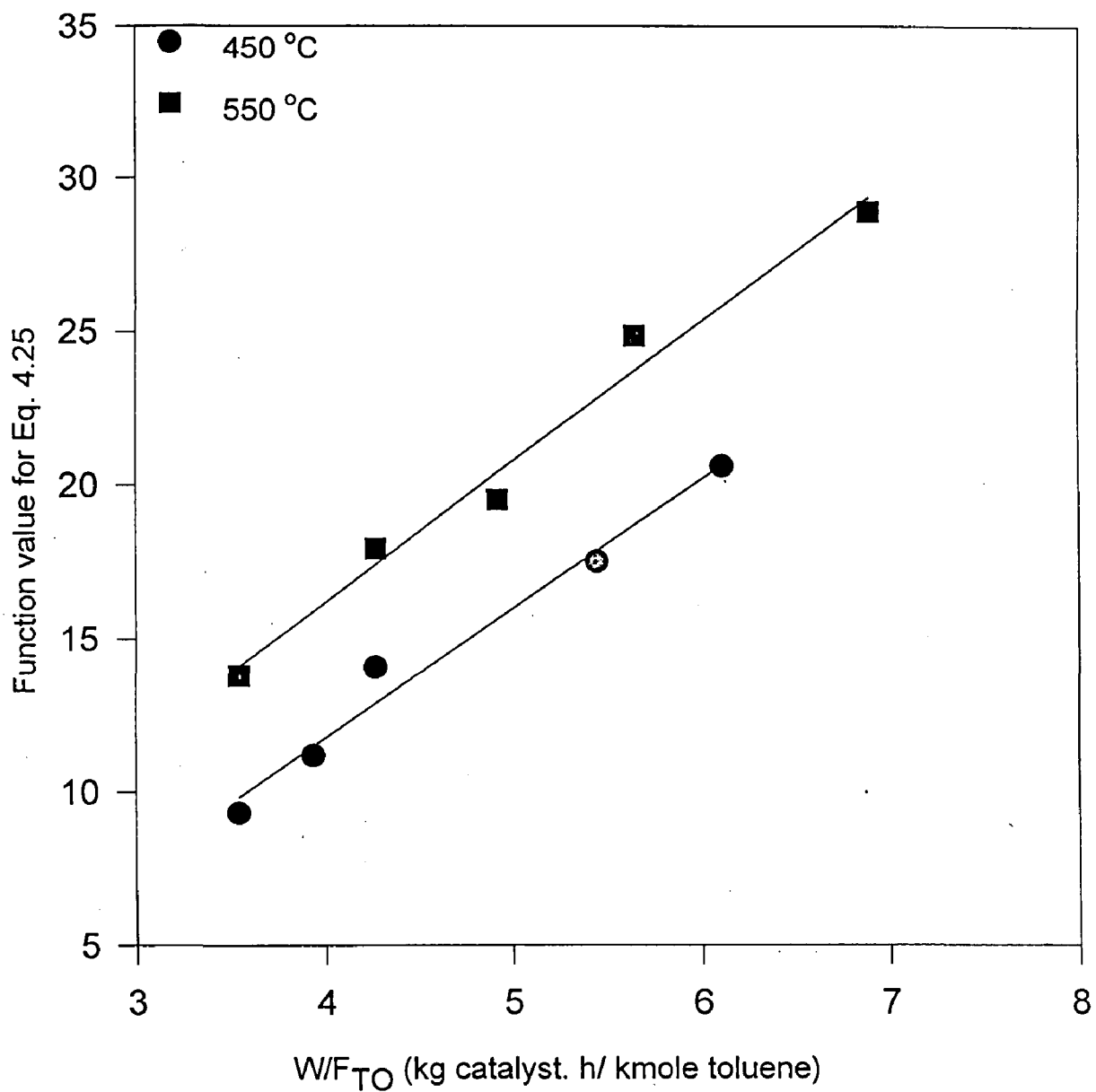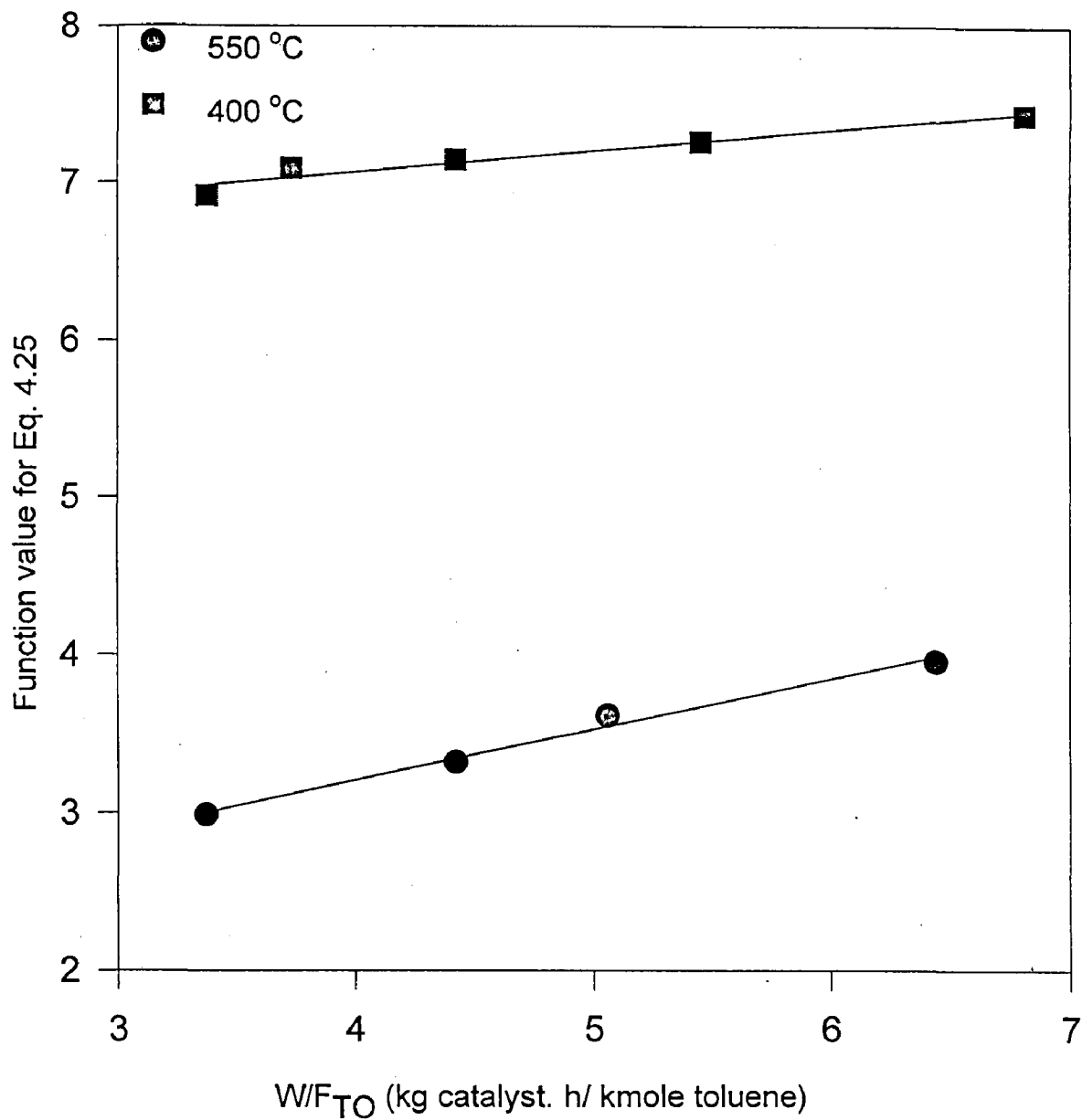FIG. 5.34 TEST FOR REVERSIBLE SECOND ORDER HETROGENEOUS
REACTION MODEL FOR (3.95%)Pb HY(SAR-3)
(SURFACE REACTION CONTROLLING)

The crystallinity of the sample has been calculated as described in Chapter 2. It has been generally found that the crystallinity which was 100% in original sample decreases after the ion exchange. The percent crystallinity value of various catalysts have been tabulated in table 2.5 of Chapter 2. The reasons for the decrease in crystallinity due to ion exchange may be attributed to the partial dealumination caused by the action of steam and thereby, disturbing the framework structure of the catalyst. Thefree $Al(OH)_3$, which is an amorphous material remains outside the lattice structure.

6.1.2 Composition and silica aluminaanalysis

The actual composition in percent by weight of exchanged cation and silica-aluminum ratio were found out by atomic absorption, ICP, and EPMA analyses HZSM- 5(SAR-32). Cation exchanged by Ni, Cu, Cr, and Pb were characterized by atomic absorption, spectrometer, HZSM-5 (SAR-32) exchanged with La and Ce and silica-alumina ratio of HZSM-5 were done by ICP instrument, whereas, silica alumna ratio of HZSM-5 (SAR 19,13) and SAR of Na-Y were done by EPMA instrument. The results of AAS and ICP for % in exchanged have been presented in table 2.6 and 2.7.

6.1.3. I.R. Analysis.

Infrared spectrograms were taken for the representative catalysts in order to see various functional groups (Si-OH-Al, SiOH, Al-OH, H-OH, M-OH, Al-O, Si-O), percentage and the relative changes in the strength of Bronsted acid sites (strong, medium and week) due to ion exchange and subsequent calculation. These properties have been reported to affect strongly the reaction mechanism and product distribution. The spectrograph of HZSM-5 (SAR-32) without exchange and in exchanged from with Ni, Cr, Cu and Ce and also HZSM-5 (SAR 60-70) were taken. Fig. 2.10 and 2.11 present the I.R. spectrograph of the all catalysts mentioned above in the range of wave number 500-4000 cm^{-1}. The functional groups with their frequency and percentage transmittance for various catalysts

have also been presented in table 2.4. The I.R. results of various catalyst have been discussed in details in chapter 2.

6.2 ACTIVITY TEST RESULTS.

6.2.1 Effect of reaction temp on toluene conversion.

Fig. 5.1 through 5.6 present the effect of reaction temperature on percent toluene conversion for HZSM-5 HY and H-Mardenite catalysts. It may be observed that among these catalyst HZSM-5 have highest activity, where as H-mardenite has least activity. The activities have been found to increase in general, with temperature. At 600°C, The % toluene conversion at 8.855 Kg catalyst.h(kmole toluene) $^{-1}$ (space time) one atmospheric reactor pressure and 3.6 molal ratio of nitrogen to toluene. The conversion obtained were about 33%, 21% and 3% for HZSM-5, HY and HM catalyst respectively. The reasons for this may be given to the peculiar acidic distribution and shape selective of ZSM5 zeolite [5]. Beltrame et al. 1985 [5]. Studies of toluene disproportionation of toulene using various zeolites and activity pattern was obtained in order.

HZSM-5(HA) > HY > HZSM -5 > HZSM-11

The activity level of particular catalyst in general is directly related to its acidic strength. The acidic strength of the framework hydrolysis of various zeolites were characterized by FTIR spectroscopy and TPD of NH_3 [30]. The acidic strength was fund in order HZSM5 > β zeolite > HY zeolite.

The surface activity of two sample of H-β zeolite (SAR-28 AND 44) , HZSM-5 and HY measured by the above technique revealed that the strong acid sides in H-β zeolites are weaker then those present in medium pore zeolite HSM-5 and stronger than present in H-Y zeolite. This conclusion as further supported by the shift in OH frequency on adsorption of base like Benzene. The shift of 337 cm^{-1} of observed for Hβ was compared with 350 and 300 cm^{-1} for HZSM-5 and HY respectively. These results on strength of acid sites on β help in understanding its relative catalytic activity and selectivity in comparison to other zeolites in acid catalyzed reaction such as toluene disproportionation.

Fig. 5.2 depicts the effect of silica aluminia ratio of HZSM-5 towards its activity for toluene disproportionation. Three catalyst with silica alumina ratio 19, 40 and 43 were used after exchange with Cr. In all these cases the exchange was done using a 4% salt solution of Cr. The actual percentage of the chromium exchanged varied with silica alumina ratil. The maximum exchange of 3.34 % was found with the lowest silica alumina ratio of 19 , where as the lowest exchange of 2.33% chromium was obtained with highest silica alumina ratio 43. The reason for this may be attributed to the number of H ions available for exchange Higher aluminum contain (Lower SAR) has the higher number of H^+ concentration. The results in figure 5.2 indicate the best conversion for Cr HZSM-5 (SAR 40). At 600 °C the conversion level was found to be about 30% , 16% and 3% for SAR 40, 19 and 43 respectively. No definite sequence have been observed in this case. It shows that the activity pattern of a given catalyst is not only dependent on silica aluminia ratio but also on several other factors like crystallinity and amount of exchange cation etc. It has been found that the percentage crystallinity of SAR-43 is very low. It is generally believed that the crstalline catalysts are far more active in comparison to amorphous (non-crystalline) catalyst at a given temperature. The other reason for lower activity of SAR-43 may be given to lowest chromium exchange level. The exchanged ions equally take part in adsorption of the reacting molecule and thereby in over all catalytic reaction.

The effect of various cation exchanged on HZSM-5 (SAR-32) on the reactivity pattern of toluene disproportionation has been presented in fig. 5.3. The different cations, Th, Ce and La at the exchange level of 3.8%, 3.7% and 3.0% respectively were used. It may be observed that among the three catalysts the activity of the Ce is the best, which is followed by La and Th. The results indicated the activities of La and Th exchanged zeolites in order of their present crystallinity. The percentage crystallinity of La, Th and Ce exchanged terms in HZSM5 found to be 91% , 73%, 63% respectively. The better activity shown by Ce exchanged catalyst inspite of its low crystallinity may be attributed to the

FIG. 5.34 TEST FOR REVERSIBLE SECOND ORDER HETROGENEOUS
REACTION MODEL FOR (3.95%)Pb HY(SAR-3)
(SURFACE REACTION CONTROLLING)

The crystallinity of the sample has been calculated as described in Chapter 2. It has been generally found that the crystallinity which was 100% in original sample decreases after the ion exchange. The percent crystallinity value of various catalysts have been tabulated in table 2.5 of Chapter 2. The reasons for the decrease in crystallinity due to ion exchange may be attributed to the partial dealumination caused by the action of steam and thereby , disturbing the framework structure of the catalyst. The free $Al(OH)_3$, which is an amorphous material remains outside the lattice structure.

6.1.2 Composition and silica aluminaanalysis

The actual composition in percent by weight of exchanged cation and silica-aluminum ratio were found out by atomic absorption, ICP, and EPMA analyses HZSM- 5(SAR-32). Cation exchanged by Ni, Cu, Cr, and Pb were characterized by atomic absorption, spectrometer, HZSM-5 (SAR-32) exchanged with La and Ce and silica-alumina ratio of HZSM-5 were done by ICP instrument, whereas, silica alumna ratio of HZSM-5 (SAR 19,13) and SAR of Na-Y were done by EPMA instrument. The results of AAS and ICP for % in exchanged have been presented in table 2.6 and 2.7.

6.1.3. I.R. Analysis.

Infrared spectrograms were taken for the representative catalysts in order to see various functional groups (Si-OH-Al, SiOH, Al-OH, H-OH, M-OH, Al-O, Si-O), percentage and the relative changes in the strength of Bronsted acid sites (strong, medium and week) due to ion exchange and subsequent calculation. These properties have been reported to affect strongly the reaction mechanism and product distribution. The spectrograph of HZSM-5 (SAR-32) without exchange and in exchanged from with Ni, Cr, Cu and Ce and also HZSM-5 (SAR 60-70) were taken. Fig. 2.10 and 2.11 present the I.R. spectrograph of the all catalysts mentioned above in the range of wave number 500-4000 cm^{-1}. The functional groups with their frequency and percentage transmittance for various catalysts
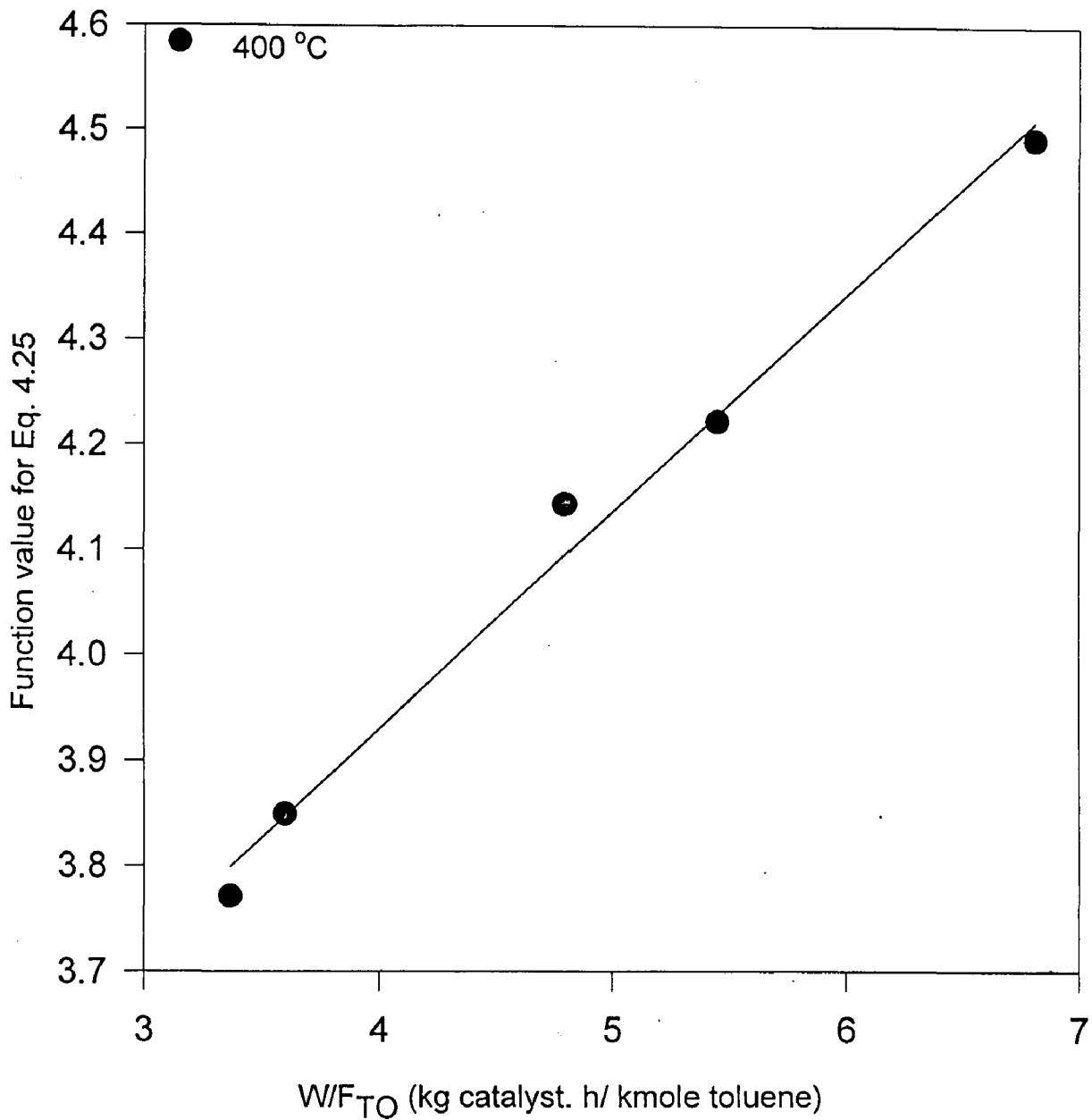
FIG. 5.34 TEST FOR REVERSIBLE SECOND ORDER HETROGENEOUS
REACTION MODEL FOR (3.95%)Pb HY(SAR-3)
(SURFACE REACTION CONTROLLING)

RESULTS AND DISCUSSION

For the study of toluene dispeorportion reaction. various zeolites, such as ZSM-5 (SAR-19, 32, 40, 43), Y zeolite (SAR-3) and H mordenite (SAR-13) were used. Since the catalyst in their usual forms having Na or H cation are not so active and selective for the desired reaction, the chosen catalysts were ion exchanged with various cation ZSM5(SAR-32) was ion exchanged with Ni, Cu, Ce, Th , La , Pb and (Cr + .Th). ZSM -5 having (SAR 19,40,43) were ion exchanged with Cr separately. The Y zeolites was used in HY form as well as ion exchanged with Pb. The mordenite catalyst was not ion exchanged and used in HM form. In all these cases, the exchange is done by taking a 4% salt (nitrate) solution. The actual percentage of ion exchange varies with the valancy of respective cation orbital structure, Si/Al ratio and temperature of ion exchange etc. The actual value of the exchange level have been found out by atomic absorption and ICP which is presented in tables 2.6 and 2.7.

6.1 CATALYST CHARACTERIZATION

6.1.1 X-ray Diffraction

X-ray diffraction of almost all the catalysts ion exchanged as well as without ion-exchange form were done in order to see the structure and estimate the percentage crystallinity. The x-ray diffractogram of some of the catalysts such as HZSM-5 (SAR-32), HZSM5(SAR-19), CrHZSM5 (SAR-32), NiHZSM-5 (SAR-32), CuHZSM-5 (SAR-32) and PbHY are presented in Figs. 2.17 to 2.19. The diffratograms show intense peaks which confirms to the structure of these zeolites as given in the literature The intensity of the peak (height) is found to decrease after the ion-exchange.

The crystallinity of the sample has been calculated as described in Chapter 2. It has been generally found that the crystallinity which was 100% in original sample decreases after the ion exchange. The percent crystallinity value of various catalysts have been tabulated in table 2.5 of Chapter 2. The reasons for the decrease in crystallinity due to ion exchange may be attributed to the partial dealumination caused by the action of steam and thereby, disturbing the framework structure of the catalyst. The free $Al(OH)_3$, which is an amorphous material remains outside the lattice structure.

6.1.2 Composition and silica aluminaanalysis

The actual composition in percent by weight of exchanged cation and silica-aluminum ratio were found out by atomic absorption, ICP, and EPMA analyses HZSM- 5(SAR-32). Cation exchanged by Ni, Cu, Cr, and Pb were characterized by atomic absorption, spectrometer, HZSM-5 (SAR-32) exchanged with La and Ce and silica-alumina ratio of HZSM-5 were done by ICP instrument, whereas, silica alumna ratio of HZSM-5 (SAR 19,13) and SAR of Na-Y were done by EPMA instrument. The results of AAS and ICP for % in exchanged have been presented in table 2.6 and 2.7.

6.1.3. I.R. Analysis.

Infrared spectrograms were taken for the representative catalysts in order to see various functional groups (Si-OH-Al, SiOH, Al-OH, H-OH, M-OH, Al-O, Si-O), percentage and the relative changes in the strength of Bronsted acid sites (strong, medium and week) due to ion exchange and subsequent calculation. These properties have been reported to affect strongly the reaction mechanism and product distribution. The spectrograph of HZSM-5 (SAR-32) without exchange and in exchanged from with Ni, Cr, Cu and Ce and also HZSM-5 (SAR 60-70) were taken. Fig. 2.10 and 2.11 present the I.R. spectrograph of the all catalysts mentioned above in the range of wave number 500-4000 cm^{-1}. The functional groups with their frequency and percentage transmittance for various catalysts
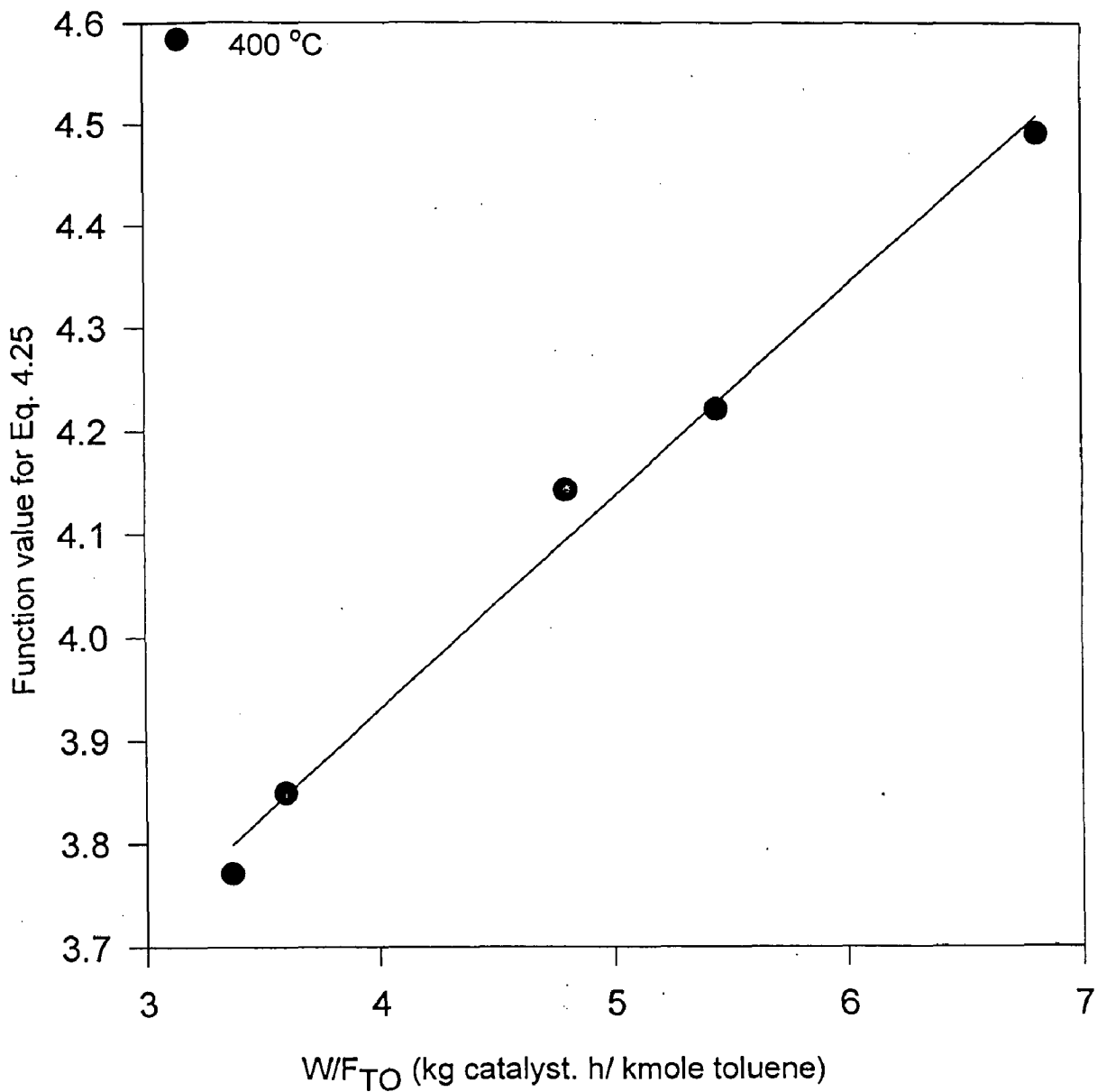
have also been presented in table 2.4. The I.R. results of various catalyst have been discussed in details in chapter 2.

6.2 ACTIVITY TEST RESULTS.

6.2.1 Effect of reaction temp on toluene conversion.

Fig. 5.1 through 5.6 present the effect of reaction temperature on percent toluene conversion for HZSM-5 HY and H-Mardenite catalysts. It may be observed that among these catalyst HZSM-5 have highest activity, where as H-mardenite has least activity. The activities have been found to increase in general, with temperature. At 600°C, The % toluene conversion at 8.855 Kg catalyst.h (kmole toluene) $^{-1}$ (space time) one atmospheric reactor pressure and 3.6 molal ratio of nitrogen to toluene. The conversion obtained were about 33%, 21% and 3% for HZSM-5, HY and HM catalyst respectively. The reasons for this may be given to the peculiar acidic distribution and shape selective of ZSM5 zeolite [5]. Beltrame et al. 1985 [5]. Studies of toluene disproportionation of toulene using various zeolites and activity pattern was obtained in order.

HZSM-5(HA) > HY > HZSM -5 > HZSM-11

The activity level of particular catalyst in general is directly related to its acidic strength. The acidic strength of the framework hydrolysis of various zeolites were characterized by FTIR spectroscopy and TPD of NH_3 [30]. The acidic strength was fund in order HZSM5 > β zeolite > HY zeolite.

The surface activity of two sample of H-β zeolite (SAR-28 AND 44) , HZSM-5 and HY measured by the above technique revealed that the strong acid sides in H-β zeolites are weaker then those present in medium pore zeolite HSM-5 and stronger than present in H-Y zeolite. This conclusion as further supported by the shift in OH frequency on adsorption of base like Benzene. The shift of 337 cm^{-1} of observed for Hβ was compared with 350 and 300 cm^{-1} for HZSM-5 and HY respectively. These results on strength of acid sites on β help in understanding its relative catalytic activity and selectivity in comparison to other zeolites in acid catalyzed reaction such as toluene disproportionation.

Fig. 5.2 depicts the effect of silica aluminia ratio of HZSM-5 towards its activity for toluene disproportionation. Three catalyst with silica alumina ratio 19, 40 and 43 were used after exchange with Cr. In all these cases the exchange was done using a 4% salt solution of Cr. The actual percentage of the chromium exchanged varied with silica alumina ratil. The maximum exchange of 3.34 % was found with the lowest silica alumina ratio of 19 , where as the lowest exchange of 2.33% chromium was obtained with highest silica alumina ratio 43. The reason for this may be attributed to the number of H ions available for exchange Higher aluminum contain (Lower SAR) has the higher number of H^+ concentration. The results in figure 5.2 indicate the best conversion for Cr HZSM-5 (SAR 40). At 600 °C the conversion level was found to be about 30% , 16% and 3% for SAR 40, 19 and 43 respectively. No definite sequence have been observed in this case. It shows that the activity pattern of a given catalyst is not only dependent on silica aluminia ratio but also on several other factors like crystallinity and amount of exchange cation etc. It has been found that the percentage crystallinity of SAR-43 is very low. It is generally believed that the crstalline catalysts are far more active in comparison to amorphous (non-crystalline) catalyst at a given temperature. The other reason for lower activity of SAR-43 may be given to lowest chromium exchange level. The exchanged ions equally take part in adsorption of the reacting molecule and thereby in over all catalytic reaction.

The effect of various cation exchanged on HZSM-5 (SAR-32) on the reactivity pattern of toluene disproportionation has been presented in fig. 5.3. The different cations, Th, Ce and La at the exchange level of 3.8%, 3.7% and 3.0% respectively were used. It may be observed that among the three catalysts the activity of the Ce is the best, which is followed by La and Th. The results indicated the activities of La and Th exchanged zeolites in order of their present crystallinity. The percentage crystallinity of La, Th and Ce exchanged terms in HZSM5 found to be 91% , 73%, 63% respectively. The better activity shown by Ce exchanged catalyst inspite of its low crystallinity may be attributed to the

unique properties of Ce cation. The Ce cation has been known for its oxygen reservoir properties. This might have led to a greater hydrophilic nature of Ce exchanged zeolite, causing it to greater dealumoination in comparison to the other two during the steaming while being ion exchanged. This might have led to formation of $Al(OH)_3$ present out side the lattice frame work and thereby contributing to conversion of toluene. The percent toluene conversion at 650 C were obtained as approximately 14.5%, 13% and 11% for Ce, La and Th exchanged catalysts respectively.

Fig. 5.4 compares the activities of HY zeolites with 3.95% PbHY and CrThHZSM-5 catalyst. The activity of HY may be compared to ion exchanged HZSM-5. The lower activity shown by HZSM-5 based catalyst may be given to the blockage of active centers by Cr and, Th. HY zeolites having a SAR equal to three has higher aluminum content and, thereby, more acidic in nature leading to greater conversions. Pb exchanged Y-zeolite have been found to be the best among all. It gave a maximum conversion of about 33% in comparison to about 7.5% for both HY and CrThHZSM-5 at 550°C. The activity of PbHY is observed to be higher up to 550°C than the other two catalysts which decrease sharply above 550°C giving the lowest activity among the three catalyst. The highest activity of PbHY at 550°C is a unique properly of Pb cation which decreases at higher temperature due to its possibly detachment as active centre and chemical vapor deposition of it at the other active center and hence blocking the activity.

Fig. 5.5 presents the effect of flow rate of the carrier gas nitrogen on percentage conversion at 550 and 600°C. The catalyst used for this test is HZSM-5 (SAR-32) .The results indicate increase in percent conversion (initially) from 0.1 lpm flow rate of nitrogen to 0.3 and there after with further increase in nitrogen flow rate from 0.3 to 0.6 lpm the conversion decreases. The above fact may be discussed based on the facts that at lower nitrogen flow rate of 0.1 lpm, the passage of toluene through the catalyst bed is in concentrated form and at slower velocity in comparison to the movement of toluene feed with 0.6 lpm nitrogen flow rate. The lower velocity may lead to lesser heat and mass transfer resulting in

a lower conversion where as a dilute feed at 0.6 lpm may also lead to a lower conversion level inspite of having a higher velocity. The optimum of the cases was found at a middle flow rate of 03 lpm nitrogen flow rate providing both an adequate concentration and velocity conditions for better conversion.

Fig. 6 presents the effect of temperature on toluene conversion with HZSM-5 (SAR-32) having different particle size. Three sizes of the catalyst, viz. 0.604 and 0.954, 1.303 mm were used. The figure clearly indicates a higher conversion at all temperature with the catalyst having smallest size. The reason for this may be attributed to large surface area of the catalyst particles.

6.2.2. Effect of Reaction Temperature on p-Xylene selectivity

Fig. 5.7 through 5.12 present the effect of reaction temperature on p-xylene selectivity using various catalysts at 8.3 to 8.9 kg catalyst.h / kmol toluene, nitrogen to toluene molal ratio 3.59 to 4.28 and 1 atm. reaction pressure. Figure 5.7 compares % p-xylene in xylenes product at various temperatures for HZSM-5 (SAR-19), HY (SAR-3) and H mordenite (SAR-3). Among the three catalysts HZSM-5 shows best performance towards p-xylene selectivity, followed by HY and HM. p-xylene formation starts at around 500 °C in case of HZSM-5, whereas the same occurs at 500 °C and 600 °C in cases of HY and HM respectively. Except in case of HY, the p-xylene selectivity was found to increase with temperature. The maximum selectivity of p-xylene was obtained at 550°C with HZSM-5 and HY which was around 26%, a little higher than equilibrium value of 24%. An increase in p-xylene selectivity at 600°C with HM may be due to formation of coke which might block the pore radius of catalyst forcing the ortho and meta components to isomerise.

Fig. 5.8 shows the effect of SAR of HZSM-5 catalyst on the p-xylene selectivity at different temperatures. In all these cases the HZSM-5 catalysts having SAR of 19,40 and 43 were exchanged with Cr using a 4% salt solution. It may be observed that among the three catalysts SAR 40 is the best at temperatures upto 550 °C. p-xylene formation started right from 350°C with SAR

- 40 and remained more or less at its equilibrium value of 24% upto 650°C. The p-xylene formation may be noticed to start at 500 °C and 600 °C respectively with SAR-19 and SAR-43. A maximum p-xylene selectivity of about 28% was found at 650°C with SAR-43. The decline in the p-xylene selectivity at 650°C below equilibrium value with SAR-19 may be due to the larger acidity leading to isomerisation of p-component on the surface of the catalyst.

Fig. 5.9 compares the activities of Th, Ce and La exchanged HZSM-5 (SAR-32) catalyst on p-xylene selectivity. Ce was found to be better than the other two. However the highest p-xylene selectivity of around 29% was obtained with Th exchanged catalyst at 600°C. At 650°C the p-xylene selectivity with all the three catalysts was near its equilibrium value.

Fig. 5.10 depicts the comparative performance of CrThHZSM-5. Though the selectivity of p-xylene is little lower for CrThHZSM-5 catalyst in comparison to HYcatalyst at 550 and 600°C, the performance of HZSM-5 catalyst have been found to be consistent even at higher temperature of 650°C. The activity towards p-xylene selectivity for HY zeolite declines at 650°C below its equilibrium level. The reason for this may be given to the isomerization of para-component to ortho and meta.

The observations mentioned above, in general, show a delayed p-xylene formation (at 500 °C) and above and the selectivity more or less in the range a little over its equilibrium value (max. 28%) . The results compare fairly poor with respect to the results reported in the literature, using HZSM-5 catalyst modified with chemical vapour deposition of Si and Mg [8]. However, the results obtained by other investigators using unmodified HZSM-5 are almost in accordance with the present result.

Fig. 5.11 presents effect of nitrogen flow rate on p-xylene selectivity. The catalyst used for this study was CuHZSM-5 (SAR-32). The plot shows the decreasing pattern in p-xylene selectivity with increasing nitrogen flow rate (with an exception of increasing p-selectivity at 600 °C and at 0.6 lpm nitrogen flow rate). The dcline in p-xylene selectivity with flow rate upto 0.5 lpm may be related

with increase in conversion level during this period and thereby leading and more isomerization of para to ortho and meta. The increase in selectivity at still higher N_2 flow rate (0.6 lpm) is due to the greater mass transfer leading to a quicker diffusion of p-xylene component from the surface of the catalyst.

An other reason of higher para selectivity at 600 °C in compare to 550 °C at 0.6 and 0.1 lpm N_2 may be attributed to the coke formation leading to slower diffusion and thereby isomerisation of ortho and meta into para inside the pores. Thus, a maximum para selectivity of the order of 32.5 % may be obtained at 600°C and 0.1 lpm N_2 flow rate.

The effect of particles size of NiHZSM-5 catalyst on para-xylene selectivity have been shown in figure 5.12 . The catalyst used for the studies was ion exchanged with nickel. The p-xylene selectivity may be found directly proportional to the size of the catalyst. The larger particle size the greater p-xylene formation. This phenomena has also been observed by other investigators [31]. The reason for this behavior may be explained on the basis of larger size, particle having larger pore lengths, which offer a slower diffusion of xylene isomers, forcing the isomerization of meta and ortho to para.

6.2.3 Effect of reaction temperature on p-xylene yield over various zeolite catalysts

It can be found from the literature [8] that the selectivity of p-xylene is increased by chemical vapour deposition of various elements like, Si, Mg, P and B etc. The mechanism for the enhancement of p-xylene in the product was suggested to be due to the blockage of the pore size of medium pore zeolites and thereby restricting the exit of ortho and meta component resulting in isomerisation. This chemical vapour deposition, at the same time, was found to reduce the conversion level due to the coverage of the active centers. The previous results, thus, reveal higher p-xylene selectivity in the product at the cost of toluene conversion. The performance of the catalyst should, therefore, be judged by both higher conversion and higher selectivity.

In an attempt to found out the combined effect of above two, the p-xylene yield was calculated for each catalyst, which is defined as

p-Xylene yield (%) = Mole of p-Xylene in products x 100 / Total mole of toluene fed

Fig. 5.13 through 5.17 present the effect of reaction temperature on p-xylene yield for various zeolite catalysts. Fig 5.13 shows the relative activities of HZSM-5, HY and H-mordenite catalyst at 8.86 kg catalyst h/ kmol toluene, Nitrogen to toluene molal ratio of 4.98 and at one atmospheric reaction pressure. HZSM-5 (SAR-19) has been found to have the best activity in terms of higher p-xylene, yield and p-xylene formation starting at much lower temperature. Maximum para xylene yield of 2.1 percent can be obtained at 550 ^{0}C with HZSM-5 (SAR-19), whereas, the p-xylene yield with H-Y catalyst is around 0.7% at 550 ^{0}C. H-mordenite has shown the start of p-xylene formation only after 600^{0}C and maximum p-xylene yield of 0.4% can be obtained at 650^{0}C.

Fig. 5.14 compares the activities of chromium exchanged HZSM-5 catalyst having different silica alumina ratios 19,40 and 43. The p-xylene yield obtained by SAR-40 is much higher 6 in comparision to other two. In general the p-xylene yield have been found to increase with temperature up to 650^{0}C. At 650^{0}C a p-xylene yield of order of 7% may be found with SAR-40 as against about 2.1% and 0.5% only with SAR-19 and 43 respectively. The reasons for this may be attributed to the better conversion and better p-xylene selectivity as explained before.

Fig. 5.15 presents the relative activities of Th,Ce and La used as exchange ions with HZSM-5 (SAR-32) for the p-xylene yield. The results indicate an increase in p-xylene yield with temperature. Ce exchanged catalyst has the highest activity in comparison to La and Th. At 650 ^{0}C percent p-xylene yield obtained by Ce exchanged catalyst is 1.277 in comparision to 1.04 and 1.00 % with La and Th xchanged catalysts respectively. The reason for better activity of cerium may be ven to both toluene conversion as well as p-xylene selectivity as explained in vious section.

Fig. 5.16 compares the activities of CrThHZSM-5, HY ad PbY catalyst, PbHY has been found to be best among three, however, its activity decline fast after attaining a maximum p-xylene yield of 1.8 percent at 550^{0}C. The yield by other two catalysts at 550^{0}C are much lower. ZSM-5 based catalysts have shown to have a steady activity which increase with temperature, giving a p-xylene yield 2.30 percent at 650^{0}C. The decline in activity towards p-xylene yield at 650^{0}C with HY catalyst may be attributed to the suggested coking of the catalyst, wereas, for PbHY it is due to possibly the detachment of Pb from active centre at high temp. Pb is known to be a very soft metal having much lower melting point.

Fig. 5.17 compares effect of catalyst partical size of Ni-HZSM-5 towards its activity and p-xylene yields. Although the lowest particle size catalyst have been shown earlier to have higher conversion in contrast to the largest particle size having better p-xylene selectivity, the combined effect of the two, that is the p-xylene yield, can be clearly seen by the lowest size dominating over bigger particle sizes in terms of higher p-xylene yield.

6.2.4 Effect of space time on performance of catalyst.

Fig. 5.18 through 5.22 present the effect for space time on the percentage toluene conversion for different zealite catalysts. All these runs were conducted at varying W/F$_{To}$ and constant nitrogen to toluene molal ratio. For this 2 gm of catalyst was placed in reactor and toluene feed rate was varied from 0.35 ml/min. to 1.1 ml/min. In order to keep the nitrogen to toluene molal ratio same the nitrogen flow rate (lpm) was kept exactly same as the toluene feed rate in ml/min. Toluene feed rate was measured by collecting the condensed toluene after passing through the reactor for definete time, whereas, the nitrogen flow rate was measured by a rotameter. In this process the partial pressure of toluene was maintained constant at 0.1776 bar and nitrogen to toluene molal ratio of 4.796. The space time (W/F$_{To}$) was varried from about 3.2 to 8.0.

Fig. 5.18 shows the percentage toluene conversion as a function of space time over HZSM-5 SBR 19 at 450 and 550^0C. It is clear that with increae in space time the toluene conversion increases. At 550^0C the conversion are much higher in comparison to 450^0C. At a value of W/F_{T_0} equal to 6.0 toluene conversion of the order of 27.5 percent may be obtained at 550^0C as against only 7% at 450^0C. The reasons for inhanced conversion at higher space time is clearly due to the greater contact time between the reactant and the catalyst.

Fig. 5.19 presents the effect of space time on percent p-xylene selectivity over HZSM-5 (SAR-19). The results show a decreasing trend in percent p-xylene selectivity with space time at both the temperatures 450 and 550^0C. A decrease of about 2% (26 to 24%) may be observed as against a decrease of about 10% (24 % to 14%) at 450 and 550^0C respectively for an increase in space time from 3.5 to 7.0. The reasons for the decline in p-xylene selectivity with space time may be due to greater residence time of para isomer on the surface of the catalyst alowing it to under go isomerisation and this isomerisation is clearly seen to be much faster at a higher temperature.

Fig. 5.20 presents the effect of space time on the performance of PbHY catalyst at 400 ^0C. At lower temperatures (below 550^0C), the activity of PbHY catalyst has been exceptionaly good as shown earlier. From the figure it may be observed that with increase in sapce time conversion increases, whereas, the p-xylene selectivity and p-xylene yield decreases.

Fig. 5.21 presents performance of CrThHZSM5 (SAR-32) as a function of space time at 550^0C. It can be seen that with increase in space time conversion increases, whereas, the p-xylene selectivity and p-Xylene yield decreases. Fig. 5.22 shows the toluene conversion as a function of space time for HZSM-5 (SAR-19) at 450^0C. As expected the % toluene conversion is found to increase with temperature.

Table 6.2 Reaction rate constant values for various catalysts calculated from plots (5.23 to 5.34)

Heterogeneous model

Catalyst	550^0C	450^0C
HZSM-5 (SAR-19)	$k_1^. = 0.3049$	$k_1 = 0.072$
	$k_2 = 4.523$	$k_2 = 4.362$
	$k_3 = 0.1257$	$k_3 = 0.0958$
CrTh HZSM-5	$k_1 = 0.0391$	$k_1 = 0.00154$ (400^0C)
(SAR-32)	$k_2 = 0.544$	$k_2 = 0.1516$ (400^0C)
	$k_3 = 0.0139$	$k_3 = 0.00105$ (400^0C)
PbHY	$k_1 = --$	$k_1 = 0.00184$ (400^0C)
	$k_2 = --$	$k_2 = 0.2359$
	$k_3 = --$	$k_3 = 0.00094$

Homogeneous model

HZSM-5 (SAR-19)	2.2058	0.67
Cr Th HZSM-5 (SAR-32)	0.241	0.0131 (400^0C)
PbY	-	0.00974 (400^0C)

6.4 CONCLUSIONS

From the present studies following conclusion may be drawn.

1. HZSM-5 catalyst is more active in comparison to HY and H-mordenite catalyst.

2. The activity of CrThHZSM-5 was found to be inferior in comparison to the HZSM-5.

3. The p-xylene selectivity of HZSM-5 having different silica-alumina ratio were compared and it was found that silica alumina ratio 40 is much better than silica alumina ratio 19 and 43.

5. Although Y-zeolites are inferior to HZSM-5 in terms of p-xylene yield, Pb exchanged Y-zeolite has shown remarkably good result at 550^0C.

Fig. 5.18 shows the percentage toluene conversion as a function of space time over HZSM-5 SBR 19 at 450 and 550°C. It is clear that with increae in space time the toluene conversion increases. At 550°C the conversion are much higher in comparison to 450°C. At a value of W/F_{To} equal to 6.0 toluene conversion of the order of 27.5 percent may be obtained at 550°C as against only 7% at 450°C. The reasons for inhanced conversion at higher space time is clearly due to the greater contact time between the reactant and the catalyst.

Fig. 5.19 presents the effect of space time on percent p-xylene selectivity over HZSM-5 (SAR-19). The results show a decreasing trend in percent p-xylene selectivity with space time at both the temperatures 450 and 550°C. A decrease of about 2% (26 to 24%) may be observed as against a decrease of about 10% (24 % to 14%) at 450 and 550°C respectively for an increase in space time from 3.5 to 7.0. The reasons for the decline in p-xylene selectivity with space time may be due to greater residence time of para isomer on the surface of the catalyst alowing it to under go isomerisation and this isomerisation is clearly seen to be much faster at a higher temperature.

Fig. 5.20 presents the effect of space time on the performance of PbHY catalyst at 400 °C. At lower temperatures (below 550°C), the activity of PbHY catalyst has been exceptionaly good as shown earlier. From the figure it may be observed that with increase in sapce time conversion increases, whereas, the p-xylene selectivity and p-xylene yield decreases.

Fig. 5.21 presents performance of CrThHZSM5 (SAR-32) as a function of space time at 550°C. It can be seen that with increase in space time conversion increases, whereas, the p-xylene selectivity and p-Xylene yield decreases. Fig. 5.22 shows the toluene conversion as a function of space time for HZSM-5 (SAR-19) at 450°C. As expected the % toluene conversion is found to increase with temperature.

6.3 KINETIC STUDY OF TOLUENE DISPROPORTIONATION REACTION

The kinetic equations based on homogeneous reaction model and as well as heterogeneous reaction model were derived and the values of the rate constant were found at various temperatures for different catalyst. The rate equation based on adsorption control of heterogeneous model is represented by equation 4.24, the surface reaction control model by equation 4.25 and desorption control by equation 4.29. The kinetic equation for homogeneous model has been presented in equation 4.40.

Experimental rate data to fit these models were taken with various catalysts at changing W/F_{To}, keeping the reaction temperature constant at a particular value. For this both toluene feed rate as well as nitrogen flow rate were increased to the same proportion in order to keep the nitrogen to toluene motal ratio constant.

The rate constant for various suggested models were calculated from the slope of the straight line obtained after plotting appropriate factors as shown in figures 5.23 to 5.34 on Y-axis as against W/F_{To} on X axis. The values of Ke used in this equation were calculated using thermodynamic vlaues as discussed in chapter IV. The values of K_e for different catalysts is tabulated in Table 4.3. The value of P_{To} used in equation was 0.1725 atm. As suggested by Uguina, 1993 [8], K_T, (adsorption of toluene equilibrium constant) was assumed to be equal to K_X (desorption of xylene equlibrium constant). This assumption was based on the fact of same number of vacant sites available during adsorption, surface reaction and desorption. The values of K_T used in above equation were calculated by equating r_{AD} (equation 4.21) and r_D (equation 4.23). Here, in order to simplify the solution, k_1 was assumed equal to k_3 (where k_1 is reaction rate constant for adsorption rate controlling and k_3 for desorption on rate controlling step). The value K_T calculated are listed below :

Table 6.1 Value of K_T for different catalyst.

Catalyst	K_T	
	450^0C	550^0C
HZSM-5 (SAR-19)	0.145	1.31
Cr Th HZSM-5 (SAR-32)	0.059	0.51
PbY	0.068 (400^0c)	-

The value of x (the toluene conversion) was taken from experimental result at given temperature. Reaction rate constant, thus, found from these plots were calculated from the constant as mention above in the value of x at the temperature 400, 450, 550^0C. Similarly for homogeneous model the reaction rate constant k_P was calculate using equation 4.40 by plotting the suggested parameters as indicated in figure 5.23 to 5.25 as ordinate Vs W/F_{T0} as abscissa. The constant values used in equations had the same values obtain earlier. Table 6.2 presents the reaction rate constant values k_1, k_2, k_3, and k_p for adsorption controlling, surface reaction controlling, desorption controlling heterogeneous model and homogenous model respectively for different catalyst at temperature 400, 450 and 550 ^0C. If we compare the k_1 values at both the temperatures the values are in order.

HZSM-5 (SAR-19)> Cr Th HZSM-5 (SAR-32) > PbY,

which is in accordance with the order of taluene conversion obtained experimentally by these catalyst as described earlier. The value of k_2, k_3, and k_p also follow the same order. For given catalyst the values of any of the reaction rate constant is found to be greater at 550^0C in compression 450^0C. This is also in agreement with the % Toluene conversion found experimentally.

Table 6.2 Reaction rate constant values for various catalysts calculated from plots (5.23 to 5.34)

Heterogeneous model

Catalyst	550^0C	450^0C
HZSM-5 (SAR-19)	$k_1' = 0.3049$	$k_1 = 0.072$
	$k_2 = 4.523$	$k_2 = 4.362$
	$k_3 = 0.1257$	$k_3 = 0.0958$
CrTh HZSM-5	$k_1 = 0.0391$	$k_1 = 0.00154$ (400^0C)
(SAR-32)	$k_2 = 0.544$	$k_2 = 0.1516$ (400^0C)
	$k_3 = 0.0139$	$k_3 = 0.00105$ (400^0C)
PbHY	$k_1 = --$	$k_1 = 0.00184$ (400^0C)
	$k_2 = --$	$k_2 = 0.2359$
	$k_3 = --$	$k_3 = 0.00094$

Homogeneous model

Catalyst	550^0C	450^0C
HZSM-5 (SAR-19)	2.2058	0.67
Cr Th HZSM-5 (SAR-32)	0.241	0.0131 (400^0C)
PbY	-	0.00974 (400^0C)

6.4 CONCLUSIONS

From the present studies following conclusion may be drawn.

1. HZSM-5 catalyst is more active in comparison to HY and H-mordenite catalyst.

2. The activity of CrThHZSM-5 was found to be inferior in comparison to the HZSM-5.

3. The p-xylene selectivity of HZSM-5 having different silica-alumina ratio were compared and it was found that silica alumina ratio 40 is much better than silica alumina ratio 19 and 43.

5. Although Y-zeolites are inferior to HZSM-5 in terms of p-xylene yield, Pb exchanged Y-zeolite has shown remarkably good result at 550^0C.

6. p-xylen yield of 7% can be obtained with 2.7% CrThHZSM-5 (SAR-40) at 650°C.

7. Kinetic study results indicate higher value of reaction rate constant for HZSM-5 (SAR-19) in comparison to CrThHZSM-5, and PbHY catalyst, conforming the better catalytic activity obtained experimentally by HZSM-5 (SAR-19).

6.5 RECOMONDATION

Following recommendations are made for future studies.

1. The catalytic activity for toluene disproportionation may be carried out by chemical vapour deposition of suitable metals on various zeolites.

2. The experimental results may also be correlated with various other charateristics of the catalyst such as acidity, TPD of NH_3 or pyridine, surface area (before and after the reaction) coke formation and pore size and pore volume measurements.

3. Toluene disproportionation may also be carried out in presence of H_2 as carrier gas.

13. D.H. Olson, G.T. Kokotailo, S.L. Lawton, "Crystal structure and structure related properties of ZSM-5", J. Phys. Chem. 1981, 85, 2238-2243.

14. D.V. Nightingale, Chem Rev 1939, 25, 329.

15. Y.Sedona and Y. Ono, "Effect of pree treatment temperature on catalytic activity of ZSM-5 zeolities", 1988, 8, 101-105.

16. B. Imalic, C. Naccache, Y.B. Tarrit, J.C. Vedrine, G. Coudurier and H. Praliaud. "Catalysis by zeolities", Elsevir Scientific Publishing Company, New York, 1990.

17. J.A. Rabo, ACS Monograph 171, "Zeolite Chemistry and catalysis", Americal Chemical Society, Washington, 1976, pp. 84-99, 121-127.

18. W.O. George, P.S. Mcintyre, "Infrared Spectroscopy", John Wiley and Sons 1987, pp. 14, 68-86.

19. W.W. Kaeding, S.A. Butter, U.S. Patent (1975) 3, 911, 041.

20. N. Cardona-Martinez, J.A. Dumesic, "Acid strength of silica - alumina and silica studied by micro calorimetric meaurements of puridine adsoption" J. of Catalysis 1990, 125, 427-444.

21. B.D. Callity, "Element of X-ray diffraction", Addison-Wesley Publishing Company, INC. 1967, pp 16-25, 144-146.

22. "X-ray diffraction operating mannual (PW 1140, 190)", University Scientific instrumentation centre, UOR, Roorkee.

23. "Scanning electron microscope mannual (Lew electron Micro copy Ltd.)" Vol. I, USIC, UOR, Roorkee.

24. "Operating mannual LABTAM 8400 spectrometer", University Scientific instrumentation centre UOR, Roorkee.

25. M. Thompson, J. Nicholas Walsh, "A hand book of Inductively Coupled Plasma Spectrometry", Blackie and Son Ltd., 1983.

26. J.M. Smith, "Chemical Engineering Kinetics", 3rd edition, McGraw Hill, New York 1982.

27. H.M. Spencer, J. Amer, Chem. Soc. 1949, 67, 1859-60.

28. M. Sounders, C.S. Mathews, C.O. Hurd, I. and C.E., 1949, 41, 1048.

6. p-xylen yield óf 7% can be obtained with 2.7% CrThHZSM-5 (SAR-40) at 650°C.

7. Kinetic study results indicate higher value of reaction rate constant for HZSM-5 (SAR-19) in comparison to CrThHZSM-5, and PbHY catalyst, conforming the better catalytic activity obtained experimentally by HZSM-5 (SAR-19).

6.5 RECOMONDATION

Following recommendations are made for future studies.

1. The catalytic activity for toluene disproportionation may be carried out by chemical vapour deposition of suitable metals on various zeolites.

2. The experimental results may also be correlated with various other charateristics of the catalyst such as acidity, TPD of NH_3 or pyridine, surface area (before and after the reaction) coke formation and pore size and pore volume measurements.

3. Toluene disproportionation may also be carried out in presence of H_2 as carrier gas.

REFERENCES

1.   R.K. Das Gupta, P. Mukherjee, "Chemical age of India 1984, 4, 35.

2.   "Chemical weekly", Nov 16, 1999.

3.   L.E. Aneke, L.A. Gerristen, P.J. Van Deg Berg, W.A. De Jang, "The disproportionation of toluene over a HY/βAlF$_3$/Cu catalyst. 1. "Preparation and characterization", J. Catl., 1979, 59, 26-36.

4.   S.S. Bhavikatti, S.R. Patwardhan, "Toluene disproportionation over nickel-loaded aluminium deficient mordenite. 2. Kinetics", Ind Eng. Chem. Pord. Res. Dev. 1981, 20 106-109.

5.   W.W. Kaeding, C. Chu, L.B. Young, S.A. Butter, "Shape-selective reactions with zeolites catalyst. 2. Selective disproportonation of toluene to produce benzene.and p-xylene", J. Catal. 1981, 69, 292-298.

6.   P. Beltrame, P.L. Beltrame, P. Carniti, L. Forni, G. Zuretti, "Toluene disproportionation catalysed by various zeolities", Zeolities, 1985, 5, 401-405.

7.   P. Beltrame, P.L. Beltrame, P. Carniti, L. Forni, G. Zuretti, "Toluene disproportionation catalysed by various zeolites". Zeolities, 1987, 7, 418-422.

8.   M.A. Uguina, J.L. Sotelo, D.P. Serrano, "Kinetics of toluene disproportionation over unmodified and modified ZSM-5 zeolites". Ind. Eng. Chem. Res. 1993, 32, (49-55).

9.   J. Das, Y.S. Bhat, A., B. Halgeri, "Selective toluene disproportionation over pore size controlled MFI zeolite", Ind. Eng. Chem. Res. 1994, 33, 246-250.

10. H.A. Benesi, J. Catal 1967, 8, 368.

11. Gates, Katzer and Schuit, "Chemistry of catalytic process" McGraw hill, New York-1982.

12. W.M. Meier, "Molecular sieve," Soc. of Chem. Ind., London -1968, pp. 10-27.

13. D.H. Olson, G.T. Kokotailo, S.L. Lawton, "Crystal structure and structure related properties of ZSM-5", J. Phys. Chem. 1981, 85, 2238-2243.

14. D.V. Nightingale, Chem Rev 1939, 25, 329.

15. Y.Sedona and Y. Ono, "Effect of pree treatment temperature on catalytic activity of ZSM-5 zeolities", 1988, 8, 101-105.

16. B. Imalic, C. Naccache, Y.B. Tarrit, J.C. Vedrine, G. Coudurier and H. Praliaud. "Catalysis by zeolities", Elsevir Scientific Publishing Company, New York, 1990.

17. J.A. Rabo, ACS Monograph 171, "Zeolite Chemistry and catalysis", Americal Chemical Society, Washington, 1976, pp. 84-99, 121-127.

18. W.O. George, P.S. Mcintyre, "Infrared Spectroscopy", John Wiley and Sons 1987, pp. 14, 68-86.

19. W.W. Kaeding, S.A. Butter, U.S. Patent (1975) 3, 911, 041.

20. N. Cardona-Martinez, J.A. Dumesic, "Acid strength of silica - alumina and silica studied by micro calorimetric meaurements of puridine adsoption" J. of Catalysis 1990, 125, 427-444.

21. B.D. Callity, "Element of X-ray diffraction", Addison-Wesley Publishing Company, INC. 1967, pp 16-25, 144-146.

22. "X-ray diffraction operating mannual (PW 1140, 190)", University Scientific instrumentation centre, UOR, Roorkee.

23. "Scanning electron microscope mannual (Lew electron Micro copy Ltd.)" Vol. I, USIC, UOR, Roorkee.

24. "Operating mannual LABTAM 8400 spectrometer", University Scientific instrumentation centre UOR, Roorkee.

25. M. Thompson, J. Nicholas Walsh, "A hand book of Inductively Coupled Plasma Spectrometry", Blackie and Son Ltd., 1983.

26. J.M. Smith, "Chemical Engineering Kinetics", 3rd edition, McGraw Hill, New York 1982.

27. H.M. Spencer, J. Amer, Chem. Soc. 1949, 67, 1859-60.

28. M. Sounders, C.S. Mathews, C.O. Hurd, I. and C.E., 1949, 41, 1048.

29. J.M. Smith, Vanness, "Introduction to chemical engineering thermodynamics", 2nd edition McGraw Hill, New York.

30. S.G. Hedge, R. Kumar, R.N. Bhat and P Ratnaswamy, Zeolite, 1989, 9, 231-236.

31. M.A. Uguina, J.L. Sotelo and D.P. Serrano, "Toluene disproportionation over ZSM-5 zeolite : Effect of crystal size, silicon to aluminum ratio, activation method and pelletization"Appl.Catalyst.1991,76,183.